T-PM-Sym1

CALCIUM SIGNALS IN MUSCLE

A Symposium Organized by RS Eisenberg,
Department of Physiology, Rush Medical College, Chicago, IL 60612.

The intracellular functions of most cells are under some form of extracellular control mediated by the cell membrane. A.V. Hill, working on skeletal muscle in 1948, was evidently the first to understand the physical need for a specialized biological mechanism coupling the cell's membrane to its intracellular organelles. The structures and molecules which form the coupling mechanism in skeletal, cardiac, and smooth muscle have been intensively investigated since that time. In particular, the role of calcium has provided a stately theme sustained through the passacaglia of subsequent research in excitation/contraction coupling.

Recently, membrane/organelle coupling in other cells has received much attention; indeed, calcium has been touted as a universal messenger in the coupling mechanism. The broadened scope of speculation and quickened pace of investigation has brought welcome progress, but also isolation of adjacent fields. The baroque passacaglia of excitation-contraction coupling is in danger of being replaced, unheard and unknown, by the romantic andante of the calcium second messenger.

The speakers in this Symposium will present our current knowledge of coupling in skeletal, cardiac, and smooth muscle, emphasizing the role of calcium. In conjunction with sibling Symposia on coupling in other cells, perhaps we can see how different, or how similar, are the mechanisms of coupling; perhaps we can listen to hear if passacaglia and andante form cacophony, or symphony.

T-PM-Sym2 EXCITATION-CONTRACTION COUPLING IN SMOOTH MUSCLE. Avril V. Somlyo and Andrew P. Somlyo. Penn. Muscle Inst., Univ. of Penn. Sch. of Med., Phila., PA 19104 U.S.A.

Electromechanical coupling (action potentials and/or graded depolarization) as well as pharmacomechanical coupling (E-C coupling independent of changes in membrane potential) trigger smooth muscle contraction via an increase in cytoplasmic free Ca^{2+}(1). Influx of extracellular $[Ca]_o$ may contribute to activation, but this presentation will emphasize the major role of the sarcoplasmic reticulum (SR) as the intracellular source and sink of activator Ca. Spontaneous, rhythmic and/or drug induced contractions occur in 0 $[Ca]_o$ (EGTA or La containing solns). Contraction in 0 $[Ca]_o$ of depolarized smooth muscle indicates that Ca-influx induced Ca-release is not a major mechanism of pharmacomechanical coupling. Recycling of intracellular Ca is indicated by repetition of drug induced maximal contractions in Ca-free solutions, and is due to the release of Ca from the junctional SR, as shown by electron probe analysis of rapidly frozen rabbit portal vein smooth muscle (2). Recent studies have also shown the release of Ca by norepinephrine from non-junctional SR (more than 200nm distant from the plasma membrane) in 1.2mM $[Ca]_o$ (Kowarski et al. Present Proceedings). The molecular mechanism(s) triggering Ca release from junctional and non-junctional SR is(are) not known, but speculations (encouraged by the Organizers!) will include: 1) release of a trigger substance such as inositol (1,4,5) triphosphate 2) propagated wave of increased Ca permeability along the SR.

REFERENCES: 1) Somlyo, A.V. & Somlyo, A.P. (1968) J. Pharmacol. & Exp. Therap. 159: 129; 2) Bond, M., Kitazawa, T., Somlyo, A.P. & Somlyo, A.V. J. Physiol. (London) 355: 677-695, 1984.

Supported by HL15835 to the Pennsylvania Muscle Institute and Training Grant HL07499.

T-PM-Sym3 CONTROL OF SARCOPLASMIC RETICULUM CALCIUM RELEASE IN SKELETAL MUSCLE. M.F. Schneider, Dept. of Physiology, Univ. of Rochester, Rochester, NY.

Electrical depolarization of the transverse tubules (TT) of a skeletal muscle fiber initiates calcium release from the adjacent but apparently electrically isolated sarcoplasmic reticulum (SR). Voltage dependent intramembrane charge movement (Schneider & Chandler, Nature 242, 244, 1973) within the TT membrane may serve as the initial voltage sensitive step in gating SR calcium release. However, a subsequent membrane to membrane signal transmission step must also occur since the intramembrane "gating" charge movement and the permeability change underlying calcium release occur in the distinct TT and SR membranes. We are measuring charge movement and the rate of SR calcium release (Melzer et al., Biophys. J. 45, 637, 1984) in frog muscle fibers in an attempt to put limits on various possible mechanisms for controling calcium release. Present results indicate that the peak rate of calcium release during a depolarizing voltage clamp pulse is uniquely determined by the charge moved in excess of the "threshold" charge required to produce detectable calcium release (B. Simon et al, these abstracts). Previous experiments using subthreshold prepulses indicated that the charge moved below threshold is also involved in the control of calcium release (Horowicz and Schneider, J. Physiol. 277, 483, 1981; Schneider et al in "Regulation of Muscle Contraction," p. 131, 1981). Such subthreshold charge movements may constitute a step preceeding the final charge transition that initiates the T-SR signal. During a 100-200 ms depolarizing pulse the rate of calcium release declines to about 1/3 of peak but there is no immobilization of intramembrane charge. Possible mechanisms for the control of calcium release will be considered in relation to these and other observations.

T-PM-Sym4 CALCIUM-INDUCED RELEASE OF CALCIUM FROM THE SARCOPLASMIC RETICULUM OF SKINNED FIBERS FROM THE FROG SEMITENDINOSUS. A. Fabiato, Department of Physiology, Medical College of Virginia, Richmond.

Bundles of myofibrils were microdissected from the frog semitendinosus with final overall dimensions of the preparation of 4-8 μm width, 2.5 μm thickness and 20-35 μm length at 2.3 μm sarcomere length. A microprocessor-controlled system of rapid microinjection-aspirations changed the solution at the outer surface of the sarcoplasmic reticulum (SR) wrapped around individual myofibrils (0.3 μm radius) by hydraulic bulk flow within ∿1 ms. Ca^{2+} release was detected (1) by simultaneous recording of tension and of aequorin bioluminescence in the presence of 0.1 mM total EGTA, or (2) by the change in the area under the curve of phasic tension induced by 20 mM caffeine in the presence of 0.2 mM total EGTA after Ca^{2+} release had been induced in the presence of 10 mM total EGTA. The temperature was 3°C and, accordingly, the pH was 7.30; the pMg was 2.50 and the pMgATP 2.50. Ca^{2+}-induced Ca^{2+} release (CICR) was triggered by an increase of [free Ca^{2+}] from pCa 7.20 to pCa 6.75. Preliminary results using increasing concentrations of the bromo-derivative of 1,2-bis(o-aminophenoxy)ethane-*N,N,N',N'*-tetraacetic acid ("bromo-BAPTA", compound 2c of Tsien, R.Y., Biochemistry 19:2396-2404, 1980) to buffer the Ca^{2+} released from the SR detected with aequorin, indicate that the rate of release was >10 times higher than that observed in skinned cardiac cells under similar conditions and, perhaps, compatible with the rate of Ca^{2+} release from the SR of intact skeletal muscle fibers. This CICR could not be obtained in skinned fibers with 10 times larger cross-sectional area because they did not present the broad separation of the myofibrils necessary for the externally applied solution to rapidly and synchronously change the [free Ca^{2+}] at the outer surface of the SR wrapped around all individual myofibrils of the preparation. (Supported by NIH #HL19138 and AHA #83-667)

T-PM-Sym5 CALCIUM IONS: THE LINK BETWEEN t DEPOLARIZATION AND SR Ca RELEASE? B.A. Curtis and R.S. Eisenberg, Depts of Physiology, University of Illinois College of Medicine at Peoria, IL 61656 and Rush Medical College, Chicago, IL 60612

Calcium uptake produced by a 150 mM potassium contracture in frog single twitch fibers was 6.7 + 0.8 pmol (21 fibers). When potassium was applied to fibers paralyzed by the combination of 30 μM D600, cold and a prior contracture, the Ca uptake fell to 3.0 + 0.7 pmol (16). Ca entry into paralyzed fibers is clearly unrelated either to e-c coupling or to contraction and is a voltage sensitive, slowly inactivating influx blocked by 4 mM Ni. It was estimated by two independent methods to be 1.1 + 0.3 pmol/min or 10 nA/cm^2 at 3°C. The paired difference in Ca uptake between contracting and paralyzed fibers is a component of influx related to e-c coupling; three independent protocols give an average of 2.0 pmol/contracture (35). Its size varies with contracture size and it occurs after tension production: ^{45}Ca applied immediately after contraction in either K or Na solutions is taken up in essentially the same amounts as ^{45}Ca added before contraction. This delayed, e-c coupling related uptake apparently refills an intracellular compartment emptied to initiate the prior contracture. We detect no e-c coupling related component of Ca uptake from the extra cellular space occurring before or during a contracture. A MODEL. The t membrane system contains a 7 pmol/fiber Ca store guarded against sudden depletion by zero Ca. Movement of this Ca store into the t-SR gap is somehow related to depolarization and charge movement and initiates Ca release from the SR. Refilling of the depleted t store with Ca may be the rate limiting event of the mechanically refractory period. Supported by NIH grants HL-20230 and NS-12038.

T-PM-A1 SPECIFICITY IN BIOLOGICAL ELECTRON TRANSFER. M. A. Cusanovich, T. E. Meyer and G. Tollin, Dept. of Biochemistry, University of Arizona, Tucson, AZ 85721.

Recent studies on electron transfer by a variety of biological electron transfer proteins, including: c-type cytochromes, cytochromes c' and high potential iron sulfur proteins have allowed us to quantitatively resolve the contribution of oxidation-reduction potential, electrostatics and steric effects on the kinetics of electron transfer. Two systems have been studied, the interaction of redox proteins with photoreduced free flavins and the reaction of the same proteins with flavodoxin from Clostridium pasteurianum. It is found that in both systems the electrostatically corrected rate constants vary with the difference in oxidation-reduction potential between reactants in a systematic fashion which can be described by a simple relationship. Moreover, the contribution of electrostatics to the reaction kinetics can be analyzed and is consistent with the charge at the site of interaction dominating, but modulated by more distant charges. Finally, deviations from expected behavior (electrostatically corrected) appear to correlate with structural differences at the presumed sites of electron transfer. In general, we find electrostatic effects, steric influence and redox potential all exert a much larger effect on reaction rate constants for the flavodoxin-cytochrome system than has been observed for free flavin-cytochrome interactions. The implications of this for determining biological specificity will be discussed.
This work was supported in part by grants from the National Institutes of Health, AM15057 (G.T.) and GM21277 (M.A.C.).

T-PM-A2 MICROHETEROGENEITY OF CORE PROTEIN 2 IN YEAST CYTOCHROME bc_1 COMPLEX PURIFIED BY A NEW METHOD Per O. Ljungdahl and Bernard L. Trumpower, Biochemistry Department, Dartmouth Medical School, Hanover, NH 03756

Enzymatically active cytochrome bc_1 complex has been purified from yeast mitochondria by a new method. The complex is solubilized from submitochondrial particles with nonionic detergent in the presence of protease inhibitors and purified by anion exchange chromatography. The purified complex contains 3.7 and 6.8 nmol of cytochromes c_1 and b per mg of protein, respectively, is free of succinate dehydrogenase and cytochrome oxidase, and exhibits 9 polypeptides on PAGE-SDS. The ubiquinol cytochrome c oxidoreductase turnover number of the purified complex is 200 s^{-1}. The purity and activity of this complex are equal to the best reported in the literature.

When examined on high resolution electrophoresis gels, core protein 2 exhibits microheterogeneity, and consists of 2 peptides of molecular weights approximately 39.5 and 38 KDa, with the smaller peptide being the more abundant. The relative amount of these 2 peptides is constant in numerous preparations of the complex, and is unaffected by the presence of protease inhibitors. These 2 peptides are also observed in bc_1 complex purified by cytochrome c affinity chromatography, and appear to be present in previous preparations reported in the literature, although not recognized or commented upon.

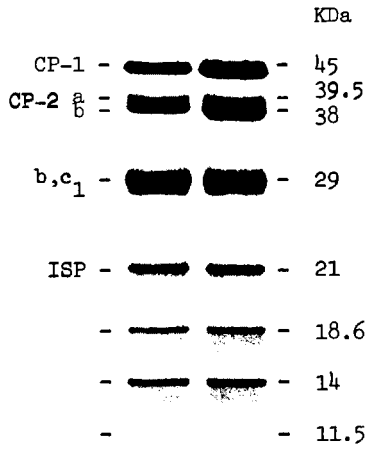

(Supported by NIH Grant GM 20379)

T-PM-A3 MEASUREMENT OF THE PROXIMITY OF CYTOCHROME c TO LIPOSOME AND MITOCHONDRIAL INNER MEMBRANES USING RESONANCE ENERGY TRANSFER. Sharmila S. Gupte and Charles R. Hackenbrock, Laboratories for Cell Biology, Department of Anatomy, University of North Carolina School of Medicine, Chapel Hill, North Carolina.

Using mitochondrial inner membranes, we determined the three dimensional diffusion of cytochrome c by measuring its diffusion coefficients and the rates of electron transfer at different ionic strengths (Gupte et al., 1984, PNAS 81:2606; Gupte & Hackenbrock, 1984, Biophys. J. 45:297a). In this communication, the proximity of cytochrome c to the membrane was directly measured using the resonance energy transfer from diphenylhexatriene (DPH) incorporated into the lipid bilayer, to the cytochrome c heme at various ionic strengths (KCl concentrations). The average distance between DPH and cytochrome c heme increased with increasing ionic strength. This increase in distance was independent of the ratio of cytochrome c to phospholipids in both liposomes and mitochondrial inner membranes. The maximum ratio of phospholipids:cytochrome c was 340:1 for both membranes and was independent of DPH concentration, which indicates that the maximum number of cytochrome c binding sites on the membrane is limited. The data reveal that the average time spent by cytochrome c on the membrane surface is minimal at physiological ionic strength (150 mM KCl) and physiological cytochrome c concentration. In intact mitochondria, the rate of electron transfer by cytochrome c is maximum at physiological ionic strength (Gupte & Hackenbrock, 1984, Biophys. J. 45:297a). Therefore, this high mobility of cytochrome c is most likely an important factor in the overall mechanism of electron transport in intact mitochondria. This work was supported by NIH Grant #GM 28704 and NSF Grants #PCM 79-10968 and PCM 8402569 to CRH.

T-PM-A4 THE ROLE OF COENZYME Q IN ENERGY-LINKED FUNCTIONS IN THE CYTOCHROME B-C_1 COMPLEX OF Q-DEFICIENT YEAST. Liviu Clejan and Diana S. Beattie, Dept. Biochem., Mt. Sinai Sch. Med., New York, N.Y. 10029

Mitochondria isolated from coenzyme Q-deficient yeast cells had no detectable NADH or succinate: cytochrome c reductase activity, but contained the normal amounts of cytochromes b and c_1 by spectral analysis. Addition of exogenous coenzyme Q derivatives including Q_1, Q_2, Q_6 and the decyl analog (DB) restored the rate of antimycin and myxothiazole-sensitive cytochrome c reduction with both substrates to that observed with reduced DBH_2. Similarly, addition of these coenzyme Q analogs increased the rate of cytochrome c reduction in wild type cells suggesting that the pool of coenzyme Q in the membrane is limiting for cytochrome c reduction in both cells. Addition of DBH_2, or succinate plus Q_6 or DB to mitochondria from the mutant resulted in an initial reduction of cytochrome b followed by a slow reduction of cytochrome c_1 with a concomitant reoxidation of cytochrome b. Antimycin caused the oxidant-induced reduction of cytochrome b without the red-shift observed in the wild-type. A few minutes after antimycin addition, a gradual reduction of cytochrome c_1 was observed indicating that the analogs cannot substitute for the tightly-bound ubiquinone in the complex. Furthermore, a slight reduction of cytochrome b was observed when succinate was added to the Q-deficient mitochondria. The subsequent addition of antimycin caused an almost 60% reduction of the total cytochrome b in a myxothiazole sensitive reaction. Again, no red-shift in the absorption of cytochrome b was observed. These results suggest that cytochrome b can be reduced by succinate in the absence of endogenous coenzyme Q. (Supported by NIH HD-04007).

T-PM-A5 IDENTIFICATION OF THE CYTOCHROME c BINDING SITE ON CYTOCHROME c_1. F. Millett, J. Stonehuerner, P. O'Brien, L. Geren, J. Steidl, L. Yu, and C.A. Yu, (Intr. by R. Koeppe, II), University of Arkansas, Fayetteville, AR, 72701 and Oklahoma State U., Stillwater, OK, 74078

Treatment of the cytochrome bc_1 complex with 2 mM 1-ethyl-3-(3-[^{14}C]trimethylaminopropyl)-carbodiimide (ETC) led to inhibition of electron transfer to cytochrome c. SDS polyacrylamide gel electrophoresis revealed that carboxyl groups on both the cyt c_1 heme peptide and the 9,175 MW "hinge" peptide were labeled by ETC. When the ETC treatment was carried out in the presence of cytochrome c, labeling of both the cyt c_1 and the hinge peptide was decreased, and two new cross-linked species were formed: cyt c-hinge peptide and cyt c-cyt c_1. Treatment of a purified cytochrome c_1 preparation containing both the heme peptide and the hinge peptide led to essentially the same labeling and cross-linking pattern as for the cytochrome bc_1 complex. In order to identify the specific carboxyl groups labeled, methylated cytochrome c_1 was treated with ETC, digested with trypsin and chymotrypsin, and the resulting peptides separated by HPLC. ETC was found to label the cyt c_1 peptides 63-81, 121-128, and 153-179, and the hinge peptides 1-17 and 48-65. All of these peptides are highly acidic and contain one or more regions of adjacent carboxyl groups. The only peptide consistently protected from labeling by cytochrome c binding was 63-81, demonstrating that the carboxyl groups at residues 66, 67, 76, and 77 are involved in binding cytochrome c. These residues are relatively close to the heme-binding cysteine residues 37 and 40, and indicate a possible site for electron transfer from cytochrome c_1 to cytochrome c. (Supported in part by NIH Grants GM 20488 and GM 30721.)

T-PM-A6 LATERAL DIFFUSION OF REDOX PROTEINS IN THE MITOCHONDRIAL INNER MEMBRANE IS AFFECTED BY THE TOTAL MEMBRANE PROTEIN CONCENTRATION. Brad Chazotte and Charles R. Hackenbrock. Laboratories for Cell Biology, Department of Anatomy, School of Medicine, University of North Carolina, Chapel Hill, NC 27514

The lateral diffusion of specific electron transfer proteins in the mitochondrial inner membrane was studied as a function of total membrane protein concentration and temperature using fluorescence recovery after photobleaching (FRAP). These results were compared and contrasted with kinetic assays of electron transfer activities of the specific redox proteins. The total protein concentration of the rat liver mitochondrial inner membrane was varied in a controlled fashion using the low pH method of Schneider, et al (PNAS77:42, 1980) which incorporates exogenous lipid into the membrane. The calcium fusion method of Chazotte, et al (Fed. Proc. 42:2170, 1983) was used to fuse these membranes to a size sufficient for FRAP. Specific redox proteins were immunofluorescently labeled in order to determine their diffusion coefficients by the FRAP technique. It was determined that the lateral diffusion coefficients for the bc1 complex increased significantly as the total membrane protein density decreased. The temperature dependence of the diffusion coefficient of the bc1 complex, analyzed by an Arrhenius treatment, showed a decrease in activation energy as the total protein concentration decreased. This parallels results showing faster lipid diffusion as the membrane protein concentration is decreased (Chazotte, et al, Biophy. J.45:296a, 1984). These results demonstrate the direct affect of membrane protein concentration on lateral diffusion, which is a catalytically important process in this membrane. Supported by NIH GM28704, and NSF PCM79-10968 and PCM84-02569 to CRH.

T-PM-A7 ATP/2e$^-$ IS GREATER THAN ONE FOR REVERSE ELECTRON TRANSFER ACROSS SITE 1. Jo A. Freedman and John J. Lemasters, Laboratories for Cell Biology, Department of Anatomy, University of North Carolina at Chapel Hill, Chapel Hill, NC 27514.

Recent measurements of ATP to oxygen flux ratios during state 3 and free energy force ratios during state 4 have led to the proposal of a new 13-proton model of chemiosmotic coupling in which proton stoichiometries are 3 for the F_1F_0-ATPase, 1 for the transport of ATP, ADP, and Pi, and 5, 4, and 4, respectively for Sites 1, 2, and 3 (Lemasters, Fed. Proc. 43, 1877). Taking into account substrate (scalar) protons, ATP/2e$^-$ ratios at the three sites are 1¼, ½, and 1¼. A striking feature of this model is its predicted high ATP ratio for Site 1. This prediction was tested by measuring the energetics of ATP-driven reverse electron transfer from succinate to acetoacetate in rat liver mitochondria. Electron transfer was initiated by addition of 5 mM ATP to a medium containing 150 mM sucrose, 1 mM EDTA, 1 mg/ml BSA, 1 mM disodium succinate, 1 mM lithium acetoacetate, 2 mM KCN, 2.5 mg/ml of mitochondrial protein, and 25 mM K-HEPES buffer, pH 7.4, 23°C. As the reaction proceeded, the phosphorylation potential (ΔG_P) and the free energy change of electron transfer or redox potential (ΔG_R) were determined from concentrations of ATP, ADP, Pi, succinate, malate, ß-hydroxybutyrate, and acetoacetate after perchloric acid quenching. ΔG_P decreased to less than 12 kcal/mol (50 kJ/mol) and ΔG_R increased to more than 13 kcal/mol (54 kJ/mol). This reverse electron transfer was ATP-dependent and fully blocked by rotenone, a specific inhibitor of electron transfer through Site 1. In the approach to quasi-equilibrium (static head), $\Delta G_R/\Delta G_P$ reached 1.18. In a nonequilibrium system, $\Delta G_R/\Delta G_P$ must be less than the mechanistic ATP/2e$^-$ ratio. Therefore, the ATP stoichiometry at Site 1 is greater than 1.18, probably close to 1¼ as predicted by the 13-proton model. Supported by GM28999 and AM30874.

T-PM-A8 Influence of Potassium Phosphate on Alamethicin Induced Changes in Mitochondrial Oxidative Phosphorylation.

A. Basu, Manoj K. Das and P. Balaram. Molecular Biophysics Unit, Indian Institute of Science, Bangalore 560 012, India.

Alamethicin, a 20-residue membrane channel forming polypeptide uncouples mitochondria in media having K^+-phosphate concentrations < 25mM. At higher phosphate levels, an inhibitory effect on respiration is observed. Studies of the time dependence of oxygen consumption rates after peptide addition, establish an initial stimulation of respiration, followed by a decrease in respiration rate. A similar effect on oxidation was also observed in presence of the tetra-acetylated derivative of melittin, a 26-residue peptide from bee venon. This effect of alamethicin or acetylmelittin on mitochondrial oxidation can be simulated by simultaneous addition of classical uncouplers like FCCP and valinomycin, a K^+-ionophore. Synergistic effects of peptide channels and carrier ionophores have been examined. Experiments with specific inhibitors and substrates, establish that the electron transport complex IV was the site of inhibition. Respiration in mitochondria, inhibited in the above manner could be restored by addition of cytochrome C. The results are rationalized in terms of changes in mitochondrial membrane properties under these conditions.

T-PM-A9 PROTONMOTIVE FORCE AND PHOTOPHOSPHORYLATION IN SINGLE SWOLLEN THYLAKOID VESICLES. M.L. Campo and H. Tedeschi, Department of Biological Sciences, State University of New York at Albany, Albany, NY 12222

Swollen vesicles generally 40 µm in diameter prepared from spinach chloroplasts appear to originate from thylakoids. The present study reports results obtained with individual vesicles using micromanipulative procedures. The electric potential across the membrane was measured with microelectrodes and the pH of the internal space was calculated from the fluorescence of the pH indicator pyranine. The individual vesicles photophosphorylate as measured with luciferin-luciferase. Impalement with microelectrodes did not affect the ability of individual vesicles to phosphorylate. However, there was no significant membrane potential either with continuous illumination or light flashes. In contrast, we found a ΔpH of 3.7 under photophosphorylative conditions and the incubation with the appropriate buffers blocked photophosphorylation. We propose that in these vesicles, the membrane potential plays no role in photophosphorylation, whereas a pH gradient is obligatory.

It has been recently argued that this is not likely to be the case in the native state, since in this case the electron transport can deliver H+ to microenvironments [e.g., Hong and Junge (1983) BBA 722, 197-208]. This is the conclusion that we favor at this time. In fact, ATP synthesis under conditions in which neither a ΔpH nor a membrane potential are likely, has been demonstrated by others [Ort et al (1976) BBA 449, 100-124].

T-PM-A10 A MITOCHONDRIAL DISEASE IN HUMAN SKELETAL TISSUE AND ITS REDOX THERAPY B. Chance. Biochem/Biophys, Univ. of Penna., S. Eleff, Dept. Anaesthesiology. Univ. of Penna., Phila., PA; N. Buist & N. Kennaway. Depts. Medical Genetics & Pediatrics, Oregon Health Sci. Univ. of Oregon. Portland, OR

As reported at last year's meeting (1), NMR examination of the resting states and recovery from arm exercise in the cytochrome b deficient skeletal muscles of a 16 year old patient (2) showed that the resting PCr/Pi together with the rate of recovery were significantly increased by dietary doses of menadione (vitamin K3) and ascorbate (vitamin C), a redox therapy. This year the resting PCr/Pi was still vastly improved (3.0). Withdrawal of the menadione caused significant discomfort and twice the previous dose was reinstituted. The resting PCr/P_i rose to over 5. This shift of the operating point of the resting tissue from PCr/P_i = 3.0 to over 5. suggests an increase in the rate of oxidative metabolism in the muscle in relation to the resting ATPase rate. The higher PCr/P_i value at the double dose of menadione also suggests that the pool of vitamin K3 accumulated in the mitochondrial space has also been increased. Thus, electron donors whose lipid solubility is greater and whose reaction kinetics may be faster would give improved effectiveness of the therapy. (1) Chance. B., et al Biophys. J. 44:93a (1984). (2) Eleff S. et al PNAS 81:3529-3533 (1984) and Darley-Usmar. V.M. et al PNAS 80:5103-5106 (1983). Support in part by Adv. Tech. Ctr. of Southeastern Penna.

T-PM-A11 APPLICATION OF METABOLIC CONTROL PRINCIPLES TO INSTABILITIES OF HEART AND BRAIN OXIDATIVE METABOLISM. J.S. Leigh, Jr., B. Chance, Dept. Biochem.Biophys. and S. Nioka, Dept. Physiol. Univ. of Penna., Phila., PA 19104

It is now possible to identify the transfer function for the rate of oxidative metabolism both in vitro (1) and in vivo (2). The intersection of the metabolic load (physiological ATPase) with this transfer function establishes a value of PCr/P_i, which is the "operating point" in steady state metabolism. Whilst this intersection is approx. orthogonal for high values of PCr/P_i (a lightly loaded system) the intersection becomes acute as the metabolic rate approaches its maximum ($\dot{V}_{O_2max}$) Under these conditions, a slight change will shift the metabolic operating point to very low values of PCr/Pi (< 1) which stimulates lactic acidosis. Acidosis causes inhibition of oxidative metabolism and shifts the PCr/P_i value directly through the proton linkage in that equilibrium. Under such conditions, a quasistable state may lead to an irreversible state with lactic acidosis, sodium or water entry into the cells with eventual cell disruption and infarction. This model has been applied to a variety of adult and neonate humans including exercised skeletal muscle (1), cardiac hypertropy (2), cytochrome b deficient skeletal tissue (3) and animal models of stroke and cardiac failure. It appears to be a simple model that affords predictive values since PCr/P_i values below 1 represent an unstable metabolic operating point and thus small perturbations may deteriorate the PCr/P_i value and render the metabolic state unstable and lead to acidosis ion and water movements and cell death. (1) Gyulai. L.et al. (1984) Soc.Mag.Res.p.285 (2) Whitman, G., et al (1984) J.Col. Cardiology In press (3) Eleff, S. et al (1984) PNAS 81:3529-3533. Supported in part by Grants AA 05662, HL 31934, Adv. Tech. Ctr. of SE Penna.

T-PM-A12 EFFECTS OF GROWTH HORMONE ON FATTY ACID OXIDATION. Sanda Clejan, Department of Pathology, City Hospital Center at Elmhurst and Mount Sinai School of Medicine, New York 10029

Growth hormone (GH) has been shown to influence fatty acid (FA) synthesis of polyunsaturated FA. Hormone effects on membrane fluidity were further studied by following the B-oxidation of saturated and polyunsaturated FA. The increased ratio of palmitoyl-carnitine to succinate oxidation in hypophysectomized rats (Hy) support the hypothesis that ketosis in Hy stems from rapid oxidation of saturated FA and increase partitioning of acetyl CoA into ketogenesis. In contrast, the rate of respiration in the presence of malonate for linolenoyl-, arachidonoyl-, and docosahexanoyl-carnitine were lower in mitochondria from Hy rats. Increasing the degree of unsaturation of the acyl group, produced a GH dependent stimulation of B-oxidation, most pronounced for docosahexanoyl carnitine (350 %). Mitochondria from GH-treated rats which was inhibited by uncoupling conditions, showed partial reactivation by adding ATP. GH-treatment increased the rotenone-sensitive rate of oxidation proportionally more than the rate of B-oxidation in absence of oxaloacetate. These results could be explained by a selective increase in the activity of the 2,4-enoyl-CoA reductase in GH treated rats. Thus, induction of the enzyme together with intramitochondrial NADPH produced by nicotinamide nucleotide transhydrogenase increased mitochondrial capacity for the degradation of polyunsaturated fatty acids.

T-PM-B1 MURINE POLYCLONAL ANTIBODIES TO THE FAT CELL BETA$_1$-ADRENERGIC RECEPTOR
Cary P. Moxham, Ana Cubero, Harvey Brandwein* and Craig C. Malbon. Dept. Pharmacological Sciences, School of Medicine, SUNY at Stony Brook, N.Y. 11794 and * the Genetic Diagnostic Corporation, Great Neck, N.Y. 11021.

The beta$_1$-adrenergic receptor (BAR) of rat fat cells has been purified and shown to be a single peptide of M_r= 67,000. Polyclonal antiserum has been raised in a Balb/C mouse by immunization with purified fat cell BAR. The immune serum has been shown to contain antibodies that are specific for the fat cell BAR by using two techniques. Using a microtiter plate coat assay we demonstrate that the immune serum is capable of detecting nanogram amounts of purified BAR at serum dilutions as great as 1:1000. Incubating the purified BAR with various dilutions of the immune serum decreases the detection of purified BAR on the microtiter plate in a competitive fashion. The immune serum has been shown by immunoprecipitation also to contain antibodies that are specific for the fat cell BAR. Incubation of the immune serum with radioiodinated, purified BAR and then goat anti-mouse antibody results in the immunoprecipitation of a 67,000-M_r peptide corresponding to the BAR. When incubated with fractions eluted from an affinity matrix the immune serum again specifically immunoprecipitates a 67,000-M_r peptide. The amount of the immunoprecipitated 67,000-M_r peptide correlates well with the amount of specific beta-adrenergic binding activity in each fraction. The effects of the immune serum upon BAR binding and adenylate cyclase activity will be discussed. (Supported jointly by USPHS grant AM 25410 from the NIH and by the Genetic Diagnostic Corporation.)

T-PM-B2 AFFINITY LABELING OF THE CALMODULIN BINDING COMPONENTS IN BOVINE LENS MEMBRANES.
Charles F. Louis, Ross Johnson, and Janet Turnquist. Department of Veterinary Biology, University of Minnesota, St. Paul, Minnesota 55108.

To determine the possible involvement of calmodulin + Ca^{2+} in the modulation of junctional permeability of lens fiber cells, we have utilized affinity labeling to identify whether MP26, the proposed junctional protein, can interact specifically with calmodulin. Affinity labeling of purified calf lens membranes (1 mg/ml) was performed in 20 mM HEPES buffer (pH 7.0), 0.1 mM $CaCl_2$, 10 mM $MgCl_2$, in the presence of ^{125}I-calmodulin (0.4 uM) and 0.1 mM dithiobis(succinimidylpropionate) (DSP)$_2$. Electrophoretic analysis in SDS demonstrated two major ^{125}I-containing products of Mr = 49,000 and 36,000. The size of these components was unchanged over a range of ^{125}I-calmodulin or DSP concentrations indicating that they represented 1:1 complexes between ^{125}I-calmodulin (Mr = 17,000), and Mr = 32,000 and 19,000 lens membrane components respectively. Labeling of these two components with ^{125}I-calmodulin, which was maximal in 1 μM Ca^{2+} and 10 mM $MgCl_2$, was inhibited by the calmodulin antagonist R24571. Treatment of lens membranes with chymotrypsin resulted in the cleavage of MP26 (the major lens membrane protein), with the appearance of a major proteolytic fragment of Mr = 22,000. This proteolysis was not associated with any significant change in either the size, or amount, of the two ^{125}I-calmodulin labeled membrane components. These results indicate that calmodulin interacts with two lens membrane components, but not significantly with MP26, in the intact lens cell membrane. Our results indicate the need to maintain caution in interpreting direct Ca^{2+} + calmodulin effects on MP26 and lens cell junctions. (Supported in part by the Graduate School of the University of Minnesota, and NIH grant EY05011).

T-PM-B3 ANTIGEN MOLECULAR STRUCTURE IS A PRIMARY CONTROLLING FACTOR IN THE REGULATION OF THE IMMUNE RESPONSE. Howard M. Dintzis, Marjorie H. Middleton and Renee Z. Dintzis, Dept. of Biophysics and Dept. of Cell Biology and Anatomy, Johns Hopkins Medical School, Baltimore, Maryland 21205.

We have previously shown for linear polyacrylamide molecules substituted with dinitrophenyl (Dnp) haptens that molecules above a certain size (Molecular weight >100,000) and substituted with more than a threshold number of haptens (20) are immunogenic (i.e. represent positive signals) in whole animals and in cell cultures. Conversely, molecules of smaller size and/or lower degree of hapten substitution can be suppressive of immune responses (i.e. represent negative signals). These findings have been interpreted in terms of B cell membrane receptor aggregation as a result of binding to multivalent antigen molecules (the immunon theory). Studies have now been extended to a series of different polymer molecules, both natural and synthetic, each containing repeating identical haptens or epitopes. The results imply that the primary control of immune response may be associated with the molecular state of the antigenic material. The array size and geometry of haptens or epitopes exposed to the cell membrane surface are determined by the molecular scaffold to which the haptens or epitopes are attached. In brief, large molecules with dense arrays of haptens or epitopes can form B cell surface receptor aggregates of sufficient size and density to stimulate the immune response, while small molecules with dense arrays are competitive inhibitors and suppressive of immune response. The relative concentrations of these two types of molecule will determine whether or not a positive immunogenic signal will be generated.

T-PM-B4 MACROPHAGE CELL SURFACE SULFHYDRYL GROUPS ARE ASSOCIATED WITH ENDOCYTOSIS BUT NOT RECOGNITION OF IMMUNE COMPLEXES. William Dereski and Howard R. Petty, Department of Biological Sciences, Wayne State University, Detroit, MI 48202.

We have previously described a fluorescein- and lactoperoxidase-conjugated ferritin-antiferritin immune complex (Biophys. J. 45:268a). Two lines of evidence indicate that cell surface SH groups play a central role in triggering endocytosis of immune complexes (IC). The membrane impermeable reagents 5,5'-dithiobis (nitrobenzoic acid), DTNB, and p-chloromercuribenzene sulphonic acid (PCMBSA) inhibit IC endocytosis, but not binding. This has been determined using crystal violet to quench bound but for internalized fluorescent IC. For DTNB, half-maximal inhibition is obtained at 20 pM DTNB. Dose-response studies indicate that complete inhibition is found at $\simeq 10^3$ molecules/cell and half-maximal at $\simeq 10^4$ molecules/cell. This is likely due to a direct effect upon the cell since pretreated cells demonstrate similar inhibition and pre-treated IC are endocytosed. Analysis of ^{14}C-DTNB labeled surface proteins show two molecules of 50K and 72K by SDS-PAGE. Local ^{125}I-labeling experiments (see ref. above) show a 2-mercaptoethanol sensitive polymerization of certain surface proteins during IC treatment, including the DTNB binding proteins listed above. We speculate that an integral feature of the zipper mechanism of antibody-dependent endocytosis is a covalent reaction involving SH groups. This may involve covalent receptor-receptor and/or receptor-ligand interactions. [Supported by a grant from the NIH AI19075.]

T-PM-B5 EFFECTS OF CATION GRADIENTS ON IMMUNE COMPLEX-STIMULATED HUMAN NEUTROPHILS, F.W. Luscinskas*, D.E.Mark*, F.J.Lionetti*, E.J. Cragoe*# and E.R.Simons, Dept of Biochem. Boston Univ. Sch. of Medicine, Boston, MA 02118 and #Merck, Sharp and Dohme Inc., West Point, PA

Neutrophils are activated by specific particulate or soluble stimuli. Other cells' (e.g. platelets') responses are regulated by changes in transmembrane cation gradients. We have examined the role of Na^+ and K^+ gradients in human neutrophils by varying these ions' extracellular concentrations and measuring immune complex-induced membrane potential changes, respiratory burst (O_2^-) initiation, and degranulation. If Na^+_{out} is replaced by K^+, the rate of stimulus-induced depolarization decreases linearly with respect to increased K^+_{out}; if it is replaced by choline, however, the rate of depolarization increases until 75% of the Na^+_{out} is replaced, and then decreases. A fast-acting amiloride analogue, blocking passive Na^+ channels, blocks only 55% of the depolarization in physiological buffers, in contrast to platelets in which 100% is blocked; when Na^+ is replaced by K^+, the effect of amiloride decreases with decreasing Na^+_{out}, but it remains at the same levels when choline is substituted for Na^+ until 75% of the Na^+ has been replaced. In contrast, O_2^- production is enhanced in low Na^+_{out}, doubling when it is totally replaced by either cation. Azurophilic granule release is similarly increased but secretion of secondary granule contents is unaffected. All of these effects exhibit dependence on the dose of immune complex utilized. Thus extracellular Na^+ is not required for these steps in the neutrophil's response to immune complex stimulation.

T-PM-B6 GENETIC ANALYSIS OF HALOBACTERIAL PHOTOTAXIS. Steven A. Sundberg and John L. Spudich, Department of Anatomy and Department of Physiology and Biophysics, Albert Einstein College of Medicine, Bronx, New York 10461.

Halobacteria modulate their swimming behavior in response to changes in light intensity. The wavelength-dependent behavioral responses (phototaxis) are retinal-dependent. In order to facilitate genetic analysis of the phototaxis pathway, we have developed a selection procedure for isolating phototaxis-deficient (pho^-) mutants of Halobacterium halobium. Our strategy has been to make use of a flashing repellent light to induce frequent reversals by responsive cells, thereby impeding their migration along a small capillary and resulting in a spatial separation of the mutagenized parent population and a fully-motile population enriched for pho^- cells.

Seventy-two mutants, obtained from five independent selections, have been classified according to three criteria: their inability to respond to a repellent blue light stimulus (pho^-), their ability to form chemotactic rings on soft agar plates (che^+), and their ability to make use of exogenous retinal in restoring photosensitivity (ret^-). Most of the cells obtained are general sensory transduction mutants as indicated by their pho^-che^- phenotype. We have also obtained several mutants with altered retinal-synthesis properties ($pho^-che^+ret^-$) which differ from those of previously isolated strains such as Flx3R, as well as a possible receptor mutant ($pho^-che^+ret^+$). Behavioral, biochemical, and spectroscopic studies of the pho^- strains are being carried out with the intent of elucidating the photosensory transduction mechanism.

T-PM-B7 SOLUBILIZATION AND ENRICHMENT OF THE SENSORY RHODOPSIN (SR) FROM HALOBACTERIUM HALOBIUM MEMBRANES. Danny Manor[a], Elena N. Spudich[a], and John L. Spudich[a,b], [a]Department of Anatomy and [b]Department of Physiology and Biophysics, Albert Einstein College of Medicine, Bronx, NY 10461

A variety of detergents which are effective in solubilizing the retinal pigments BR and HR while maintaining their visible absorption cause rapid destruction of SR color. Using the zwitterionic detergent CHAPS, we have developed conditions for solubilizing SR in a stable form from the membrane while maintaining its native chromophore absorption. Membranes are prepared by the sonication method or by dialysis against 100mM NaCl followed by ultracentrifugation to obtain an enriched membrane fraction, as described for HR purification (Taylor et al. PNAS USA 80: 6172, 1984; Steiner and Oesterhelt, EMBO J. 2:1379, 1984). SR is solubilized from the membrane by 10mM CHAPS, 10mM HEPES, pH 7.0 and the chromophore is maintained in a stable form (at least 2 weeks) both in high (4 M) and low (0.1 M) NaCl, and has essentially the same absorption spectrum as in the membrane. Properties of CHAPS-solubilized SR (e.g. pH effects on absorption, kinetics of pigment formation by addition of retinal to the solubilized apoprotein) are similar to those of membrane-integrated SR. Chromatography on Sephacryl S-300 in low NaCl yields c. 2.3-fold enriched preparation.

BR = bacteriorhodopsin; HR = halorhodopsin; SR = slow-cycling rhodopsin-like pigment.

T-PM-B8 BIOCHEMICAL AND PHYSIOLOGICAL EVIDENCE FOR THE INVOLVEMENT OF INOSITOL 1,4,5-TRISPHOSPHATE IN VISUAL TRANSDUCTION. E. Szuts, M. Reid, R. Payne, D.W. Corson and A. Fein, Marine Biological Laboratory, Woods Hole, MA.

Intracellular pressure injection of inositol 1,4,5-trisphosphate ($InsP_3$) results in excitation and adaptation of Limulus ventral photoreceptors (Fein et al., 1984, Nature 311:157). These effects of $InsP_3$ appear to result from a rise in intracellular calcium (Ca_i) since: 1) An $InsP_3$-induced rise in Ca_i can be detected with aequorin, 2) injection of the calcium buffer EGTA blocks $InsP_3$ -induced excitation and adaptation, 3) pressure injection of calcium induced excitation and adaptation. If $InsP_3$ is involved in excitation and adaptation in microvillar photoreceptors, one would expect to see a rapid light-induced rise in $InsP_3$. To test for this, isolated squid eyecups were incubated with [^{3}H]inositol for two hours in the dark (oxygenated saline at 10°C). Chemical reactions were stopped by plunging the eyecup into ice-cold 15% trichloroacetic acid, either without exposure to light or immediately (~1s) after illumination by a strobe flash. Inositol phosphates in the aqueous phase were separated by column chromatography. The amount of [^{3}H]$InsP_3$ in an eye was expressed as a percent of the total [^{3}H]inositol phosphates. For four experiments the light/dark ratio of $InsP_3$ was 3.4 ± 1.6 (mean ± s.d.). These findings suggest that the light-induced elevation in $InsP_3$ may be rapid enough to be involved in visual transduction.

T-PM-B9 GABA RECEPTOR CHANNELS IN ADRENAL CHROMAFFIN CELLS. J. Bormann and D. Clapham*, Max-Planck-Institut für biophysikalische Chemie , Göttingen, W. Germany /*Present address: Cardiovascular Division, Brigham & Women's Hospital, Boston, MA 02115 USA.

Recently Kataoka et al (PNAS 81:3218) reported high-affinity binding sites for the GABA (gamma-aminobutyric acid) receptor agonist muscimol in adrenal chromaffin cells, indicating the presence of GABA receptors in this area of the peripheral nervous system. Using patch-clamp techniques on cultured single bovine adrenal chromaffin cells, we found GABA-activated chloride channels similar in their properties to GABA receptor channels in the central nervous system. The GABA-activated channels are chloride-selective, blocked by the GABA antagonist bicuculline, potentiated by benzodiazepines, and reversibly desensitize at high concentrations.

In whole-cell recordings we found the chloride substitution by isethionate shifted the reversal potential in accord with the Nernst relation. In symmetrical 145mM Cl, the dose-response curve to GABA had a slope of 2 on a Hill plot, indicating a bimolecular binding of GABA to the receptor. Desensitization followed a biexponential delay (τ_1=2.8s,τ_2=20.8s; 20μM GABA). Recovery from desensitization followed a single exponential time course (τ=23s). Bicuculline (5-25μM) decreased while diazepam (10μM) doubled the net whole-cell Cl current induced by GABA.

Single channel measurements from outside-out patches showed a main conductance state of 46pS and subconductance states of 30, 18 and 12pS, closely corresponding to GABA-activated Cl^- channels in spinal cord neurons. Glycine had no effect on our channels. A model of the gating properties of the GABA-activated chloride channels in chromaffin cells is presented. Supported by the Deutsche Forschungsgemeinschaft and an award from the North Atlantic Treaty Organization (NATO).

T-PM-B10 MECHANO-RECEPTOR ION CHANNELS ARE NOT NICOTINIC. F. Guharay & F. Sachs, Department of Biophysics, SUNY, Buffalo, N.Y. 14214.

There is an ion channel in the membrane of tissue-cultured chick skeletal muscle which is activated by membrane stretch (Guharay & Sachs, J. Physiol. 352:885, 1984). This stretch-activated (SA) channel has a conductance of 35 pS and a reversal potential of -30 mV in normal saline. The dominant nicotinic channel in this preparation also has a conductance of 35 pS but the reversal potential is 0 mV. Since the two conductances were similar, we examined the possibility that the SA channels were a form of nicotinic channel. The two channels are completely distinct based upon the following evidence:

1) Nicotinic channels activated by suberyldicholine are insensitive to membrane tension.
2) α-bungarotoxin blocks nicotinic activity but has no effect on SA channels.
3) Desensitizing doses of suberyldicholine eliminate nicotinic activity but have no effect on SA channel activation.
4) The difference in reversal potential between the two types of channels is maintained when the extracellular solution is changed to isotonic CsCl.
5) Changes in extracellular pH have no effect on SA channel conductance, but have a large effect on nicotinic channel conductance (Goldberg & Lass, J. Physiol. 343:349, 1983).
6) The probability of the SA channel being open increases while the probability of the nicotinic channel being open channel decreases with depolarization.

Supported by NINCDS-13194

T-PM-B11 CELL DENSITY DEPENDENT CHANGES IN THE LATERAL DIFFUSION OF MHC MOLECULES. Marjorie L. Wier and Michael Edidin, Department of Biology, Johns Hopkins University, Baltimore, MD 21218.

We have used the fluorescence recovery after photobleaching (FRAP) technique to study the effects of cell density on the translational motions of Class I major histocompatibility (MHC) antigens in the plasma membranes of cultured fibroblasts. The lateral diffusion of MHC molecules was decreased in cells cultured at high cell density. The most pronounced change was an increase in the proportion of cells which showed no recovery. In confluent cultures 20-50% of the cells exhibited only immobile receptors, while in sparse cultures >90% of the cells typcially showed some recovery. In addition, cells with mobile receptors from dense cultures showed a decrease (from 8.3 x 10-10 to 4.5 x 10-10 cm2/sec) in the diffusion coefficient of the mobile receptors. In nonconfluent cultures, both the diffusion coefficent and the mobile fraction were decreased as the number of cell-cell contacts increased. In contrast to the changes in lateral diffusion of MHC antigens, the diffusion of a lipid soluble fluorescent dye, DiI-C16, was not affected by cell density. In preliminary experiments, cells plated at low cell density on extracellular matrix produced by confluent cells showed decreased mobile fractions with little change in diffusion coefficient. These results suggest that cell-cell contact can induce changes in the translational mobility of specific membrane proteins. The mechanisms by which these changes are induced are currently under investigation.

T-PM-C1 MONTE CARLO STUDIES OF LIPID WATER INTERFACES. H. L. Scott Jr. Dept. of Physics, Oklahoma State University, Stillwater, Oklahoma 74078.

The results of a series of numerical simulations of the aqueous interface near several types of lipid bilayer headgroups are presented. The Monte Carlo method was used to study 172 water molecules located between two lipid bilayers separated by 24.5 A. The types of headgroups used in the studies include phosphorylcholine, ethanolamine, and serine. The quantities calculated were molecular density, dipolar orientation, and number of hydrogen bonds as functions of the distance from the interfacial regions. The data point out important differences in the organization of the interfacial water for each of the three different lipids.

T-PM-C2 DEPTH OF WATER PENETRATION INTO PHOSPHOLIPID BILAYERS. T.J. McIntosh and S.A. Simon, Departments of Anatomy and Physiology, Duke University Medical Center, Durham, N.C. 27710.

The depth to which water penetrates phospholipid bilayers has been determined by combining x-ray diffraction data from multilamellar liposomes and specific capacitance data from single planar bilayers of the same lipid composition. As measured from the phospholipid head group, water penetrates into the bilayer a distance $dw = \frac{1}{2}(d_b - d_e)$, where d_b is the bilayer thickness obtained from x-ray diffraction and d_e is the thickness of the low dielectric constant region of the bilayer obtained by capacitance measurements. We have previously found (Science 216, 65-67) that dw is about 2.5Å larger for bacterial phosphatidylethanolamine (BPE) bilayers than for 1:1 BPE:cholesterol bilayers, which implies that cholesterol displaces the deepest water molecules in the bilayer from near the lipid carbonyl groups. To directly test this conclusion we have measured the thickness of the water layer in fully hydrated BPE and BPE:cholesterol bilayers by the use of neutron diffraction and H_2O/D_2O exchange. The neutron results are in agreement with the x-ray data and show that the thickness of the bulk water layers between adjacent bilayers are virtually unchanged by cholesterol. However, the water profiles obtained by neutron diffraction do not detect the removal of the one or two water molecules per phospholipid which reside in the carbonyl region of the bilayer. On the other hand, the capacitance measurements appear to be extremely sensitive to these deepest water molecules since they determine the position of the electrical potential drop across the bilayer. Thus, capacitance experiments, when combined with x-ray or neutron diffraction measurements of d_b, can provide a precise localization of the water/hydrocarbon interface.

T-PM-C3 COMPUTER GRAPHICS REPRESENTATION OF THE CRYSTAL STRUCTURE OF THE DIMYRISTOYL PHOSPHATIDYLCHOLINE BILAYER. Bruce P. Gaber and Ronald M. Brown, Bio/Molecular Engineering Branch and ENEWS Program, Codes 6190 and 5707.4, Naval Research Laboratory, Washington, DC 20375-5000

The first computer graphics representations of a phospholipid bilayer are shown. Using the coordinates and crystal symmetry of 1,2-dimyristoyl-sn-glycero-3-phosphorylcholine (DMPC) (R. H. Pearson and I. Pascher, Nature, (1979) 28: 499-501) as input data, we have generated high resolution space-filling images of a section of bilayer containing 36 DMPC molecules in each of the "upper" and "lower" monolayers. The Pascal code we have written permits rotation, translation, and scaling of either the entire bilayer or individual molecules. Stereo pairs may be generated for 3-D viewing of the image. Continuous shading and suppression of hidden surfaces assist in spatial cueing in the model. The images were realized on a VAX 11-780 and post-processed on a Dicomed D148C Color Graphic Computer to produce color photographs at a resolution of 4000 x 4000 pixels. (The authors gratefully acknowledge Dr. Robert H. Pearson for providing the atomic coordinates for the two DMPC molecules of the asymmetric unit and Dr. Janet L. Smith for assistance in establishing the bilayer model from the primary data.)

T-PM-C4 STRUCTURE AND THERMOTROPIC PROPERTIES OF MIXED CHAIN 1-STEAROYL-2-MYRISTOYL-PHOSPHATIDYLCHOLINE (SMPC) AND 1-MYRISTOYL-2-STEAROYL-PHOSPHATIDYLCHOLINE (MSPC) BILAYER MEMBRANES. J. Mattai and G.G. Shipley. Biophysics Institute, Boston Univ. Schl. Med., Boston, MA.

X-ray diffraction and differential scanning calorimetry have been used to investigate the structure and thermotropic properties of hydrated mixed chain SMPC and MSPC. After prolonged storage at -3°C, SMPC exhibits two transitions at 18.8°C (ΔH = 0.9 Kcal/mol) and 33.2°C (ΔH = 6.3 Kcal /mol) while MSPC undergoes two transitions at higher temperatures, 22°C (ΔH = 2.8 Kcal/mol) and 37.2°C (ΔH = 8.1 Kcal/mol). While the high temperature transitions for both SMPC and MSPC show reversible behavior, the enthalpy of the lower temperature transition is gradually recovered with increasing incubation time at low temperatures.

Below the low temperature transition, x-ray diffraction of SMPC shows a characteristic L_{β}' bilayer gel phase with tilted hydrocarbon chains (d = 64.4Å). Between the two transitions is the rippled gel phase, P_{β}', with hexagonal chain packing (d = 71.6Å; ripple periodicity ∿ 120Å). Above the high temperature transition is the liquid crystalline bilayer phase, L_{α} (d = 68.4Å) with melted chains. These structural changes are reversible on cooling. In contrast, MSPC at low temperatures show a crystalline bilayer L_c phase (d = 61.7Å) with an ordered hydrocarbon chain packing mode characterized by multiple wide angle reflections. On heating, this phase converts to the P_{β}' phase (d = 71.0Å, ripple periodicity ∿ 118Å) which on further heating gives rise to the L_{α} phase (d = 66.6Å). On cooling, the L_{α} phase reverts to P_{β}' and then to a different bilayer gel phase which exhibits a time and temperature dependent conversion to the L_c phase. The more pronounced asymmetry of the hydrocarbon chains of SMPC, attributed partly to the conformation of the sn-2 acyl chain at the glycerol backbone, does not allow for the formation of the crystalline L_c phase.

T-PM-C5 STRUCTURAL PROPERTIES OF 1,3-DIPAMITOYL-GLYCERO-2-PHOSPHOCHOLINE(β-DPPC) BILAYERS: A RAMAN SPECTROSCOPIC STUDY. J. P. Sheridan, Naval Research Laboratory, Bio/Molecular Engineering Branch, Code 6507/6190, Washington, DC 20375-5000

The changes in structure which accompany the endothermic phase transitions of fully hydrated dispersions of β-DPPC have been monitored by Raman spectroscopy. Multibilayer preparations of β-DPPC, incubated near 0°C, yield Raman data which are indicative of a highly ordered "crystalline-like" bilayer structure: (1) The skeletal/optical (SOM) and acoustical regions of the spectrum strongly suggest the presence of fully extended all-trans acyl chains; (2) the relative intensity of the symmetric and antisymmetric CH stretching modes is close to that for a crystalline hydrocarbon; (3) the CH_2 bending spectrum is consistent with an orthorhombic-type sub-cell, and (4) the presence of a doublet in the carbonyl stretching region suggests partial dehydration at the head-group. Crossing the low temperature transition (LTT) at 27°C yields a phase which appears to be hexagonal and possesses a somewhat more disorder and looser packing as reflected by the SOM, CH stretching and bending modes. In addition, changes in the carbonyl bands indicate an increase in hydration. Finally, upon crossing the high temperature transition (HTT) at 37°C, "melting" of the acyl chains occurs and a fluid-like phase is obtained which is qualitatively similar to that observed for d-DPPC at 45°C. Upon cooling, the HTT is reversible while the LTT is not. Cooling to 10°C results in fairly rapid recrystallization of the chains, but equilibration to the close-packed, low-hydration structure occurs via a rather complicated kinetic pathway and on a much slower time scale.

T-PM-C6 SUB-MICROSCOPIC IRREGULARITIES (RIPPLES?) IN GIANT DMPC VESICLE BILAYERS BELOW THE ACYL CHAIN CRYSTALLIZATION TEMPERATURE DEPEND ON THE VESICLE STRESS-HISTORY. D. Needham, E. Evans, Pathology, Univ. of British Columbia, Vancouver, B.C. V6T 1W5

Micropipet aspiration of giant (2×10^{-3} cm diameter) dimyristoylphosphatidylcholine (DMPC) bilayer vesicles was used to regulate membrane tension levels and to provide sensitive detection of vesicle surface area changes (0.1% area). It was observed that cooling giant DMPC vesicles from above T_m (24°C) to temperatures in a range from 5° - 23°C resulted in vesicle rupture at the transition which resealed and left the vesicle in a distorted shape. At the final temperature, application of small pipet suction pressure produced membrane tensions (0.1 dyn/cm) sufficient to force the vesicle into a smooth spherical shape. Two different tests were then performed: (1) The vesicle was heated to above T_m and the increase in relative area was observed (typically 20% for this experiment). The vesicle was then refrozen but exhibited only about an 11% decrease in area for the transition. (2) The other test was to stress the spherical vesicle at the low temperature by application of large pipet suction. The vesicle area versus membrane tension was essentially elastic up to a threshold tension (1 dyn/cm) beyond which the vesicle area increased steadily (over 5 minutes or more) until it had expanded about 8-9% where it stopped. Further increase in membrane tension up to the breaking point (6 dyn/cm) produced miniscule area changes that were perfectly elastic. Subsequent reduction of the pressure to zero left the vesicle permanently deformed. Finally, heating this vesicle to above T_m exhibited an 11% increase in area followed by the same value on refreezing. In summary, it was apparent that initial vesicle freezing which involved rupture was accompanied by formation of sub-microscopic surface irregularities and that these irregularities were pulled out slowly at large tensions after which they did not reappear.

T-PM-C7 CROSS-RELAXATION PATHWAYS IN PHOSPHOLIPID VESICLES AS REVEALED BY TWO-DIMENSIONAL ^1H NMR. David S. Cafiso, Department of Chemistry, University of Virginia, Charlottesville, Virginia 22901.

For small molecules, the measurement of nuclear overhauser effects (NOEs) provides a measure of magnetization transfer between nuclei which can yield information on internuclear distances and conformation. In membrane systems, the measurement of proton NOEs has not been widely utilized because of strong zero-quantum exchange processes. In this case the dominance of these energy conserving transitions results in a diffusion of magnetization and a loss of spacial information normally provided by the steady-state NOE experiment. In membrane vesicle systems, the build-up rates of cross-peaks in two-dimensional cross-relaxation spectra can be used to recover this spacial information. Spin-diffusion is clearly indicated in these 2D membrane vesicle spectra and occurs over limited distances and within limited domains of the vesicle bilayer. The extent and pattern of cross-relaxation varies as a function of the type and state of the lipid. Because of the limited spin-diffusion in these systems, the development of cross-relaxation between nuclei at early mixing times can be taken as a strong indication of proximity between nuclei. Cross-relaxation between the hydrophobic ion tetraphenylborate and the lipid resonances of egg phosphatidylcholine vesicles has been measured and indicates that intermolecular dipole exchange is possible in these systems. Furthermore, the development of cross-peaks from this magnetization exchange can be used to locate this ligand within the lipid matrix. Thus, 2D cross-relaxation spectroscopy can provide a means to localize ligands in small membrane vesicle systems.
(This work was supported by the Camille and Henry Dreyfus Foundation and NSF grant BNS-83-02840.)

T-PM-C8 KINETICS OF MEMBRANE VOLUME FLUCTUATIONS, Michael L. Johnson, William van Osdol, Susan G. Frasier and Rodney L. Biltonen, University of Virginia, Charlottesville, VA. 22908.

We have recently developed a novel volume perturbation calorimeter which we are using to study the dynamics of model membrane system. Our volume perturbation calorimeter functions by forcing a suspension of membranes to undergo a bidirectional adiabatic volume change and then monitors the relaxation of the chemical processes to their new equilibrium position. The relaxation is currently monitored by observing the decay of the pressure and temperature of the solution. These thermodynamic variables can then be related to temperature and frequency dependence of the thermal expansivity, adiabatic and isothermal compressibility, and density fluctuations of the membrane. The kinetic data from this instrument is used in conjunction with thermodynamic data obtained by differential scanning calorimetry to study the dynamics of membrane processes.

Initially the project has concentrated on a study of the dynamics of the main phase transitions in single and multi lamellar vesicles of pure phospholipids. The object being to develop an understanding of how the individual constituent parts of a phospholipid molecule contribute to the overall dynamics of the artifical membranes. These preliminary studies will be used as a framework for the interpretation of the results which we plan to obtain on more complex vesicles with mixtures of phospholipids and non-phospholipid constituents such as cholesterol, anesthetics and proteins (such as bovine rhodopsin).

The kinetic calorimeter will be described as well as examples of the results which we are obtaining.

T-PM-C9 THE CHEMICAL SHIELDING TENSORS OF THE CARBON-13 CARBONYL GROUPS IN PHOSPHOLIPIDS. Bruce Cornell, Commonwealth Scientific and Industrial Research Organisation, Australia, P.O.Box 52 North Ryde N.S.W. 2113, Australia.

A Quantitative interpretation of the chemical shift anisotropy obtained from solid state carbon-13 NMR spectra requires a knowledge of both the magnitude and orientation of the relevent chemical shielding tensor. In this presentation a study of the shielding tensors for the carbonyl groups in dimethyl oxalate and dimethyl succinate will be reported and compared with previously reported data obtained from oxalic acid (1) and dimethyl oxalate (2). These data will be used as the basis for an interpretation of the carbonyl group chemical shift anisotropy obtained from phospholipids in model and biological membranes. (3,4,5)

1. R.G. Griffin, A.Pines, S. Pausak and J.S. Waugh 1975. J. Chem. Phys. 63 1267-1271.
2. A. Pines and E. Abramson 1974. J. Chem. Phys. 60 5130-5131.
3. R.J. Wittebort, C.F. Schmidt and R.G. Griffin 1981 Biochemistry 20 4223-4228.
4. B.A. Cornell 1980 Chem. Phys. Lett. 72 462-465.
5. B.A. Cornell 1981 Chem. Phys. Lipids 28 69-78.

T-PM-C10 DESTABILIZATION OF PLANAR LIPID BILAYERS BY ALPHA PARTICLES FROM POLONIUM-210 Gene A. Nelson, Technicon Instruments Inc., Tarrytown, NY

A system for measuring the interaction between alpha particles from a Polonium-210 source on a micrometer advance and planar lipid bilayers is described. Membrane capacitance, which was used to determine thinning, and conductance were simultaneously measured with a voltage clamp. Data consisted of measurements of the conductance of the planar membrane while advancing or withdrawing the Polonium-210 source from the bilayer.

Conductance records showed an abrupt failure of the bilayer when the source was approximately 30 microns or less from the bilayer. Comparisons of conductance noise characteristics just prior to membrane breakage and noise characteristics with a source - bilayer separation of 50 microns or greater showed no difference. The openning and closing of channels was not observed within the system bandwidth.

The range of the alpha particles inferred from observations of membrane failure is consistent with the expected maximum range of approximately 35 microns for alpha particles from the particular gold-covered source in water. Evidence from the addition of aqueous phase free radical scavengers supports the hypothesis that free radicals generated in the bilayer, as opposed to aqueous phase free radicals, are the most important agent for bilayer destabilization.

T-PM-C11 CHARGE-REVERSAL STUDIES OF PHOSPHATIDYLSERINE MEMBRANES.
Joel A. Cohen, Dept. of Physiology, University of the Pacific, San Francisco, CA 94115.

Particle electrophoresis has been used to determine the concentrations of divalent cations that exactly neutralize the negative surface charge of multilamellar PS vesicles in the presence of various monovalent salts. The null condition of zero electrophoretic mobility and of charge neutrality is subject to particularly unambiguous theoretical interpretation. Since neither hydrodynamic nor interfacial-electrostatic analysis is needed, uncertainties related to the position of the shear surface and to the assumptions of diffuse-double-layer theory become irrelevant. The aqueous concentrations of monovalent cations (M) and divalent cations (D) at the membrane surface are equal to their bulk values. The value of [D] that produces neutrality or charge reversal of the membrane is called $[D]_{rev}$. Since the bound charge density is comprised of both M and D, the [M] dependence of $[D]_{rev}$ yields direct information on M vs. D competition for PS binding sites. $[Ca]_{rev}$ was determined by measurment of PS electrophoretic mobilities (or zeta potentials) at 25, 50, and 150 mM $CaCl_2$. In the former two cases the mobilities are negative and in the latter positive. A quadratic fit of zeta vs. log [Ca] gives the value of [Ca] at which zeta crosses zero. Careful error analysis yields values of $[Ca]_{rev}$ with standard errors of several mM. Preliminary data show $[Ca]_{rev}$ = 82±2 mM in 0.1 M NaCl and 92±4 mM in 0.2 M NaCl. Na vs. Ca competition for PS binding sites predicts that $[Ca]_{rev}$ be independent of [Na], whereas lack of competition predicts that $[Ca]_{rev}$ decrease with increasing [Na]. The experimental result is inconsistent with both of these possibilities. The data suggest that a new phenomenon, such as anion binding to the neutralized PS membrane, must be considered.

T-PM-C12 QUANTITATIVE DETERMINATION OF THE NUMBER OF LAMELLAE IN GIANT LIPOSOMES USING FLUORESCENT MICROSCOPY Mark N. Melkerson and John J. McGrath, Mechanical Engineering Department, Michigan State University, East Lansing, Michigan 48824

A technique has been developed to quantify the number of lamellae in giant liposome membranes on a light microscope. This fluorescent technique allows for the selection of single bilayer lipid vesicles "in situ" prior to their use in the quantitative determination of such membrane characteristics as passive transport properties, thermomechanical properties and phase transition behavior.

Fluorochromes were excited using an argon laser in a highly attenuated photobleaching configuration. Bilayer lipid membranes (BLMs) were formed from a mixture of egg phosphatidylcholine (EPC) and cholesterol doped at a molar ratio of 1:1000 with dil-C18(3) (1,1'-dioctadecyl - 3,3,3',3'-tetramethyl-indocarbocyanine). The BLM was observed to thin to blackness (assumed to be a single bilayer; H.T. Tien, BLM: THEORY AND PRACTICE, 1974) in a BLM forming chamber which also contained 10μm diameter fluorescent polystyrene microspheres (Duke Scientific).

The microscope using epi-illumination and 400X magnification focused the laser beam to a diameter of approximately 1μm as limited by diffraction. The laser beam was used to excite a small spot on the single bilayer BLM and on the fluorescent microspheres. Absolute fluorescent intensities were measured photometrically after passing the emitted light through a 0.1μm diaphragm. The intensity of the BLM fluorescence was normalized with respect to that of the fluorescent microspheres.

Giant liposomes were formed from a mixture of egg phosphatidylcholine (EPC) and cholesterol doped at a molar ratio of 1:1000 with dil-C18(3). Fluorescent microspheres were added to or adjacent to the liposome sample and fluorescent intensities of the liposome membranes were normalized with respect to that of the microspheres.

The normalized intensities of the liposomes that were collected showed a distinct band of lower intensity readings. The distribution of this lower band of intensities was found not to be statistically different than the normalized BLM distribution, providing an "unilamellar intensity distribution." Thus all future "in situ" measurements similarly normalized within two standard deviations of the mean intensity of the "unilamellar distribution" (95% confidence level) can be considered unilamellar liposomes.

T-PM-D1 MOLECULAR DYNAMICS SIMULATION OF THE PHOTODISSOCIATION OF CARBON MONOXIDE FROM HEMOGLOBIN. Eric R. Henry and William A. Eaton, Laboratory of Chemical Physics, NIADDK, NIH, Bethesda, MD 20205, and Michael Levitt, Department of Chemical Physics, Weizmann Institute of Science, Rehovot Israel.

We have used the technique of molecular dynamics to simulate the photodissociation of carbon monoxide from the alpha subunit of hemoglobin. Equilibrated trajectories of the liganded molecule were generated at room temperature by applying continuous small random momentum increments to all the atoms to increase the average kinetic energy of the molecule. The photodissociation event was simulated by interrupting such a trajectory, deleting the iron-ligand bond from the potential function, and changing the heme potential function to produce the equilibrium deoxyheme conformation. Heme potentials were chosen to reproduce the out-of-plane energies and forces on the iron atom from quantum mechanical calculations. Photodissociation of the ligand from a free heme complex in vacuum was also simulated to assess the effect of the protein on the subsequent heme conformational change. The half-time for the displacement of the iron atom from the porphyrin plane was between 50 and 150 femtoseconds for both the protein and the free heme complexes. These results support the interpretation of optical absorption studies (Martin, et al., Proc. Nat. Acad. Sci. 80, 173 (1983)) that the iron is displaced from the porphyrin plane within 350 femtoseconds in both hemoglobin and a free heme complex in solution. These trajectories are being analyzed to identify possible conformational changes of the surrounding protein in response to photodissociation of ligands.

T-PM-D2 COMPUTER SIMULATIONS OF PROTEIN DYNAMICS: THEORY AND EXPERIMENT, Ronald M. Levy, Department of Chemistry, Rutgers University, New Brunswick, New Jersey 08903

The use of computer simulations to study the internal dynamics of globular proteins has attracted a great deal of attention in recent years. These simulations constitute the most detailed theoretical approach available for studying internal motions and structural flexibility of proteins. Ultimately, the extent to which the simulations reproduce the properties of molecular systems for which they are models, depends on the required precision of the potential functions used to describe the atomic and molecular interactions. Since the potential functions for proteins necessarily involve many approximations, it is essential that there be a continuing effort to develop procedures for comparing the results of simulations with a wide variety of experimental measurements. Recent work concerned with the use of computer simulations for the interpretation of, and comparison with NMR and x-ray diffraction experiments will be reviewed. Future directions, including the combined use of classical and quantum simulations for studying vibrational spectroscopic properties of proteins will also be discussed. The examples will be drawn from molecular dynamics studies of myoglobin and turkey ovomucoid third domain.

T-PM-D3 AMIDE PROTON EXCHANGE IN REDUCED AND OXIDIZED CYTOCHROME C BY TWO-DIMENSIONAL NMR. A.J. Wand, H. Roder, S.Altman and S.W. Englander. Department of Biochemistry and Biophysics, University of Pennsylvania School of Medicine, Philadelphia, PA 19104.

Solvent exchange rates for numerous individually assigned protons in cytochrome c (horse heart) were measured by two-dimensional correlated ^{1}H-NMR spectroscopy (COSY). Buffered ^2H_2O solutions of oxidized and reduced cytochrome c at p^{2}H 7 were kept at 20^{o}C for time periods up to 30 days. COSY spectra were recorded at p^{2}H 5 where exchange is relatively slow. The time course of exchange for individual amide protons was obtained from the intensity of the NH-C_αH cross-peaks as a function of exchange time. The most slowly exchanging amide protons were studied by one-dimensional ^{1}H-NMR spectroscopy. The NH exchange results provide detailed structural and dynamic information, and in addition indicate which parts of the protein structure are energetically sensitive to the redox state.

T-PM-D4 MAPPING STRUCTURAL PERTURBATIONS IN E. COLI ASPARTATE TRANSCARBAMYLASE BY MEDIUM RESOLUTION HYDROGEN EXCHANGE. D. S. Burz and N. M. Allewell, Wesleyan University, Middletown CT 06457.

Medium resolution hydrogen exchange has been used to identify regions of the regulatory subunit (r_2) perturbed by binding of nucleotide effectors, CTP and ATP. Following Rosa and Richards (1979) and Englander et al. (1983), exchange curves for segments of the native protein have been derived by digesting the protein with pepsin at various times during exchange out, separating the resulting peptides by HPLC and determining the radioactivity associated with each peak. Digestion and separation were performed under conditions where exchange is largely quenched and corrections were made for exchange during analysis. Peptides were identified from their amino acid compositions, determined by HPLC analysis of their constituent amino acids. Twenty peptides have been identified; to date the exchange behaviors of seven (2-6, 76-89, 76-97, 77-84, 108-114, 114-125, and 127-147) have been examined. Peptides were not recovered from residues 11-76, presumably because of the high density of pepsin-sensitive sites in this region. 2.6 mM ATP alters rates of exchange by factors ranging from 1 (114-125) to 20 (2-6, 76-89, 76-97, and 77-84). The latter are in the nucleotide binding domain.

Supported by NIH grant AM-17335.

T-PM-D5 PICOSECOND ANISOTROPY DECAY OF A SINGLE-TYROSINE PROTEIN - J. H. Sommer, X.-Y. Liu & T.M. Nordlund (intr. by R.S. Knox)

Lima bean trypsin inhibitor (LBTI) is a small (MW∿9000) protein with one tyrosine and no tryptophan residues. The tyrosine appears buried in the protein interior, its 300 ps fluorescence lifetime unaffected by 0.88 M citrate. We have studied the fluorescence antisotropy decay of this protein (dissolved in pH 6.5 20 mM bis-tris/100 mM NaCl buffer at ambient temperatures) with a streak camera based instrument. Excitation was from a quadrupled active/passive mode-locked Nd:YAG laser (266 nm, 20 ps FWHM). We saw two anisotropy decay processes. A slow nanosecond process was attributed to protein rotational diffusion; a faster process (∿140 ps) appears due to internal motions of the tyrosine within the protein. The amplitude of this process is 0.06±0.015 anisotropy units (a.u.). We measured the limiting anisotropy of N-acetyltyrosinamide in glycerol to be 0.13±0.015 a.u. Since the limiting anisotropy of LBTI was also found to be 0.13±0.015 a.u., we may conclude that the subpicosecond motion of the buried tyrosine in LBTI is small.

This work was supported by NSF grants PCM-80-18488, PCM-83-03004 and PCM-83-02601 and by the sponsors of the Laser Fusion Feasibility Project at the Laboratory for Laser Energetics of the University of Rochester.

T-PM-D6 STUDY OF INTERNAL PROTEIN MOTION BY FLUORESCENCE AND PHOSPHORESCENCE QUENCHING. D. B. Calhoun, J.M. Vanderkooi, S.W. Englander, Dept. of Biochemistry & Biophysics, University of Pennsylvania, Philadelphia PA 19104.

We are developing the capability for studying internal protein motions by fluorescence and phosphorescence quenching methods. A variety of molecules have been identified--having differing size, polarity, and charge-- that can quench the photoluminescence of protein tryptophans on contact. Quenching patterns exhibited by these allow one to distinguish between the various modes of quencher-tryptophan encounters. When quenching occurs by quencher penetration into a protein, the rate is very sensitive to quencher size, etc. When contact occurs with tryptophan at the protein surface, different quenchers show similar efficiencies. In the latter case, Try that have some solvent exposure in the native state can be distinguished, by their level of sensitivity to quenching, from those brought to the surface via transient "opening" reactions. Trp partially exposed in the native state are reached by solven quenchers with rates from 1 to 0.01 of the diffusion-limited rate, depending on their relative exposure. Those exposed by transient opening reactions are quenched orders of magnitude more slowly, on the phosphorescence time scale. Once the quenching mode is recognized, information on the motions involved can be obtained. Examples will be shown. (Sponsored by NIH grant GM 34448)

T-PM-D7 DISTRIBUTION OF DISTANCES IN MACROMOLECULES FROM FREQUENCY-DOMAIN FLUOROMETRY, by J.R. Lakowicz, B. Maliwal and S. Keating, University of Maryland School of Medicine, Baltimore and M. Johnson, University of Virginia School of Medicine, Charlottesville.

Fluorescence energy transfer is widely used to measure the distance between donors(D) and acceptors(A). A single static D-A distance exists in certain cases, such as a protein in the native state labeled at two specific locations. A single donor-acceptor distance is not expected in many other cases of interest, such as denatured macromolecules, lipid distributions in membranes, and ion distributions around DNA and other macromolecules.

We describe the use of energy transfer to determine the distance probability distribution of donor-accpetor pairs. The information is contained in the time-dependent decays of fluorescence intensity, which are measured by frequency-swept (1-200 MHz) phase-modulation fluorometry. Simulations will be described which illustrate the potential resolution of this method. Additionally, data will be described for donors and acceptors bound to lipid bilayers and for cobolt ions bound to ethidium bromide-labeled DNA. The preliminary results indicate that substantial resolution of the distance distribution is available from the frequency-domain measurements.

T-PM-D8 DYNAMICS OF THE NaCl INDUCED CONFORMATIONAL TRANSFORMATION OF POLY-(dG.dC)-POLY (dG.dC). Yash P. Myer, Department of Chemistry, State University of New York, Albany, NY 12303

It is generally acknowledged that the change of the right-handed helical form of poly (dG-dC)-poly (dG-dC), the B form, to the left-handed helical form, the Z form, is a single step, highly cooperative process, whereas the reverse change involves a well-defined intermediate form, Ψ form. We have examined kinetically the dynamics of the B to Z transition using the NaCl concentration jump technique and both circular dichroism and absorption as probes. The CD studies were conducted at 293 nm, the negative Cotton effect, and 266.4 nm, the cross-over point of the B form. Control investigations were also made at 279.0 nm, the isodichroic point during the latter stages of the reaction. Absorption measurements were conducted at 293, 280, 250 and 240 nm, the four well-defined inflections in the difference spectrum for the Z-B form. The decay profiles in all cases were consistently biphasic with a slow and a rapid reaction. Pseudo- first-order rate constants showed a linear dependence upon the final NaCl concentrations, above 2.15 M, with apparent second-order rate constants of $2.1 \pm 0.2 \times 10^{-4}$ and $1.2 \pm 0.1 \times 10^{-3}$ $M^{-1}s^{-1}$ from CD studies and $4.5 \pm 0.2 \times 10^{-4}$ and $2.3 \pm 0.2 \times 10^{-3}$ $M^{-1}s^{-1}$ from the absorption-based studies for the slow and the fast reactions respectively. Kinetically and thermodynamically, the change is a highly cooperative transition centered in a relatively small NaCl concentration range, 2.15 to 2.3 M. Preliminary studies of the Z to B transition showed this is also a two-step process, but the rate constants are about 10-20 times larger. The simplest possible model that conforms to these findings is the single-intermediate mechanism, $B \rightleftharpoons I \rightleftharpoons Z$.

T-PM-D9 STRUCTURAL CHANGES IN HEMOGLOBIN MEASURED BY TRANSIENT ABSORPTION SPECTROSCOPY
J. Hofrichter, E. R. Henry, J. H. Sommer, R. D. Deutsch and W. A. Eaton, NIADDK, NIH, Bethesda, MD; M. Ikeda-Saito and T. Yonetani, U. of Pennsylvania, Philadelphia, PA USA

Rapid structural changes in hemoglobin A are probed by measuring accurate, time-resolved, absorption spectra. The spectrum of deoxyhemoglobin in the Soret band is used to probe the protein structure at the heme binding site. Three distinct structural relaxations are observed. The first, occurring at ∿100 ns, is accompanied by 'geminate' rebinding of the photodissociated ligand. Measurements on partially photolyzed Hb and studies of iron-cobalt hybrid hemoglobins, both show that this structural relaxation is localized in individual subunits of the tetrameric Hb molecule. It is not yet possible to determine how this event is linked to the geminate rebinding reaction. The structural change could either result from a change in heme stereochemistry on ligand dissociation which acts to decrease the rate of ligand binding at the heme or it could result from the displacement of the ligand from the heme pocket. A second relaxation is observed at 1-2 μs. Data on the $\alpha(Co)\beta(Fe)$ hybrid show that the $\alpha(Co)$ subunits are slightly altered during this relaxation, but much larger changes are seen in the $\beta(Fe)$ spectrum. In $\alpha(Fe)\beta(Co)$, the spectral changes in this relaxation are confined to the $\alpha(Fe)$ subunits. In the quaternary relaxation at 20 μs the spectra of both α and β hemes show changes of roughly equal magnitude, independent of the position of the Co substitution. Accordingly, the first structural change can be viewed as a pure tertiary relaxation, localized in a single α or β subunit. Structural information appears to be propagated from the β to the α subunit in the second relaxation, but the perturbation is small compared to that which results from the change in quaternary structure.

T-PM-D10 DETECTION OF FLEXIBILITY DIFFERENCES BETWEEN RHODANESE CATALYTIC INTERMEDIATES USING DEPOLARIZATION OF INTRINSIC FLUORESCENCE. Paul Horowitz and Nick Criscimagna, Biochemistry Dept., U. Texas Health Science Center, San Antonio, TX 78284.

The enzyme rhodanese cycles between a free form, E and a sulfur-substituted form, ES. Solution studies suggest that rhodanese is flexible and obligatory conformational changes accompany catalysis. Polarization of rhodanese intrinsic fluorescence has been used to directly detect overall protein motion and local motion near tryptophan residues. The limiting polarizations for both the E and ES forms were lower than for N-acetyl tryptophanamide at all excitation wavelengths through the red edge of the spectrum. Rotational relaxation times were determined from polarization measurements by varying either temperature or viscosity. In both cases, the rotational relaxation time was 36nsec for E and 53nsec for ES. This compares with 47nsec based on ultracentrifuge measurements. Lifetime resolved anisotropy measurements were performed using acrylamide to quench fluorescence. Due to extensive static quenching, only a subset of quite flexible tryptophans contributed to these anisotropy measurements. In general, E is more flexible than ES in both overall and internal motion. These results are interpreted using the x-ray structure of rhodanese and are consistent with a model requiring that cyclic changes in flexibility accompany the interconversion of enzyme conformers during catalysis. (Supported by NIH grant GM-25177 and Welch grant AQ-723).

T-PM-E1 ELECTRON TRANSFER IN MIXED-METAL [ZN, FE] HYBRID HEMOGLOBINS. J. L. McGourty, S. E. Peterson-Kennedy and B. M. Hoffman, Departments of Chemistry and Biochemistry, Molecular Biology and Cell Biology, Northwestern University, Evanston, IL 60201.

Mixed-metal [Zn, Fe] hybrid hemoglobins provide a unique matrix in which to study electron transfer. The chromophores in this protein matrix are rigidly held at fixed and crystallographically known distance and orientation, providing a well defined electron transfer unit between the different metalloporphyrins. The excited zinc triplet state, ^{3}ZnP, formed by flash photolysis in the [Zn, Fe(II)] hybrid, decays with a rate of $\sim 55 s^{-1}$. When the hybrid is oxidized to the [Zn, Fe(III)] state, the triplet decays with a rate of $\sim 155 s^{-1}$. The difference between the rates of decay in these two oxidation states is the rate of electron transfer from the excited ^{3}ZnP in one chain of the hemoglobin hybrid to the Fe(III)P, aquoferriheme, in the opposite chain. Transfer in the reverse direction occurs at a much faster rate. In addition, irreversible reduction of the Fe(III)P upon ^{3}ZnP formation provides further evidence for electron transfer between subunits and indicates aspects of participation by the protein matrix.

Direct measurements of the ZnP $\rightarrow$ (ZnP^+) redox potential have been made and permit calculation of the redox potential for the overall electron transfer process: For the forward process of electron transfer, $^3ZnP + Fe(III)P \rightarrow (ZnP^+) + Fe(II)P$, $\Delta E_0' \simeq 0.8V$, while for the back transfer, $(ZnP^+) + Fe(II)P \rightarrow ZnP + Fe(III)P$, $\Delta E_0' \simeq 1.0V$. Binding of various anions alters the spin state and geometry of the ferriheme as well as the redox potential of the Fe(II) $\rightarrow$ Fe(III) couple. The rate of electron transfer in these ligated species is greatly reduced.

T-PM-E2 TEMPERATURE DEPENDENCE OF ELECTRON TUNNELING IN [ZN,FE] HEMOGLOBIN HYBRIDS. S. E. Peterson-Kennedy, J. L. McGourty, B. M. Hoffman. Departments of Chemistry and Biochemistry, Molecular Biology and Cell Biology, Northwestern University, Evanston, IL 60201

The full temperature dependence of electron tunneling across a crystallographically known distance (25Å) was measured by flash photolysis. Rate constants were acquired for multiple samples in three solvent systems over a temperature range from 4K to 313K, on both the [α-Zn, β-met] hybrid and the [α-met, β-Zn] hybrid. The temperature dependence is comparable to the classic biological study of nonadiabatic electron tunneling from cytochrome to chlorophyll in C. Vinosum.[1] Both systems exhibit a temperature dependent region indicative of coupling of the transfer process to thermal vibrations and/or fluctuations, and a temperature independent region characteristic of a transfer process involving nonadiabatic electron tunneling in which the accompanying nuclear rearrangement proceeds by nuclear tunneling.

The rate constants for the [α-Zn, β-met] hemoglobin hybrid are a smooth function of the temperature. In contrast, the rate constants for the opposite [α-met, β-Zn] hybrid show a plateau region from 240K to 270K. Prompted by these results, we measured the relative extinction coefficients of the Soret bands of the [Zn, Fe] hybrids as a function of temperature and found that the plateau in the electron transfer rate constant correlated to an anomaly in the temperature dependence of the [α-met] Soret band extinction coefficients.

1. DeVault, D.; Chance, B. Biophys. J. 1966, 6, 825-847.

T-PM-E3 LASER PHOTOLYSIS MEASUREMENTS OF THE TETRAMER-DIMER DISSOCIATION CONSTANT OF DEOXYHEMOGLOBIN IN THE pH RANGE 9.5 TO 11.2. C. A. Sawicki and M. A. Khaleque, Physics Department, North Dakota State University, Fargo, North Dakota 58105.

Laser photolysis of deoxyhemoglobin samples with fractional CO saturations of less than 3% has been used to determine $K^u_{4,2}$ the tetramer-dimer dissociation constant of human deoxyhemoglobin. As the pH was increased from 9.5 to 11.2 $K^u_{4,2}$ was found to increase monotonically from 0.037 μM to 640 μM. Our results agree reasonably well with earlier ultracentrifugation measurements (Andersen, M. E. Moffat, J. K., and Gibson Q. H. 1976. J. Biol. Chem. 246:2796-2807) which show a much larger scatter than our data. In the present experiments the large difference (about a factor of 30) between the rate constants describing binding of CO to deoxy tetramers and deoxy dimers makes possible detection of small concentrations of deoxy dimers and determination of $K^u_{4,2}$. With presently available equipment determinations of $K^u_{4,2}$ with this method are only possible in the range 0.01 μM to 1000 μM.

T-PM-E4 KINETICS OF CHANGES IN QUATERNARY STRUCTURE, SPIN-STATE, AND CARBON MONOXIDE BINDING IN VALENCE HYBRIDS OF HEMOGLOBIN. John S. Philo, Ulrich Dreyer, & Todd M. Schuster, Biochemistry & Biophysics Section, Biological Sciences Group, University of Connecticut, Storrs, CT 06268

As part of our studies of the linkage between quaternary structure and spin-states in hemoglobin, we have undertaken kinetic studies of valence hybrid hemoglobins in which the ferric subunits are in a 'mixed-spin' state (both high- and low-spin states in thermal equilibrium). Like normal hemoglobin, such hybrids adopt the T conformation when the ferrous subunits are unligated, and the R conformation when they are ligated. According to the Perutz model, changes between R and T should be strongly linked to changes in spin-state of the ferric subunits. We are trying to measure this coupling by following the kinetics after laser photolysis of CO-hybrids using both Time REsolved Magnetic Susceptibility (TREMS) and optical detection methods. The photolysis initiates several processes: (1) a switch from R to T; (2) a possible shift in spin-states in the ferric subunits as a consequence of the R to T change; and (3) rebinding of CO, which competes with the switch to T. By using the complementary information from the magnetic and optical data we hope to completely characterize these kinetics. We have studied both $\alpha^{+}\beta$CO and αCOβ^{+} hybrids with azide, thiocyanate, and formate ferric ligands at 20°C. Qualitatively, the magnetic data fail to show that the R->T change gives any large change in spin distribution of the ferric subunits. Both magnetic and optical data show that the R->T change is quite rapid (~100 μs) for fully deoxy hybrids.

(Supported by grants NIH HL-24644 and NSF PCM 79-03964 & 81-11320)

T-PM-E5 Picosecond Dynamics in Hemoglobin: Implications for the Mechanism of Cooperative Ligand Binding J. M. Friedman*, M. R. Ondrias**, E. W. Findsen**, and S. R. Simon***, *AT&T Bell Laboratories, Murray Hill, NJ 07974, **Dept. of Chem. U. of N.M., Albuquerque, NM 87106, ***Dept. of Biochem. SUNY at Stony Brook, Stony Brook, NY 11794

Picosecond transient absorption studies reveal that the magnitude of the ultra fast (<400 ps) geminate rebinding of O_2 in a large variety of mammalian, reptilian and fish hemoglobins, is highly sensitive to protein tertiary structure. Both proximal and distal effects are observed. A systematic correlation exists between the geminate yield and the frequency of the iron-proximal histidine stretching mode ν(Fe-His) for deoxytransients occurring within 10ns of photolysis. Picosecond Raman studies reveal that these quaternary structure dependent values for ν(Fe-His) seen at 10ns are already apparent within 25ps of dissociation. The above findings point to a model in which the iron coordinate is strongly coupled to the protein through the proximal histidine. The effect of quaternary structure on the spontaneous off rates for ligand dissociation is now understandable in terms of the effect of tertiary structure on the geminate yield and the influence of protein modulated fluctuations in the iron coordinate on the intrinsic rupture rate of the iron ligand bond. These findings provide a smooth connection between the distributed and localized strain models of hemoglobin reactivity.

T-PM-E6 CALCULATIONS OF DEPOLARIZED SCATTERED LIGHT FROM SICKLE HEMOGLOBIN POLYMERS. Alice R. W. Presley and Marilyn F. Bishop, Department of Physics and Atmospheric Science, Drexel University, Philadelphia, PA 19104.

We have calculated the intensity and polarization of linearly polarized light scattered from a dilute solution of long sickle hemoglobin polymers. We assumed that the polymers are long rigid cylindrical rods that lie in a plane perpendicular to the incident beam. For light backscattered at a small angle relative to the incident beam, we calculated the intensities of the polarized and depolarized components of the scattered light. For randomly oriented polymers, the ratio of polarized to depolarized scattered light is three to one. For uniformly oriented rods, the ratio has a maximum of one and a minimum of zero, depending on the direction of orientation. The maximum ratio occurs if the rods are tilted at an angle of 45° with respect to the incident electric field, and the minimum if they are aligned either along the field or perpendicular to it. Our calculations suggest that the alignment of sickle hemoglobin polymers could be detected by measuring the polarization of scattered light.

Work supported by NIH grant HL31549.

T-PM-E7 REMARKABLY LOW AFFINITY POPULATIONS OF HEMES IN THE HEMOGLOBINS OF FISH FROM THE FAMILY MACROURIDAE. R.W.Noble*, L.D.Kwiatkowski*, A.DeYoung*, L.-T.Tam**, A.F.Riggs**, B.J.Davis*, and R.L.Haedrich††, *Department of Medicine and Biochemistry, SUNY at Buffalo, V.A. Medical Center, Buffalo, NY 14215, **Department of Zoology, University of Texas, Austin, TX 78712, *Department of Biological Sciences, San Francisco State University, San Francisco, CA 94132, ††Newfoundland Institute for Cold Ocean Science, Memorial University, St. John's, N.F. A1B 3X7, Canada.

Many fish use their hemoglobins, Hbs, as sources of O_2 for filling their swim bladders. They accomplish this with a gas gland in which the blood is acidified. The Hbs of such fish have exaggerated Bohr effects or Root effects and acidification commonly shifts the R↔T equilibrium so much that the molecule remains in the T state even when fully liganded. We have examined the Hbs of several species of MACROURIDAE which possess well developed swim bladders and live in water depths ranging to over 4000 meters. We hoped to determine if these Hbs have unusual properties which might facilitate the release of O_2 into a gas phase at elevated hydrostatic pressures. At low pH in the presence of organic phosphate these Hbs exhibit two distinct populations of hemes whose ligand affinities differ by more than 100-fold. The low affinity sites have $P_{50}(CO)$ values of 30mm for Macrourus berglax and Coryphaenoides rupestris and 100mm for Coryphaenoides armatus, the deepest dwelling of these species. Rates of CO dissociation from these low affinity sites are in the normal range, but CO combination rates are extremely slow with second order rate constants on the order of $10^3 M^{-1} sec^{-1}$. Supported by NSF Grants PCM-8023166 and PCM-8202760, Research Funds from the Veterans Administration, NIH Grant HL-12524, R.A. Welch Foundation Grant F-213, and ISERT Grant A-7230.

T-PM-E8 EFFECTS OF CROSS-LINKING ON THE THERMAL DENATURATION OF HUMAN HEMOGLOBIN. Frank L. White, John Gashkoff and Kenneth W. Olsen. Department of Chemistry, Loyola University, Chicago, IL 60626

Two different methods of cross-linking have been tested for their ability to stabilize hemoglobin. The first method uses a double-headed aspirin, bis(3,5-dibromosalicyl)fumarate(Walder et al., Biochemistry 18, 4265-4270, (1979), known to be a potent acylating agent, to selectively cross-link hemoglobin A between Lys 82 β1 and Lys 82 β2. The thermal denaturation was done in 0.9M guanidine, 0.01M MOPS, pH 7. The hemoglobin was first oxidized to methemoglobin by making the solution 10^{-5}M in $K_3Fe(CN)_6$. Changes in absorbance, followed at 8 different wavelengths between 190 and 650nm, were monitored on a HP 8451A Diode Array Spectrophotometer, using a heating rate of 0.3°C/min, between 25°C to 70°C. As expected, the apparent single transition for hemoglobin A was very broad, due to the multi-state nature of this denaturation. This transition for uncross-linked hemoglobin had a mid-point temperature of 43°C. The cross-linked hemoglobin A showed at least two distinct transition temperatures at 42°C and 57°C. These results seem to indicate that this cross-link stabilizes some portions of the protein but not others. The second method, using dimethylsuberimidate, was also expected to stabilize hemoglobin A by making random cross-links between lysine residues. Surprisingly, the modified hemoglobin A showed no marked increase in the stability. This result suggests that the cross-linking reaction conditions and reagents directly influence the effect on the hemoglobin stability.

*Supported by a grant from Loyola University Research Stimulation Fund.

T-PM-E9 **THE RATE OF ALLOSTERIC CHANGE FOR TRILIGATED HEMOGLOBIN A.** Frank A. Ferrone, Anthony J. Martino, and Soumen Basak, Department of Physics and Atmospheric Science, Drexel University, Philadelphia, PA 19104.

Using modulated excitation we have measured the rate of change between the R and T conformations of tri-ligated carboxy-hemoglobin A at pH 6.5 and pH 7.0 in 0.1 M phosphate buffer. We find the R to T rates to be 1.2×10^3 sec^{-1} and 1.0×10^3 sec^{-1} (for pH 6.5 and 7.0 respectively) while the T to R rates are found to be 3.6×10^3 sec^{-1} and 3.1×10^3 sec^{-1}. The rates for both pH's yield allosteric equilibrium constants, L_3, of about 0.32, in good agreement with values determined from equilibrium binding measurements. A spectral feature near the HbCO Soret peak has been identified as a structural marker arising from perturbations of the liganded hemes, and is similar in size and shape to the perturbation of the Trout I spectrum by IHP. The data obtained here also is quantitatively consistent with the results of Ferrone and Hopfield (1976, Proc. Nat. Acad. Sci. [USA], 73: 4497-4501) using a revised analysis to account for the multiple excitations in the former work.

Taken together with measured R to T rates for unliganded and singly liganded molecules, this data suggests that the transition state for transitions between R and T structures is very T-like. This can be rationalized by the suggestion of Baldwin and Chothia (1979, J. Mol. Biol.,129:175-220) that the structural change is principally impeded by the motion of His β97 past Thrα41 if one further assumes that the addition of ligands destabilizes the T state (rather than adding to the stability of the R state).

Work supported by NIH grant AM30239.

T-PM-E10 FORMATION OF LOW SPIN DEOXYHEMOGLOBIN IN PARTIALLY LIGATED Hb. Abraham Levy and Joseph M. Rifkind, National Institutes of Health, Gerontology Research Center, Baltimore, Maryland 21224

The study of the temperature dependence of deoxyhemoglobin (Hb) reveals the presence of a conformation in which the iron is in the low spin state. This state was attributed to a conformation where the N_E his(E_7) binds to the empty iron sixth ligand position. The relative population of this conformation is temperature dependent and a study of the protein dynamics suggests that excitation of conformational fluctuations are needed to allow for its formation, which peaks around 250K. In order to relate this phenomenon to ligand binding, we have performed a series of measurements on a number of partially liganded oxyhemoglobins at different temperatures where we monitored the formation of the low spin deoxyhemoglobin conformation. The same study was carried out on carboxyhemoglobin (HbCO). Evidence is found for subunit interactions which produce enhanced protein mobility for unliganded subunits as a result of ligand binding. The results will also deal with the different protein dynamics exhibited by HbO_2 and HbCO.

T-PM-E11 THERMODYNAMIC CHARACTERIZATION OF 2,3-DIPHOSPHOGLYCERATE BINDING TO HUMAN HEMOGLOBIN A_0. M.K. Hobish and D.A. Powers, Department of Biology, Johns Hopkins University, Baltimore, MD 21218.

The binding of 2,3-diphosphoglycerate to human oxy- and deoxyhemoglobin as a function of pH and temperature was determined using rate equilibrium dialysis. One major binding site was found on both oxy- and deoxyhemoglobin, and a second, minor and likely physiologically unimportant site was found on deoxyhemoglobin. The data were fitted to several equilibrium thermodynamic models using nonlinear least squares regression analysis. The fitted curves resemble titration isotherms which, at a given temperature, are shifted approximately 1.5 pH units for the oxy- relative to the deoxy- data. The isotherms appear to converge at high and low pH, with apparent association constants of approximately 10^2 and 10^5, respectively. The slopes of these isotherms were calculated as a function of pH to determine the numbers of protons involved in the binding phenomena, yielding a maximum of two protons for the binding to oxyhemoglobin, and one proton for the deoxy- protein, although this value is pH-dependent. Contributions to the Bohr Effect at 21.5° and 30° were calculated. Thermodynamic parameters (ΔG, ΔH, ΔS) as a function of pH were calculated from the fitted curves. The implications of these findings for regulation of hemoglobin function will be discussed.

T-PM-F1 CHARACTERIZATION OF TETRAHYMENA DYNEIN FRAGMENTS PRODUCED BY PROTEOLYTIC DIGESTION.
Daniel B. Clutter and Kenneth A. Johnson, Biochemistry Program, Pennsylvania State University, University Park, PA 16802

Tetrahymena 22S dynein was bound to bovine brain microtubules under conditions known to favor the binding of the three dynein heads to the microtubule and the complex was subjected to proteolytic digestion with elastase. The digested dynein-microtubule complex was pelleted and then resuspended in the presence of ATP to release the dynein fragments. The fragments were resolved by sedimentation on a sucrose gradient and examined by electron microscopy, gel electrophoresis and assayed for ATPase activity. Three different fragments were produced: a 13S, single-headed species; an 18S, two-headed species; and a 21S, three-headed species, the latter of which appeared to be a nicked form of the three-headed dynein. The specific ATPase activities of the dynein fragments were 0.28, 0.35, and 0.25 μmoles/mg-min for the 13S, 18S, and 21S fragments, respectively; compared to a value of 0.31 μmole/mg-min for intact dynein. Each fragment rebound to microtubules in an ATP-sensitive manner. Mass analysis of the individual fragments by scanning transmission electron microscopy (STEM) has given molecular weights of 300,000 930,000 and 1,390,000 for the three fragments, respectively. The single-headed, 13S species has only one heavy chain greater than 250 kdaltons while the two-headed, 18S species has two heavy chains greater than 250 kdaltons. The large fragment has three heavy chains, each of which is slightly smaller than the native chains. Supported by NIH GM32023.

T-PM-F2 STRUCTURES AND MASSES OF 14S DYNEIN FROM TETRAHYMENA CILIA AND 19S DYNEIN FROM BULL SPERM.
S. P. Marchese-Ragona[1], M. Belles Isles[2], C. Gagnon[2], J. S. Wall[3] and K. A. Johnson[1]. [1]Biochemistry Program, Penn. State University, University Park, PA. [2]Molec. and Cell. Bioregulation Unit, Centre Hosp. de Univ. Laval, Quebec, Canada. [3]Biology Dept., Brookhaven Natl. Lab, Upton, NY.

The structure and mass of Tetrahymena 14S dynein were determined using the Brookhaven scanning transmission electron microscope (STEM) and by conventional TEM. Negatively stained 14S dynein consisted of globular particles 12 nm in diameter and, in addition, nearly half of the particles exhibited a thin projection or tail ~23 nm in length. Unstained 14S particles, adsorbed to carbon films and freeze dried, showed the same morphology. Mass analysis of individual unstained particles by integration of electron scattering intensities gave a mass of 510 ± 90 kdaltons for particles with tails. The globular heads of both types of particles exhibited a net mass of 330 ± 60 kdaltons, leaving a mass of 180 kdaltons for the tails.

A 19S dynein was isolated from bull sperm by high salt extraction and purified by sucrose gradient sedimentation. SDS-PAGE analysis showed two heavy chains of greater than 300 kdaltons. Examination of the 19S dynein by STEM revealed particles with two 10-12 nm globular heads connected to an extended base by two flexible strands. The longest dimension from the base to the top of each head was 35 nm. Mass measurement by integration of electron scattering intensities gave a mean of 1.6 ± 0.2 million daltons. Thus, with the exception of the somewhat larger mass, the bull sperm dynein resembles the two-headed Chlamydomonas 18S dynein described previously. Supported by NIH grant GM32023 to KAJ.

T-PM-F3 ACTIVATION OF DYNEIN ATPASE BY MICROTUBULES.
C. K. Omoto, and K. A. Johnson. Biochemistry Program, Pennsylvania State University, University Park, PA 16802

Activation of the dynein ATPase by repolymerized microtubules was examined by steady state and transient kinetic methods. Bovine brain and Tetrahymena axonemal microtubules were purified on DEAE-Sephacel and repolymerized using 7% DMSO. These microtubules did not have any measurable ATPase activity. Tetrahymena 22S dynein associated with the microtubules at a 24 nm periodicity. The rate of association was approximately 20-fold faster than in the presence of MAPs. ATP induced the dissociation of the microtubule-dynein complex at a rate a factor of two slower than that reported previously in the presence of MAPs. Following the ATP-induced dissociation, the dynein rebound to the microtubules with a time course inversely proportional to the amount of ATP added. At any one ATP concentration, the rate of rebinding increased with increasing tubulin concentration. The microtubule concentration dependence of the ATPase activity was measured directly at both high (1mM) and low (μM range) ATP concentration. We observed a 5- to 10-fold activation of the ATPase by the microtubules at both ATP concentrations. However, a lower concentration of microtubules was sufficient to activate dynein at low ATP concentrations. This can be understood in terms of multiple ATP and microtubule binding sites on Tetrahymena 22S dynein as described previously. Moreover, these data provide the first definitive evidence for an activation of the dynein ATPase by microtubules in solution and they support a model in which the rebinding of the dynein-ADP-P_i intermediate to the microtubule enhances the rate of product release. The enhanced ATPase activity is comparable to that coupled to motility in sea urchin spermatozoa, and sufficient to account for one ATP per dynein per beat. Supported by NIH GM33027 and GM26726.

T-PM-F4 **ENERGETICS OF THE DYNEIN ATPASE CYCLE. Erika L.F. Holzbaur and Kenneth A. Johnson. Biochemistry Program, The Pennsylvania State University, University Park, PA 16802.**

The mechanism of energy transduction by the motility enzyme dynein can be assessed if the forward and reverse rate constants for each step in the dynein ATPase pathway are known. We have measured the rate constants for ATP synthesis by dynein by two methods. The rate of ATP synthesis by dynein in the presence of 2 mM ADP and 4 mM phosphate was measured in a fluorescence coupled assay system using hexokinase and glucose-6-phosphate dehydrogenase. In this system the dissociation of the enzyme-ATP complex was the limiting step and the rate constant for release of ATP was determined to be 0.1 s^{-1} at pH 7, 28 C. Medium exchange reactions were performed in which 0.1 μM dynein was incubated with 0.1 μM ADP and 20 mM $P^{18}O_4$, and the rate of loss of the labeled phosphate oxygens to the unlabeled medium H_2O was monitored by ^{31}P-NMR. The partition coefficient for the process was 0.307, which is equal to the ratio $k_{-2}/(k_{-2} + k_3)$, where k_{-2} is the rate of synthesis of ATP on the enzyme, and k_3 is the rate of release of phosphate from the dynein-ADP-P_i complex. A measurement of the rate of product release of 8 s^{-1} (K.A. Johnson (1983) J. Biol. Chem., 258: 13825-13832) allowed the determination of k_{-2} as 3 s^{-1}. An estimate of 8,000 $M^{-1}s^{-1}$ for the rate of phosphate binding was also determined from the time course of loss of $P^{18}O_4$. Thus, at physiological ATP, ADP, and P_i concentrations, the free energy change for ATP binding would be: ΔG=-27 kJ/mol. ATP hydrolysis occurs on the enzyme with a much smaller energy change: ΔG=-7 kJ/mol. Product release is also accompanied by a significant decrease, ΔG= -26 kJ/mol. Thus, large free energy changes are associated with nucleotide binding and release which are coupled to the dissociation and reformation of the microtubule-dynein complex. (Supported by NIH GM26272).

T-PM-F5 SOLUBLE FACTORS FROM THE SQUID GIANT AXON SUPPORT ATP-POWERED MOVEMENTS OF ORGANELLES AND LATEX BEADS ALONG PURIFIED MICROTUBULES. R.D. Vale, B.J. Schnapp, T.S. Reese, M.P. Sheetz. Neurobiology Dept., Stanford Med. School, Lab.of Neurobiology, NINCDS, at the Marine Biological Lab. Woods Hole MA, 02543, and the Physiology Dept., Univ. of Connecticut Health Center.

Our previous work has shown that single microtubules dissociated from the axoplasm of the squid giant axon support directed movements of endogenous organelles for hours in the presence of ATP. In order to study their molecular basis, we developed a procedure for producing these, and related movements, in reconstituted preparations. Significant numbers of axoplasmic organelles, previously purified in a sucrose gradient, moved along taxol-polymerized, MAP-free microtubules from squid optic lobes provided ATP and a soluble supernatant from axoplasm were added. The rate (1.6 um/s) and other characteristics of these movements were indistinguishable from movements of endogenous organelles along filaments extracted directly from the axon. Furthermore, purified microtubules moved along the glass coverslip and carboxylated latex beads moved along microtubules at 0.5 um/s in the presence of ATP, provided the supernatant fraction was either added or previously used to treat these substrates. The direction of organelle movement was opposite to that of the microtubule movement on glass, but beads and organelles typically moved in the same direction. The supernatant factors promoting movement of organelles, beads, and microtubules were non-dialyzable, inactivated by trypsin or heat, and blocked by 100 um vanadate. These results suggest that the three types of microtubule-dependent movements could be driven by the same ATPase, and that the reconstituted preparations can be used to assay its activity during purification. (Supported by NIH grant GM 33351 to M.P.S.)

T-PM-F6 STRUCTURE OF THE PRINCIPAL SUBASSEMBLY OF INTERMEDIATE FILAMENTS : Martin Potschka , Inst.for theor. chemistry, Univ. of Vienna, Währingerstraße 17,A-1090 Vienna,Austria.

Due to the limited coherence length in fiber diffraction of Intermediate Filaments, structure prediction methods are an indispensible tool for resolving their quarternary structure in solution. To this end, amino acid sequences were numerically coded according to various criteria, such as charge, hydrophobicity, volume or to particular amino acids. The autocorrelation function of this coded array, padded by multiple duplications, was then fourier transformed. To assess statistical significance, this frequency spectrum was normalized by repeated randomisation of the given sequence. The published hydrophobicity codes turned out to perform quite differently. Their capability to faithfully reproduce known alpha-coiled coil domains in various fibrous proteins was used to assess their respective validity. The surface of the dimer coiled coil was also analyzed with special double-cosine-function filters and helical averaging. This analysis revealed the presence of an hydrophobic axis which defines the packing within the tetramer assembly of intermediate filaments. Taken together with hydrodynamic measurements on the intermediate filament protein Vimentin, the structure of this principal subassembly of Intermediate Filaments can be defined close to 1nm resolution.

T-PM-F7 STUDIES OF ACTIN COMPLEXES BY NEUTRON SCATTERING USING "INVISIBLE" ACTIN. Curmi, P.M.[1], Stone, D.B.[1], Schneider D.[3], Spudich, J.A.[2], and Mendelson, R.A.[1]. [1]CVRI and Biochem/Biophys, Univ. of Calif., San Francisco, CA, [2]Cell Biology, Stanford Univ., Stanford, CA and [3]Brookhaven Nat. Lab., Upton, N.Y.

Neutron scattering from complexes of deuterated and protonated proteins allows structural data to be obtained from one member of the complex with minimal interference from the other. Either deuterated or protonated protein can be made to appear "invisible" to the neutron beam by solvent contrast matching. We have adopted this strategy to study problems of force generation and its control in muscle and non-muscle systems.

Deuterated actin has been extracted from amoebae of the cellular slime mold, Dictyostelium discoideum, and purified (>99%) in sufficient quantity to carry out neutron scattering experiments. Conditions were found such that the actin was about 75% deuterated, this being the predicted level for optimal contrast matching. The level of deuteration was measured by ^{1}H-NMR and verified by neutron scattering. This deuterated actin was shown to form Mg^{2+}-paracrystals and to bind to myosin. Preliminary neutron scattering data on the structure of S-1 bound to deuterated actin will be presented.

Supported by NIH (HL-16683, GM-25240), MDA, AHA and Postgraduate Medical Foundation, Univ. of Sydney grants.

T-PM-F8 FACTORS IN G-ACTIN CONFORMATION. Kunihiko Konno & Manuel F. Morales. CVRI, U. of Calif., San Francisco, CA 94143.

We have extended recent findings of Mornet & Ue (PNAS 81: 3680, 1984) and Faulstich, et al. (Biochemistry 23: 1608, 1984): (I) With Ca^{2+} in place, N-terminal 9 kDa region is proteolyzed, but C-terminal 33 kDa "core" is not; with no Ca^{2+} both regions are proteolyzed. (II) Conformational indicators --- titratable thiols, n_{SH}, and fluorescence intensity of ANS-equilibrated actin --- were studied as functions of [ATP], for 0 and 0.2 mM Ca^{2+}; also as functions of [Ca^{2+}], for fixed [ATP]s. For one Ca^{2+} affin. const. $\approx 10^{-8}$M. At high [ATP], n_{SH}(zero Ca^{2+}) - n_{SH}(mM Ca^{2+}) = 1. (III) Actin incubated with fluorescein-s-maleimide and 0.2 mM Ca^{2+} yields single fluorescent band due to Cys-374 modification, but with no Ca^{2+} another, slower band also appears. Bands were individually cut out, treated with NH_2OH, and re-run. Original band is now 40 kDa but still fluorescent; slower band is now faster but non-fluorescent. Relating (II) to (III), we think thiol exposed by Ca^{2+} removal at high [ATP] and affected by NH_2OH is Cys-10. (IV) ϵATP behaves differently from ATP, possibly due to lower affinity: its release was detected by decrease in, (a) polarization, & (b) total fluorescence when bulk phase contained acrylamide. With ϵATP release always accompanied Ca^{2+} release. Help of A. Kasprzak with (IV) & support of AHA and NHLBI are gratefully acknowledged.

T-PM-F9 ACTIN-BINDING PROTEINS MODULATE ANGULAR DISORDER OF ACTIN FILAMENTS. David L. Stokes and David J. DeRosier, Biophysics Graduate Program and Rosenstiel Center, Brandeis University Waltham, MA 02254

Single actin filaments exhibit a variable twist arising from a $\pm 10°$ variation in individual subunit positions; this is called cumulative angular disorder. This disorder may play a biological role when for example the actin filament, with nonhexagonal symmetry, is incorporated into a hexagonal lattice such as the actin bundle or striated muscle. Since actin-binding proteins mediate the interactions holding an actin assembly together, these proteins may modulate actin's intrinsic angular flexibility. We have therefore quantified the cumulative angular disorder in negatively-stained single filaments of actin, actin + scruin, actin + troponin (Tn) + tropomyosin (Tm), and actin decorated with the S1 fragment of myosin. This was accomplished by measuring the projected intensities of the 1st and 6th layer lines from Fourier transforms; cumulative angular disorder attenuates these intensities depending on the Bessel order of the layer line and on the length of the transformed filament. The shape of the nonlinear curve relating intensity ratio to filament length determines the RMS deviation per subunit <d>. The results for negatively-stained specimens are as follows: for actin <d>=10°, for actin+Tn+Tm <d>=15°, for actin+scruin <d> <3°, and for actin+S1 <d> <3°. The ability of these actin-binding proteins to modulate angular disorder in actin may well depend on the biological function of the actin assembly. In muscle, thin filaments must be flexible to allow for freer interaction with myosin. Scruin may actually control the twist of actin to interconvert the 3 forms of the acrosomal bundle from Limulus sperm. Similiarly, myosin S1 may impart rigidity by binding to more than 1 actin monomer, thereby reducing angular flexibility. (Supported by NIH grants GM21189 & GM26357. Thanks to Lynne Coluccio, Don Winkelmann and Peter Vibert for specimens.)

T-PM-F10 A MODEL FOR ACTIN POLYMERIZATION. Dominique Pantaloni, Marie-France Carlier and Edward D. Korn, Laboratory of Cell Biology, NHLBI, NIH, Bethesda, MD 20205.

This model is based on the known structure of the actin filament and on recent kinetic data on filament elongation as a function of the concentration of monomeric actin. The following three assumptions are made: 1) ATP hydrolysis is not necessarily coupled to ATP-actin polymerization, so that ATP-subunits can exist at the ends of filaments, while the subunits inside the filament have ADP bound. 2) The kinetic and thermodynamic properties of the filament depend on the nature of the three terminal subunits. Four types of filaments are distinguished: F_0, F_1, F_2, F_3 in which the three terminal subunits consist of 0, 1, 2, or 3 ATP-subunits. 3) The four types of filament ends undergo mutual interconversions by association or dissociation of an ATP-actin subunit or hydrolysis of ATP. The proportions of the four types of filaments therefore change with the concentration of monomeric ATP-actin. F_0 is the major component in the depolymerization phase; F_3 is dominant in the rapid polymerization phase. The model is characterized by the hypothesis that, in the region of the critical concentration, the four types of filament ends F_0, F_1, F_2, F_3 coexist at a steady state in which continuous depolymerization of F_0 is compensated by continuous polymerization of F_3; intermediate complexes F_1 and F_2 would represent the major very stable components, which impose the usually observed low critical concentration of 0.35 μM. The model also accounts for the critical concentrations of 3 μM found by us for the polymerization of ATP-actin at very high actin concentration where F_3 will predominate. In agreement with T.L. Hill (in press), the model predicts that the frequency with which F_0 becomes F_3 will greatly affect the length fluctuations of actin filaments at steady state.

T-PM-F11 THEORETICAL MODELS PREDICT THE EFFECT OF CAPPING PROTEIN ON THE KINETICS OF ACTIN POLYMERIZATION. John A. Cooper and Thomas D. Pollard. Department of Cell Biology and Anatomy, Johns Hopkins University School of Medicine, Baltimore, MD 21205.

Acanthamoeba capping protein increased the rate of actin polymerization from monomers. Various theoretical models were tested for their ability to predict the effect of capping protein on the full time course of actin polymerization. Three models in which capping protein accelerated, but did not bypass, nucleation predicted the data well. In the best one, capping protein resembled a non-dissociable actin dimer. In the other two, capping protein either resembled an actin monomer or captured actin dimers. Two models that predicted the experimental data poorly were 1) capping protein was similar to actin filaments, bypassing nucleation, and 2) capping protein fragmented actin filaments. Experimentally, capping protein increased the rate of polymerization in buffers with either Ca^{++} or Mg^{++}/EGTA, but it increased the critical concentration for polymerization only in Mg^{++}/EGTA. The modeling of kinetics was performed on data from experiments with Ca^{++} to simplify the models.

Several lines of evidence have supported the idea that capping protein blocks the barbed end of actin filaments, preventing the addition and loss of monomers. This mechanism was also supported in these experiments by the effect of capping protein on the kinetics of actin polymerization that was nucleated by preformed actin filaments. Low capping protein concentrations slowed nucleated polymerization, presumably because capping protein blocked elongation at barbed ends of filaments. High capping protein concentrations accelerated nucleated polymerization because of capping protein's ability to interact with monomers and accelerate nucleation.

T-PM-F12 COMPUTING THE DYNAMICS OF CONTRACTILE NETWORKS IN TWO DIMENSIONS. Micah Dembo, Theoretical Biology and Biophysics, MS K710, Los Alamos National Laboratory, Los Alamos, NM 87545

The reactive fluid model is a dynamical model of contractile actin-myosin polymer networks. The model is based on the formalism of multifield fluid mechanics. It describes the transport of momentum and mass in a finally interpenetrating mixture of network filaments and aqueous solvant. Contractile stresses in the filament phase and the possibility of chemical assembly and dissassembly are included in the model. Except in special cases solution of the model requires application of finite element techniques. Computer generated movies illustrating some computations of an elementary sort will be demonstrated.

T-PM-G1 VOLTAGE-DEPENDENT H^+ CURRENTS COMPLICATE ANALYSIS OF LOW INTERNAL pH EFFECTS ON Ca^{2+} AND K CURRENTS IN INTERNALLY PERFUSED LYMNAEA NEURONS. William Moody & Lou Byerly, Dept. of Zoology, University of Washington and Dept. Biol. Sci., University of Southern California

We have studied the effects of low internal pH (pH_i) on the delayed K current, the A-current, and the Ca current in internally perfused neurons of the snail, Lymnaea. When pH_i was lowered, voltage-dependent outward H^+ currents became substantial at voltages positive to ~20mV (Byerly et al., J. Physiol. 351:199). The kinetics and amplitude of these currents were such that they did not interfere with A-current measurements at low pH_i, but did severely contaminate both delayed K and Ca currents. Low pH_i blocked the A-current; the titration curve indicated that 2 H^+ ions bind to a site with pK=6.05. Low pH_i appeared to block slow inactivation of the delayed K current, as judged by the loss of relaxation of current during long voltage pulses, and by loss of holding potential dependence of peak current. However, this was found to result from the superposition of two other separate effects of low pH_i: a reduction in delayed K current by about 75% (pH_i 5.9) with no change in inactivation, and an increase in H^+ current. At pH_i 5.9 the H^+ current was about 75% of the total outward current at potentials negative to +20mV, so that in many cells the peak outward current was little changed by low pH_i. The Ca current was also decreased at low pH_i, but the presence of H^+ currents which increased at low pH_i made this block seem greater and more reversible than it actually was. These results indicate that H^+ currents may severly contaminate measurements of the effects of low pH_i on other ion currents.

T-PM-G2 EFFECTS OF N-ALKANOLS ON K^+CURRENT KINETICS IN GIANT AXONS OF LOLIGO FORBESI. Y. Pichon, M. Paternostre and Y. Larmet, Département de Biophysique, Laboratoire de Neurobiologie Cellulaire du C.N.R.S., F-91190 Gif sur Yvette, France.

In the present study, we have analysed the effects of external application of several N-alkanols on the kinetics of the potassium current recorded under voltage-clamp conditions. TTX (0.5 μM) was used to eliminate the sodium current. Current traces corresponding to square depolarizations of the axonal membrane were digitized and stored on digital cartridge tape. They were analysed off-line using an algorithm derived from the Hodgkin and Huxley (J. Physiol., 117, 500, 1952) equations with a fixed exponent of 4. Besides their effects on the intensity of the current, alkanols were found to induce three modifications in K^+current kinetics: (1) a double shift of the $\bar{G}n$ versus potential curve towards more positive potentials and shorter time constants; (2) a marked increase in the K^+ activation delay (i.e. the delay which separates the turning-on of the K^+ current as extrapolated from the linearized current traces and the beginning of the depolarizing voltage pulse); (3) a slow inactivation. No obvious correlation was found between these changes and the effects on the maximum conductance: alcohol concentrations which induce an increase in $\bar{g}K$ such as 1 mM heptanol have the same effects on the kinetics as those which reduce $\bar{g}K$ such as 4 mM heptanol (Paternostre and Pichon, J. Physiol., 328, 31P, 1982). These data strongly suggest that alcohol molecules interfere with several of the successive steps which govern the voltage-dependent opening and closing of potassium channels. Preliminary experiments indicate that N-alkanols have similar effects on the sodium current kinetics, suggesting common mechanisms for the two ionic conductances.
Experiments were performed at the Station Biologique, F-29211, Roscoff, France.

T-PM-G3 EVIDENCE FOR THE PRESENCE OF HISTIDINE ON THE EXTERNAL SURFACE OF THE POTASSIUM CHANNEL AND ITS INVOLVEMENT IN CHANNEL GATING. Sherrill Spires and Ted Begenisich, Department of Physiology, University of Rochester Medical Center, Rochester, NY 14642.

We have investigated the action of the histidine modifying reagent, diethylpyrocarbonate (DEP) on potassium channel ionic and displacement (gating) currents. Ionic currents were measured using an artificial sea water (ASW) containing an elevated potassium concentration (50 mM) to reduce effects of K accumulation in the periaxonal space. The internal solution contained 350 mM K. A temperature of 15 or 20°C was used. The gating currents were measured in a Na-free (Tris) ASW with nitrate as the anion and with 0.2 mM dibucaine at 20°C. These steps (and a somewhat depolarized holding potential) selectively reduced sodium channel gating currents. The internal solution for the gating current measurements contained Cs and 1 mM 3,4- diaminopyridine.

DEP (.25-.35 mM) added to the external solution at pH 6 produced a rapid (2-5 min) slowing of potassium channel ionic current kinetics with a small reduction in steady-state levels. In contrast internal application had no effect on kinetics. The modification of kinetics is specific for potassium channels: Na channel kinetics are not altered. In contrast to the effects on ionic currents, DEP had very little effect on the kinetics of potassium channel gating currents. These results suggest that there is (are) a histidyl group(s) on the external surface of the potassium channel protein involved in a voltage-independent step in channel gating. Supported by USPHS grant NS-14138.

T-PM-G4 POTASSIUM CHANNEL KINETICS AND CURRENT-VOLTAGE RELATIONS IN SQUID AXONS WITH ELEVATED LEVELS OF EXTERNAL POTASSIUM ION CONCENTRATION. John R. Clay, Lab. of Biophysics, NINCDS, NIH, at the MBL, Woods Hole, MA 02543.

Measurements of potassium channel current in squid axons are complicated by effects of ion accumulation or depletion in the periaxonal space. This problem can be circumvented by elevating K_o so that E_K is within the range of activation of the conductance (-60 to +20 mV). Consequently, a prepulse to E_K activates channels without significant current flow. The current immediately after a second step away from E_K provides a measurement of membrane current with minimal complications due to accumulation/depletion. This procedure is based on the observation that increases in K_o do not alter either the activation kinetics or the g_K-V curve. Experiments of this type reveal that the instantaneous I_K-V is, in general, a non-linear function of $(V-E_K)$, when $K_o \neq K_i$, and that I_K at any given potential does not appear to saturate with increases in either K_o or K_i. The time course of channel activation can be measured by varying the duration of the prepulse to E_K. The current upon return to holding level, V_H, as a function of prepulse duration, provides a relative measure of $g_K(t)$ at $V=E_K$. The original HH n^4 model is consistent with these results for $t \leq 100$ ms and $V_H = -80$ or -100 mV. These results together with tail current kinetics indicate that squid axons possess only a single type of gated K channel. Inactivation of g_K occurs in two phases with time constants of 5 and 40 sec, respectively, at V=0 mV and T = 10°C. Inactivation at V=0 mV is incomplete. Reactivation at V = -100 mV also occurs with two time constants following a delay of 100 msec. Full reactivation occurs within 10 sec.

T-PM-G5 SATURATION AND PERMEABILITY OF VOLTAGE-DEPENDENT K CHANNELS IN SYMMETRICAL AND ASYMMETRICAL PERMEANT CATION SOLUTIONS. K.W. May and G.S. Oxford (Intr. by M.M. Goldner). Department of Physiology, University of North Carolina, Chapel Hill, NC 27514.

Conductance-activity relationships and permeability ratios were examined in delayed rectifier K channels of perfused squid axons using instantaneous I_K-V measurements. Experiments were performed for the permeant monovalent cations, K^+, NH_4^+, Rb^+ and Tl^+ under symmetrical activity conditions and under asymmetrical conditions for K^+. Accumulation of permeant cations in the periaxonal space was reduced by limiting the amplitude and duration of activating voltage prepulses. As the activity of K^+ was increased from 100 to 650mM on one or both sides of the membrane, the conductance increased. Further increases in activity to 1.5M resulted in conductance decreases. This biphasic response to increasing K^+ activity was seen for activity ratios (out/in) ranging from 0.02 to 1.0. Similar changes in the conductances to NH_4^+ and Rb^+ w5re seen for symmetrical elevation of their activities. This pattern was not observed in control experiments in which urea or glycine served to elevate osmolality, although at the highest osmotic strengths (and/or viscosity) the conductance was reduced. The selectivity sequence for monovalent cations was the same as previously observed. After correction for junction potentials and ion accumulation, the absolute permeability ratios for NH_4^+ and Rb^+ relative to K^+ were different for external vs. internal substitutions. Tl^+ currents exhibited a negative conductance region at potentials above +80 mv suggesting a "self-block" of K channels by Tl^+. These results are consistent with recent predictions of multi-ion pore models for K channels.
(Supported by NSF grant BNS82-11580 and the Grass Foundation).

T-PM-G6 TWO TYPES OF POTASSIUM CHANNELS IN THE CUT-OPEN SQUID GIANT AXON. I. Llano and F. Bezanilla. Dept. of Physiology, University of Pennsylvania, Philadelphia, PA, Dept. of Physiology UCLA, Los Angeles CA and MBL, Woods Hole, MA.

We have used the modified cut-open axon preparation (Levis et al., Biophys. J. 45: 11a, 1984) to record single channel events associated with the potassium currents in the squid giant axon. The axon was cut open in artificial sea water with 200 nM TTX, the axoplasm was removed mechanically and small patch pipettes filled with a solution containing 375 mM K-glutamate, 25 mM KF and 10 mM tris were used to seal against the internal side of the membrane and to control the potential of the patch. Gigaohm seals were obtained frequently but often they did not last or became noisy. In stable patches, two types of single channel events were observed which differed in their single channel conductance and in their frequency of activation under voltage clamp pulses. The first channel type was studied with both single channel records and channel fluctuation. Direct measurements of its conductance and ensemble analysis of channel fluctuation yield a single channel conductance of 14 to 20 pS. Estimates of its mean open time are of the order of 5 ms at 100 mV. The second type of channel has a larger conductance (40 to 45 pS) and it opens infrequently for repetitive large depolarizing pulses. The probability of at least one opening for a 40 ms pulse to 180 mV is 0.21. The current obtained by averaging shows that the activation kinetics of the large channel is slower than the small channel.

Supported by USPHS grant GM30376.

T-PM-G7 ATP REGULATES THE RESTING K CONDUCTANCE OF SQUID GIANT AXON. David C. Gadsby, Paul De Weer and R.F. Rakowski, Marine Biological Laboratory, Woods Hole, MA 02543.

Metabolic inhibitors elicit membrane hyperpolarization in a variety of cells. The reversible CN-induced hyperpolarization of squid giant axon is not due to intracellular acidification or Ca release (De Weer, Ann. N.Y. Acad. Sci., 307:427-430,1978). We have tested the hypothesis that the resting K conductance, g_K, of squid giant axon is reversibly inhibited (directly or indirectly) by intracellular ATP. Axons (diam 400-600μm) were internally dialyzed with solutions containing 50 mM Na, 270, 100, or 34 mM K (replaced by N-methylglucamine), 12.5 mM Mg, and 100 mM HEPES, with and without 5 mM ATP, were bathed in 10 mM-K seawater containing 100 μM ouabain and 0.2 μM TTX, and clamped at voltages between -65 and -35 mV. Relative changes in steady-state g_K due to washing out and readmitting intracellular ATP were determined at a fixed holding potential, V_H, by measuring changes in holding current, I_H, caused by intermittently lowering external [K] from 10 to 7.5 mM. When V_H was positioned between the calculated K equilibrium potentials for these two [K], washout of ATP caused an inward shift of I_H at 10 mM K_o but an outward shift of I_H at 7.5 mM K_o, confirming that ATP removal leads to an increase in steady-state g_K. That increase developed slowly ($t_{0.5} \sim$ 30-70 min) on removal of ATP, could be abolished by 1 mM 3,4-diaminopyridine, and was rapidly ($t_{0.5}$ ~5-10 min) and completely reversed by readmitting ATP. Its relative magnitude showed a steep dependence on V_H, ranging from ~7-fold at -65 mV to barely measurable at -35 mV. Injection of protein kinase inhibitor together with cyclic nucleotide phosphodiesterase did not prevent inhibition of g_K by ATP. We conclude that ATP causes a reversible reduction in steady-state g_K of squid giant axon at potentials more negative than ~-35 mV. Supported by NIH grants NS 11223 to P.D.W. and NS 19393 to R.F.R., and an Established Fellowship of the N.Y. Heart Association to D.C.G.

T-PM-G8 K CURRENT IN SQUID AXON IS MODULATED BY ATP. Bezanilla, F., DiPolo, R., Caputo, C., Rojas, H. and Torres, M.E. Dept. of Physiology, UCLA, Los Angeles, CA, CBB, IVIC, Caracas, Venezuela.

Experiments with dialyzed and voltage clamped squid axons revealed that potassium currents were decreased when the dialysis solution contained no ATP, and the effect was reversed by addition of this compound. This effect of ATP was studied in more detail using an internal dialysis medium containing (in mM): 310 K; 40 Na; 30 TRIS; 98 Cl; 310 Aspartate; 330 glicine; 1 EGTA; 4 Mg in excess of ATP; pH 7.3; (16-18°C). The external medium was artificial sea water with 1 mM cyanide and 300 nM TTX. In axons dialyzed free of ATP, its addition, at 1-2 mM, increased the outward K currents up to 200% in response to large depolarizations. Furthermore, ATP produced a slowing down of the turn-on kinetics of the K currents. The effect of ATP is complex, because the conductance is decreased for V <-30 and is increased for V>-30 mV. These effects are not compatible with a simple increase in the number of conducting channels, or an increase of the single channel conductance, and they suggest a change in the relative proportion of two populations of K channels. The effect has a $K_{\frac{1}{2}}$ of about 300 μM. ADP, AMP, and cyclic AMP did not show any effect. The ATP effect seems to involve a phosphorilating step because: a) Mg is required; b) a non-hydrolizable ATP analogue (AMP-PCP) had no effect, and c) experiments with internal perfusion only showed the effect when ATP and Mg were added in the presence of the catalytic subunit of protein kinase. The effect on current kinetics was very reproducible, but we found a wide variation in the effect of ATP on the magnitude of the K currents in different batches of squids. (Supported by CONICIT S1-1144, S1-1148, CONICIT-NSF joint program INT-8312953, S1-1556; USPHS GM-30376.)

T-PM-G9 IONIC CURRENTS FROM GIANT FIBRE LOBE NEURONS OF THE SQUID. Richard J. Bookman, Isabel Llano & Clay M. Armstrong. Dept. of Physiology, Univ. of Pa., Philadelphia, PA 19104.

The giant axon of the squid arises from the fusion of hundreds of individual axons emerging from neurons located in the giant-fibre lobe of the stellate ganglion. We have developed a method for the isolation, dissociation, and culturing of these neurons. The stellate ganglion is removed from the mantle and the connective tissue capsule is dissected away from the giant fibre lobe prior to cutting the lobe from the ganglion. The lobe is soaked in ASW containing 10mg/ml of pronase for 40-60 minutes. The cells are then rinsed and dissociated mechanically in a vortexer. The cells are grown in a culture medium (L-15) supplemented with serum, salts, glucose, and antibiotics and are viable for at least two weeks. These cultures show axon fragments and cell bodies, some of which have processes which may develop growth cones after a few days in culture.

We have recorded ionic currents from axon-free cell bodies, 25-50μm in diameter, using the whole cell variant of the patch clamp technique. The preparation was bathed in ASW at 10°C. With an internal K solution pipettes had resistances of 500k to 1Mohm. Depolarizing pulses from a HP of -90mV elicit large outward currents (0.5-2.0 $pA/\mu m^2$ at +50mV). When internal K is replaced by impermeant ions (nMG), small inward currents (0.02-0.06 $pA/\mu m^2$) were seen. Two components of this current are distinguishable based on their TTX sensitivity. The TTX-sentitive current (I_{Na}) activates rapidly (time to peak 700 us at +10 mV) and inactivates during a 10 ms pulse. The other component (presumably I_{Ca}) activates more slowly reaching steady state with a time constant of 2.6 ms at 0 mV and does not inactivate during a 50 ms pulse.
Supported by an MDA Fellowship to I.Ll. & USPHS grant 5-R01-NS12547.

T-PM-G10 THE K^+ CONDUCTANCE OF SQUID GIANT FIBRE LOBE NEURONS. Isabel Llano and Richard J. Bookman. Dept. of Physiology, University of Pennsylvania, Philadelphia, Pa., 19104.

The properties of the K channel from giant fibre lobe neurons isolated from squid stellate ganglion were characterized by the analysis of both whole cell currents and currents from excised patches. These currents were recorded from cells bathed in ASW at 10°C, with patch pipettes filled with a solution of 250 KGlutamate, 25 KF, 10 Hepes, 10 EGTA. The G_K -V relation and activation time course of the macroscopic current closely resemble those of the delayed rectifier in the squid axon, the time to half peak being ~2.9ms for an activating pulse to +50 mV. However this current partially inactivates, decreasing to ~80% of its peak value at the end of a 50ms depolarization to +50 mV. This inactivation proceeds with a time constant of 20-50ms. Measurements of the instantaneous I-V relation during the falling phase of the current reveal a clear decrement of the conductance with time and a small (7-10 mV) shift in the reversal potential for K^+ ions. The steady-state inactivation curve has a midpoint at -40mV and saturates around -10mV. 40 mM internal TEA blocks this current, but has little effect when applied to the outside.

In a few cases, single channel events were observed in cell-attached patches. However, most attempts to record single-channel currents were hindered by the large current density (100-300 pA/patch at +20mV). Thus, ensemble fluctuation analysis of currents recorded from outside-out excised patches was used to estimate the single channel conductance. For membrane potentials ranging from -20 to +30 mV, estimates of γ were 13-14 pS, and were independent of both the membrane potential during the activating pulse and the holding potential.

Supported by an MDA fellowship to I.Ll. & USPHS grant 5-NR01-NS12547.

T-PM-G11 **MODIFICATION OF DELAYED RECTIFICATION BY CATECHOLAMINES IN HEART.** P.B. Bennett, L.C. McKinney, R.S. Kass and T. Begenisich, Department of Physiology, University of Rochester, Rochester, NY 14642.

The effects of norepinephrine (NE) and isoproterenol on a time dependent potassium current (Ix) were investigated in calf cardiac Purkinje fibers and enzymatically dissociated ventricular myocytes from guinea pig. Purkinje fibers (PF) were voltage clamped using a conventional 2-microelectrode arrangement. Necessary and sufficient conditions were defined to allow measurement of Ix in PF without interference from K+ accumulation or from other ionic currents. NE increased the magnitude of deactivating Ix-tails in a concentration dependent manner. A maximally effective concentration of NE (2 uM) produced a 2-5 fold increase in Ix-tail magnitude. The Ix reversal potential (Vx) was measured in several [K]o and was very near the eqilibrium potential for a potassium selective channel (-51 mV in 16mM K o). NE produced a small (-3mV) shift in Vx suggesting a small increase in K-selectivity or an increase in [K]i. Ix deactivation had 2 time constants ($\tau 1$ & $\tau 2$). $\tau 1$ was not affected by NE but $\tau 2$ was decreased at most voltages. The voltage dependence of Ix activation was not shifted by NE. The results are described by a 3-state model for Ix with catecholamines altering the volatge dependence of one of the rate constants. Ventricular cells were voltage clamped using the whole cell variation of the patch clamp method. Voltage clamp protocols were the same as in PF but experiments were at 20°C instead of 37°C resulting in a much slower time course. Other features of the current were quite similar to PF. The results suggest that the currents have similar properties and that catecholamines produce similar effects in the single- and multi-cellular preparations.

T-PM-G12 RESTING K^+ CHANNELS IN SINGLE GUINEA-PIG ATRIAL AND VENTRICULAR MYOCYTES ARE DIFFERENT. A. Uehara and J.R. Hume (Intr. by D.G. McConnell), Department of Pharmacology/Toxicology, Michigan State University, East Lansing, MI 48824. We have used a single suction micropipette technique for whole-cell current and voltage clamp and the cell-attached configuration of the patch clamp technique (Hamill et al., Pflugers Arch. 391: 85-100, 1981) in order to compare the properties of resting K^+ channels in atrial and ventricular myocytes. The isochronal (5 sec) current-voltage relationship of single ventricular myocytes exhibited a region of prominent negative slope conductance and elevation of $(K^+)_o$ produced cross-over; a negative slope conductance region was absent in atrial cells and elevation of $(K^+)_o$ failed to produce a cross-over. Hyperpolarizing voltage pulses applied from holding potentials of -50 mV elicited inward current in ventricular cells which decayed with time; similar voltage clamp pulses in atrial cells elicited inward currents which fail to decay. Single K^+ channel current measurements (Fig.) confirmed the existence of different resting K^+ channels in single atrial and ventricular myocytes. Resting K^+ channels in both types of cells had similar single channel conductances (30-32 pS with $(K^+)_o$ = 145 mM) but ventricular K^+ channels had significantly slower gating kinetics compared to atrial K^+ channels (ventricular K^+ channel mean open time = 223 msec; atrial K^+ channel mean open time = 1 msec at Vr = -20 mV and 25°C). The different properties of resting K^+ channels may contribute significantly to the different action potential configurations of atrial and ventricular myocardium.

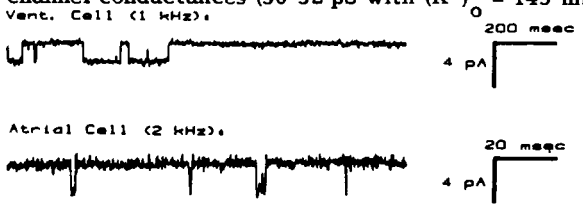

Supported by N.I.H. grant HL30143.

T-Pos1 **STATISTICAL ANALYSIS FOR THE PREDICTION OF PROTEIN CODING REGIONS IN DNA SEQUENCES.**
Kotoko Nakata, Minoru Kanehisa and Charles DeLisi, Laboratory of Mathematical Biology, NCI, NIH, Bethesda, Maryland 20205

We developed a general method based on the statistical technique of discriminant analysis to distinguish coding regions and non-coding regions in DNA sequences. Protein coding regions and their boundaries exhibit a number of characteristic patterns including consensus sequences of promoters in DNA, splice junctions in RNA, and the periodic appearance of specific bases reflecting the non-random usage of degenerate codons. We used this information in conjunction with a pattern recognition algorithm called the perceptron method. Although the perceptron algorithm allows 100% discriminantion between coding and non-coding regions in a training set of sequences, its predictive ability, i.e. its ability to distinguish coding from non-coding regions in sequences that are not in the training set, is less reliable. By discriminant analysis we can combine information processed by the perceptron algorithm, e.g. boundary consensus sequence patterns, with information obtained by other methods, e.g. base composition and periodicity, and improve the degree of predictive ability in unknown sequences. We have applied this method to distinguishing translation initiation sites, termination sites, exon/intron and intron/exon boundaries from merely fortuitous sequences, using the GenBank database. To asses the discriminatory power of these variables, we allocated additional sequences that have been newly included in the data base.

T-Pos2 INTERRELATEDNESS OF 5S RNA SEQUENCES STUDIED BY CORRESPONDANCE ANALYSIS.
C.A. Mannella, J. Frank and N. Delihas.[+] Wadsworth Center for Laboratories and Research, New York State Dept. of Health, Albany, NY 12201 and [+]Dept. of Microbiology, State Univ. of New York, Stony Brook, NY 11794. (Intro. by D.S. Berns)

The primary structure of a nucleic acid can be represented by a 5N-dimensional vector, in which N is the number of base positions, each of which can be occupied by one of 4 bases or be blank. Thus, a set of P aligned sequences can be represented as a "cloud" of P points in 5N-space, with the chi-square distances between points being a measure of the overall relatedness of the corresponding sequences. The directions in 5N-space along which inter-sequence variance is greatest can be determined by correspondance analysis. Subsequent projection of the data cloud into low-dimensional spaces defined by these directions (or "factor axes") may be used to reveal clustering of related sequences. Applying this procedure to a set of 64 5S RNA sequences, we find that (1) eucaryotes and eubacteria fall on either end of factor axis 1, with archaebacteria in the middle, closer to the eucaryotes; (2) chloroplasts cluster near the cyanobacteria in maps involving the first five factorial directions; (3) mitochondrial 5S RNA falls on the eubacterial side of factor axis 1 but is totally isolated on higher factor axes. Correspondance analysis also identifies those base positions at which the systematic changes occur which are responsible for clustering of the sequences. For factor axes 1-5, these "important" base positions are unevenly distributed along the molecule, with highest frequency in helix 4 and in the unpaired regions at either end of the molecule adjacent to helix 1 (see model in Delihas and Andersen, Nucleic Acids Res. 10:7323). (Supported by NIH grant GM 29169 and NSF grant PCM 83-02127.)

T-Pos3 STATISTICAL MECHANICS OF SUPERCOILING-INDUCED B-TO-Z TRANSITIONS IN A CLOSED CIRCULAR DNA: S. Miyazawa and A. Sarai, Lab. of Math. Biol., NCI, NIH, Bethesda, MD 20205

A configurational partition function for transitions from the right handed B helix to left handed Z helix in a closed circular double stranded DNA is formulated on the basis of an idealized model. A double quadratic twisting potential with minima at the B- and Z-forms for base pair twists and a harmonic potential for nearest neighbor interactions between twists are assumed. Long range interactions among the twists, which are attributable to the conservation of linking number (L_k) between two closed DNA strands, are approximated to be a harmonic potential with regard to the writhing number (W_r); $L_k=T_w+W_r$; the twisting number T_w is equal to the total twists. Interactions between phonon and structures such as B- and Z- regions and B-Z junctions are neglected. The configurational partition functions are formulated for two cases; one that all base pair can take the Z form, and another that only part of DNA can take the Z- and B-forms. These partition functions are consistent with the fact that the equilibrium ensemble of B-form closed DNAs over L_k obeys the Gaussian distribution with the variance of L_k, kTN/κ; N is the total length of DNA. It is proved that the variance of T_w in a closed DNA is smaller than that of a linear DNA, because of the long range interactions. The characteristics of B-to-Z transitions induced by reducing L_k of a closed circular DNA are examined in details; the dependences of the transition linking number on external variables such as the total length of DNA and the length of a DNA segment that can take the Z form are analytically derived among others. Also, the relative energy of Z-form to B-form, the energy for forming a B-Z junction, and $\kappa/2$ have been estimated by curve-fitting of transition curves to the experimental data (Peck & Wang, 1983) to be $0.84 \cdot kT$, $8.28 \cdot kT$ and $1490 \cdot kT$.

T-Pos4 STATISTICAL MECHANICAL ANALYSIS OF LOCALLY CONSTRAINED STRUCTURES, N. L. Marky and W. K. Olson, Department of Chemistry, Rutgers University, New Brunswick, New Jersey 08903

Nucleic acid molecules adopt a variety of structures in nature, some of which results from specific, localized constraints in the chain molecule. The constraints in structures such as closed figures, loops, knots, hairpins and bulges can be described by the ends of a theoretically equivalent chain. The probability of formation, Q, of any of these structures is then obtained with a set of correlated probability functions of the various parameters, which define the constraints, $Q = [W(r_o)\delta r]\ [2\Gamma_r(\gamma_o)\delta\gamma]\ [2\Lambda_{r,\gamma}(\lambda_o)\delta\lambda]\ [2E_{r,\gamma,\lambda}(\varepsilon_o)\delta\varepsilon]\ [2B_{r,\gamma,\lambda,\varepsilon}(\beta_o)\delta\beta]$. In this expression W(r) is the spatial density distribution of the end-to-end chain separation, r, while $\Gamma(\gamma)$, $\Lambda(\lambda)$, $E(\varepsilon)$ and $B(\beta)$ are angular correlation functions describing the conditional probability of the chain ends meeting a required angular orientation when the previous constraints have been met. In closed figures, the only functions needed to calculate Q are W(r=0) and $\Gamma_{r=0}(\gamma=\gamma_o)$. The values of $W(r=r_o)$, $\Gamma(\gamma=\gamma_o)$ and $\Lambda(\lambda=\lambda_o)$ are usually necessary for loops and knots, while for structures like hairpins, internal loops and bulges, where side chains need to be "bonded", all five functions are needed. To illustrate the model, bulges and internal loops of A-RNA are studied. Both structures show a maximum probability with 1 residue. A comparison between a 1 residue bulge and a 1-residue internal loop slightly favors the bulge over the internal loop. A 1-residue bulge, accompanied by intercalation side has a lower probability than a bulge of the same length without it. (Supported by USPHS Grant #20861).

T-Pos5 THE RAMAN SPECTRA OF POLY(dA-dT)·POLY(dA-dT): INVESTIGATION OF THE B-TO-A TRANSITION IN DNA CONTAINING ONLY ADENINE-THYMINE BASE PAIRS. James M. Benevides and George J. Thomas, Jr., Department of Chemistry, Southeastern Massachusetts University, North Dartmouth, MA 02747

Recently, much interest has been focussed on the secondary structure of poly(dA-dT)·poly(dA-dT). NMR data indicate a B-helix structure at the same conditions for which certain A-helix characteristics are indicated by both equilibrium and dynamic Raman studies.[1-3] The stability of an A helix lacking GC pairs has also been questioned on the basis of x-ray evidence.[4] In this work poly(dA-dT)·poly(dA-dT) is shown by laser Raman spectroscopy to exist predominantly in the B-DNA conformation in aqueous solution and in the A-DNA conformation in fibers at 75% relative humidity. The Raman spectrum of the A-form, which has not been reported previously, differs strikingly from that of the aqueous B-form not only in the conformation sensitive modes of the backbone but also in the in-plane ring modes of adenine and thymine which are sensitive to base stacking, and in the carbonyl stretching modes of the thymine 2C=O and 4C=O groups which are sensitive to base pairing. The present results suggest that thymidine, like deoxyguanosine, contains a vibrational mode of the base which is coupled to deoxyribose through the glycosidic bond and is therefore sensitive to nucleoside conformation. (N.I.H. Grant AI18758.)

1. Assa-Munt, N. & Kearns, D.R. (1984) Biochemistry 23, 791-796.
2. Thomas, G.A. & Peticolas, W.L. (1984) J. Am. Chem. Soc. 105, 993-996.
3. Benevides, J.M., & Thomas, G.J., Jr. (1985) Biopolymers 24 (in press).
4. Dickerson, R.E. & al. (1983) CSH Symp. Quant. Biol. 47, 13-24.

T-Pos6 MINIMIZED SEMI-EMPIRICAL CONFORMATIONAL POTENTIAL ENERGY CALCULATIONS FOR d(GpCpGpC) MODIFIED BY THE CARCINOGEN 2-AMINOFLUORENE. B. Hingerty, Health and Safety Research Division, Oak Ridge National Laboratory, Oak Ridge, TN 37830, and S. Broyde, Biology Dept., New York University, New York, New York 10003.

A program to compute conformations of carcinogen modified nucleic acids, employing potentials devised by Olson and Srinivasan (1), has been used to elucidate the conformations of the tetramer d(GpCpGpC) modified at carbon-8 of the central guanine with the carcinogen 2-aminofluorene (AF). Low energy conformers previously computed (2) for the modified dimer d(CpG)-AF were incorporated into A,B and Z form adjacent sites, and the energy of these structures was minimized. Both carcinogen-base stacked states and base-base stacked states were energy minima in the tetramer, as was previously inferred from the dimer minima and model building.

(1) Srinivasan, A. and Olson, W. (1980). Fed. Proc., Fed. Am. Soc. Exp. Biol. 39. 2199.
(2) Broyde, S. and Hingerty, B. (1983). Biopol. 22, 2423.

This work was supported jointly by PHS Grant #1R01 CA28038-04(SB), DOE Contract #DE-AC02-81ER60015 (SB), and by the Office of Health and Environmental Research, U.S. Dept. of Energy, under Contract #DE-AC05-840R21400 with Martin-Marietta Energy Systems, Inc. (BH).

T-Pos7 **A SIMPLE MODEL TO REVEAL THE GROSS TERTIARY STRUCTURE OF B-DNA HELIX FROM PRIMARY SEQUENCE.** **Chang-Shung Tung, T-10, MS-K710, Los Alamos National Laboratory, Los Alamos, NM 87545.**

Based on the prediction scheme of helix twist angles and changes of base-pair roll angle for DNA double helix developed by Tung & Harvey, a simple model is constructed to reveal the gross three dimensional structure of DNA double helix. With the sequence being specified, this model plots the DNA double helix in stereo view so that one can actually see the three dimensional structure. The plot of the 51 basepair bending locus of the trypanosome kinetoplast DNA (Wu, H.-M. & Crothers, D. M. Nature 308, 509-513 (1984)) has shown that this particular piece of DNA is close to being planar and that the bending is about 30°. Also discussed are the possible applications of the model being used to study the role of local structural variations as a means for proteins to recognize specific DNA sequences.

T-Pos8 THE INFLUENCE OF DANGLING ENDS ON THE STABILITY AND CONFORMATIONAL PREFERENCES OF DNA DUPLEXES. Mary M. Senior, Roger A. Jones, and Kenneth J. Breslauer, Department of Chemistry, Rutgers, The State University of New Jersey, New Brunswick, New Jersey 08903.

We have evaluated the influence of thymidine (T) dangling ends (both 5' and 3') on the thermal stabilities and salt-dependent conformational preferences of a family of oligomer sequences. Specifically, we have studied the following six duplex structures: $[d(CG)_3]_2$; $[dT_2(CG)_3]_2$; $[d(CG)_3T_2]_2$; $[d(GC)_3]_2$; $[dT_2(GC)_3]_2$; and $[d(GC)_3T_2]_2$. All six sequences were synthesized using a modified phosphite triester method, and purified by hplc. The thermal stabilities of each duplex were determined from optical melting curves. We found that 5' dangling T residues increase thermal stabilities to a greater extent than do 3' dangling T's with respect to the core duplexes (Δt_m's of 8-9°C for two 5' dangling T's versus 3-5°C for two dangling 3' T's). Interestingly, this observed trend in stability, based upon dangling thymidine position, is the reverse of that reported by Freier and Turner for RNA duplexes. From model building and computer graphics (B conformation is assumed), we propose that 3' dangling T stabilization results from additional intrastrand stacking of the T residues, while 5' stabilization reflects both inter- and intrastrand stacking of the T bases over the adjacent terminal GC pairs.

We have also used CD spectroscopy to evaluate the influence of dangling ends on the conformational preferences of each duplex. We have found that the addition of dangling T residues does not alter the low salt "B" conformation of either core duplex at 25°C. In 5 M salt (25°C), $d[(CG)_3TT]_2$ displays a partially inverted CD spectrum similar to the "Z-like" conformation observed for $[d(CG)_3]_2$ in high salt. The salt dependent conformational behavior of $[dT_2(CG)_3]_2$ is still under investigation. This work was supported by a grant from the National Institutes of Health (GM23509).

T-Pos9 SPECTROSCOPIC EVIDENCE FOR STRONG INTERACTIONS BETWEEN DNA DOUBLE HELICES IN THE CONDENSED STATE. C. DeMarco, S.M. Lindsay, M. Pokorny and J. Powell, Physics Department, Arizona State University, Tempe, AZ. 85287 and A. Rupprecht, Arrhenius Laboratory, University of Stockholm, S-106 91 Stockholm, Sweden.

We have studied the acoustic and lowest lying optic modes in Li- and Na-DNA fibers and films as a function of their degree of hydration. In Na-DNA at 66% r.h. we find bands at 34, 25, 15 and possibly 12 cm^{-1}. The 25 cm^{-1} band softens on hydration, the 34 cm^{-1} band does not. In Li-DNA (66% r.h.) we find a band at 30 cm^{-1} (which softens to about 19 cm^{-1} by 90% r.h., stabilizing at higher r.h.) and a band at 12 cm^{-1}. The acoustic data show that the longitudinal sound speed falls from about 4 to 2 km/s in both samples as they are hydrated, with a break in gradient at the point of decrystallization (80% r.h., Li-DNA, 92% r.h., Na-DNA). The most extensively crystalline films show a negative elastic anisotropy. The phonon attenuation also passes through a loss maximum on decrystallization of the samples. The rate of equilibration of a new conformation is controlled by the extent of the crystallinity of the samples. We interpret these data as evidence for strong interdouble-helical interactions and propose that the soft mode which drives conformation change is sensitive to these interactions.

T-Pos10 EFFECT OF HYDROXYL FREE RADICAL ON dTpA.

Aruna V. Arakali, James L. Alderfer and Harold C. Box, Biophysics Department, Roswell Park Memorial Institute, Buffalo, New York 14263, USA.

Formation of glycol modification is initiated by hydroxyl radical attack and occurs in X-ray irradiated aqueous solution of the dinucleoside monophosphate, thymidyl(3'-5')-2'-deoxyadenosine (dTpA). Four stereoisomers of the glycol modification are possible. We have examined the cis configurations, dTpA I and II that are also produced chemically by permanganate oxidation. ^{1}H, ^{13}C and ^{31}P NMR studies of dTpA I and II were carried out in aqueous solution. Relative to dTpA, the thymine glycol modifications I and II have these spectral characteristics: (a) upfield shifts of 6-H and 5-CH_3 and (b) the downfield shift of the 4-C=O and 5-CH_3; the upfield shift of 5-C and 6-C carbon resonances consistent with 5,6-saturation of the double bond of thymine ring, (c) downfield shift in phosphorus resonance, (d) changes in δ values of sugar protons. The changes in chemical shift values were consistent with those reported for thymine glycols. This initial study demonstrates that the HPLC and NMR techniques should be valuable tools for studying lesions induced by radiation and how these lesions alter the conformation of the DNA molecule.

T-Pos11 MAGNESIUM EFFECTS ON THE ANTICODON LOOP OF TRANSFER RNA. Steve Seifried and Barbara Wells. Chemistry Department. University of Wisconsin-Milwaukee. Milwaukee, WI. 53201

As magnesium is required for biological function, there has been considerable interest in the structural effects of magnesium on nucleic acids. The fluorescence of Y base in yeast $tRNA^{Phe}$ is quite sensitive to the addition of magnesium. We have measured the fluorescence lifetime of Y as a function of added magnesium using phase modulation effects. 470 MHz proton NMR of the methyl region was also followed using the same experimental conditions.

The Y base shows two fluorescence lifetimes (about 2 and 6 nseconds), the relative contributions of each component is magnesium dependent. Y base also has 4 methyl groups, which prompted us to use NMR to complement the fluorescence data. The methyl NMR is also sensitive to magnesium. Magnesium caused a number of resonances to change in chemical shift. Resonances assigned to Y base were perturbed, as were resonances assigned to bases in other regions of tRNA.

Supported by NIH GM 30700.

T-Pos12 TRANSIENT ELECTRICAL BIREFRINGENCE MEASUREMENTS OF THYMINE DIMER INDUCED DISTORTIONS IN SHORT RESTRICTION FRAGMENTS OF PLASMID DNA. CHRISTOPHER FARNSWORTH AND DON EDEN, DEPT. OF CHEMISTRY, SAN FRANCISCO STATE UNIV., SAN FRANCISCO, CA 94132.

It is possible to estimate the degree of bending, resulting from the induction of a cis-syn cyclobutane type thymine-thymine dimer in short restriction fragments of plasmid DNA by observing the changes in the rotational diffusion coefficient. Transient electrical birefringence measurements on dilute (4-9 μg/mL) monodisperse solutions of DNA permit the experimental determination of the rotational decay constants for rod-like or bent cylinders from the field free decay of the birefringence. Two fragments from sites 2375-2416 (Fragment A) and 941-991 (Fragment B) of pBR 322 were prepared by double endonuclease digestions, purified and irradiated with high pressure Hg lines at 313 and 365 nm in the presence of the photosensitizer, acetophenone. The resulting birefringence is relatively weak, only 30% of the amplitude from the birefringence of buffer alone. A reference Kerr cell which can provide a 100 fold rejection of the buffer birefringence was therefore incorporated into an improved birefringence apparatus with 10 ns resolution and 350 ns pulse width at low field strengths (3000-4500 V/cm). Preliminary results of samples in 0.5 mM magnesium acetate at 4 C suggest that neither Fragment A, with a single dimer at sites 2393-2394, nor Fragment B, with two dimers at sites 961-962 and 970-971, displayed significantly different τ_r's from those of non-irradiated control samples. For Fragment B, which contains two dimers and would be expected to express the largest change in the rotational decay, +light = 280 ns, control = 270 ns. These results contain a 5 ns uncertainty which imposes an upper limit of 15 degrees to the bend angle which may result from the presence of a thymine dimer within the helix. This work was supported by NIH #GM31674.

T-Pos13 CONFORMATION OF 5-FLUOROCYTIDINE: X-RAY AND NMR DETERMINATION.
S. D. Soni, T. Srikrishnan and J. L. Alderfer, Biophysics Department, Roswell Park Memorial Institute, Buffalo, NY 14263

5-Fluorocytidine (5FC) is an important antimycotic agent which also has antiviral and antitumor properties. We compare here the conformation of 5FC in the solid state as determined by single crystal X-ray diffraction with that in aqueous solution as determined by NMR. Crystals of 5FC are orthorhombic, space group $P2_12_12_1$, a = 9.853, b = 15.012, c = 15.290 A°, Z = 8 (two molecules/asymmetric unit), D = 1.52, D_c = 1.534 gms. cm^{-3}. Complete three dimensional data (to $2\theta \leq 154°$) was collected on a CAD-4 diffractometer using $\omega/2\theta$ scan. The structure was obtained by a combination of multisolution technique and trial and error methods and refined by full-matrix least squares to a final R value of 0.040 for 2333 observed reflections. Both the molecules are in the anti conformation, sugar pucker C3'-endo, and γ(C4'-C5') is g^+. The three-bond carbon-proton coupling constants between the base and the sugar are used to measure χ, and three-bond proton-proton couplings are used to measure sugar pucker and γ(C4'-C5'). The results showed that the molecules are in the anti-conformation. Sugar pucker is 36% C2'-endo and 64% C3'-endo. Exocyclic furanose conformation of γ is 74% (g^+), 19% (t) and 7% (g^-). (Supported by PSH CA-25438, National Cancer Institute, DHSS and Grant NIH GM 24864.)

T-Pos14 THE hisT GENE IS PART OF A MULTIGENE OPERON IN ESCHERICHIA COLI K-12.
Peggy Arps[1], Christopher Marvel[2], Beth Rubin[1], and Malcolm Winkler[1], [1]Northwestern Univ. Medical School Chicago, IL: [2]Naval Biomedical Research Laboratory of the Univ. of California, Berkeley, CA.

The Escherichia coli K-12 hisT gene has been cloned and its organization and expression analyzed on multicopy plasmids. The hisT gene, which encodes tRNA pseudouridine synthase I (PSUI), was isolated on a Clarke-Carbon plasmid known to contain the purF gene. The presence of the hisT gene on this plasmid was suggested by its ability to restore production of PSUI enzymatic activity and to restore suppression of amber mutations in a hisT mutant strain. A 2.3 kilobase HindIII-ClaI restriction fragment containing the hisT gene was subcloned into plasmid pBR322 and the resulting plasmid (designated 300) was mapped with restriction enzymes. Complementation analysis with different kinds of hisT mutations and tRNA structural analysis confirmed that plasmid 300 contained the hisT structural gene. Restriction fragments from plasmid 300 inserted downstream from the lac promoter established that the hisT gene is oriented from the HindIII site toward the ClaI site. Other subclones and derivatives of plasmid 300 containing insertion or deletion mutations were constructed and assayed for production of PSUI activity and production of proteins in minicells. These experiments showed: (1) the proximal 1.3 kilobase HindIII-BssHII restriction fragment contains a promoter for the hisT gene and encodes a 45,000 dalton polypeptide that is not PSUI; (2) the distal 1.0 kilobase BssHII restriction fragment encodes the 31,000 dalton PSUI polypeptide: (3) the 45,000 dalton polypeptide is synthesized in approximately an 8-fold excess compared to PSUI: and (4) synthesis of the two polypeptides is coupled, suggesting that the two genes are part of an operon. Insertion mutations and DNA sequence analysis confirmed that hisT is the downstream gene in the operon.

T-Pos15 BROWNIAN DYNAMICS SIMULATION OF THE SUPEROXIDE DISMUTASE-SUPEROXIDE REACTION. S. Allison, Dept. of Chem., Georgia State University, Atlanta, GA 30303; G. Ganti and J.A. McCammon, Dept. of Chem., University of Houston, Houston, TX 77004.

A Brownian dynamics trajectory method is used to study the diffusion controlled reaction between superoxide dismutase (SOD) and superoxide. The SOD dimer is modelled as a sphere with two reactive patches placed on opposite poles. Charges were embedded within the sphere to mimic the actual charge distribution of the protein and were derived from the known x-ray structure of bovine erythrocyte SOD. The net protonic charge of SOD is -4 at neutral pH. A dielectric constant of 78 was assumed throughout the system in this initial work. Electrostatic interactions are found to bias the substrate trajectories toward the active sites of the enzyme leading to a 40% enhancement in reaction rate relative to the simple model in which all the charge of SOD is concentrated at its center. Furthermore, a simple 5 charge model (which reproduces well the monopole through quadrupole moments of SOD) yields rate enhancements in excellent agreement with those based on more complex models. The effects of added salt are studied using simple Debye-Hückel screening between charges. Above an ionic strength of .03, increasing salt decreases the reaction rate as observed experimentally.

T-Pos16 A RESTRICTED SEARCH ALGORITHM PREDICTS THE FOLDING PATTERN OF LATTICE MODEL PROTEINS WITHOUT REFERENCE TO SPECIFIC LONG-RANGE INTERACTIONS

Stephen H. Bryant[1] and L. Mario Amzel[2] 1-Department of Biostatistics, Johns Hopkins University School of Hygiene and Public Health, 615 N. Wolfe St. Baltimore, MD 21205 2-Department of Biophysics, Johns Hopkins University School of Medicine, 725 N. Wolfe St. Baltimore, MD 21205

Simplified models of proteins as points on a chain traversing a two-dimensional lattice have been used previously by several researchers in theoretical studies of protein folding. In computer simulations of the lattice protein folding process conventional energy minimization algorithms generally converge to local minima, and do not correctly predict overall chain topology. Monte Carlo methods have been shown to converge to the correctly folded structure only when interactions between specific residues which are not adjacent on the chain have been included in the model. The present work describes a method which systematically searches all configurations where the conformational enthalpy associated with local segments of the lattice protein chain does not rise above a sliding minimum. Conformational enthalpy is calculated as a function of the number of contacts between any hydrophobic and between any hydrophilic and hydrophobic residues. The method successfully predicts the folding pattern of several lattice proteins. The requirement for minimum enthalpies over local chain segments is discussed with reference to actual protein folding topologies. Such restricted search methods may provide insight on how to overcome the local minima encountered in calculation of chain topology from linear sequence data.

T-Pos17 KINETICS OF COOPERATIVE MACROMOLECULAR BINDING IN THE CONTINUUM LIMIT. Charles P. Woodbury, Jr., Department of Medicinal Chemistry and Pharmacognosy, University of Illinois at Chicago, Chicago, IL 60680.

As a model for macromolecular binding we had proposed a "continuum" model (Biopolymers 20, 2225 [1981]) where the ligands were not bound to specific sites but instead could slide continuously over all positions on the macromolecule. We have now developed a treatment of the binding kinetics for this model in two important limiting cases: 1) irreversible (i.e. covalent) attachment of a ligand to its initial point of binding, and 2) reversible binding to a chain where the bound ligands very rapidly rearrange themselves to a new equilibrium distribution. We include the effects of binding cooperativity and of binding site exclusion.

T-Pos18 THE ROLE OF PROTEIN CONFORMATIONAL STATICS AND DYNAMICS

R.H. Austin, J.D. LeGrange, B. Tsuei, J. Glockner (Princeton University, Dept. of Physics)

3 experiments will be discussed that probe modern concepts of disordered systems as applied to globular proteins. The first experiment comprises a test of the Agmon-Hopfield conjecture that the low temperature recombination kinetics of heme proteins can be perturbed by maintaining the molecule in the deoxy state through the glass transition. The second experiment uses the time-resolved emission from terbium/Calmodulin to test the $\exp(-t^b)$ relaxation law for disordered system below the glass transition. The third experiment uses a unique differential dielectric relaxation cell to observe the dielectric relaxation of protein solutions as a function of temperature (to liquid nitrogen) and frequency.

We will discuss the relevance of these experiments to protein function and stress the new insights that condensed matter theory is providing in understanding the dynamics of macromolecules.

T-Pos19 ARE RINGS ON HELICAL SEGMENTS ALIGNED WITH THE HELIX' FIELD? H.R. Faber, R.S. Morgan, S. Snedden, R.J. Zauhar, Pennsylvania State University

Electrostatic theory suggests that the most favorable orientation of polarizable aromatic rings occurs when their normals are perpendicular to the electric field at their centers. Aromatic side-chains from Phe, Tyr, Trp & His residues which occur on helical segments in proteins necessarily lie in strong electrostatic fields produced by the cooperative action of the peptide dipoles. How are such rings oriented with respect to the helix' field? We have started to answer this question by computing the net fields due to the 4 helical segments of HEW lysozyme. We find that His 15 (in H1), Trp 28 and Phe 34 (both in H2) are aligned with the net field at their centers as expected. Results from the study of other proteins will be presented.

T-Pos20 AN APPROACH TO MODELLING THE STRUCTURAL EFFECT OF MUTATIONS ON SURFACE RESIDUES OF PROTEINS. Mark E. Snow and L. Mario Amzel, Department of Biophysics, The Johns Hopkins University School of Medicine, Baltimore, Md. 21205

A package of computer programs (Protein Conformational Analysis Package, PCAP) for the representation and modification of protein structures and for the calculation and minimization of their conformational energies has been developed. Conformational energies are calculated using a semi-empirical potential which includes charge-charge and van der Waals interactions as well as deviations from ideal geometry (bond lengths, bond angles, single and double bond dihedral angles). Single amino acid replacements are modelled by attaching the new side-chain in a standard geometry to the backbone and performing a local energy minimization. Larger changes are modelled as a series of single amino acid replacements, insertions and deletions. The coefficients for the different energy terms are calculated using a least square procedure to minimize the square of the forces on the atoms in the initial x-ray structure. The procedure can be used to determine coefficients locally so that they best represent the local characteristics of the structure. The ability to determine coefficients locally is also useful, for example, to calculate the effective dielectric constant as a function of the distance from the surface of the molecule. The programs are currently being used to analyze the combining sites of immunoglobulins. Results from this system will be discussed. (Supported by N.I.H. Grant AI20293).

T-Pos21 Differential Scanning Microcalorimetric (DSC) Study of A Partial Unfolding Transition of αα-Tropomyosin around 38°C. Peter K. Lambooy and Tian Y. Tsong. Department of Biological Chemistry, Johns Hopkins University School of Medicine, Baltimore, Maryland 21205

We report here the conformational stability of rabbit skeletal muscle αα-tropomyosin in the Cys-190 reduced (SH) and oxidized (SS) forms. The endotherms of both SH- and SS-tropomyosins were found sensitive to pH around 7.0, and most thermograms in the temperature range 20 to 70°C could be resolved into 3 two-state-like transitions. Among these three, the low temperature one (Tm1) was also found to depend on the oxidation state of Cys-190: the melting point was 47°C for the SH form and 30°C for the SS form, at pH 7.0. The Tm1 of SH-tropomyosin changed with pH: it shifted upward from 41°C at pH 6 to 48°C at 7.5, with an inflection point at pH 6.5. In contrast, the Tm1 of SS-tropomyosin shifted downward from 41°C at pH 6.0 to 30°C at pH 7.5, with an inflection point of pH 6.8. The two higher temperature transitions (Tm2=52°C and Tm3=59°C at pH 7.0) were not sensitive to the oxidation state of Cys-190, although they were slightly sensitive to pH. The enthalphy change associated with Tm1 was 100 kcal/mol at pH 6.0 and increased to 140 kcal/mol at pH 8.0 for the SH-tropomyosin. For the SS-tropomyosin, this value was 36 kcal/mol at pH 6.0 and decreased slightly to 28 kcal/mol at pH 8.0. The above results indicate that at 38°C, a partial unfolding of tropomyosin can be triggered either by the oxidation of Cys-190 or by the de-protonation of an ionizable amino acid residue, possibly His-153, around neutral pH. The DSC study is being extended to histidine modified tropomyosins and proteolytically cleaved tropomyosin fragments. This work was supported by NSF Grant PCM8408579.

T-Pos22 THE NATURE OF THE DOMAIN ASSOCIATION STEP IN THE FOLDING OF THE α SUBUNIT OF TRYPTOPHAN SYNTHASE. C. R. Matthews, M. R. Hurle and M. M. Crisanti, Department of Chemistry, The Pennsylvania State University, University Park, PA 16802.

The folding of the α subunit of tryptophan synthase (E.coli) from high concentrations of urea has previously been shown to involve stable intermediates which reflect the independent folding of two stable domains and their subsequent association. Studies of the effects of temperature, ionic strength and pH on the equilibrium and rate constants of refolding are helpful in constructing a model for the domain association reaction. The dissociation of the two domains is principally entropy-controlled, with an activation entropy of -47±2 cal/deg-mol. This may reflect ordering of solvent about hydrophobic groups buried at the interface between the folded domains of the protein. Ionic strength studies show small effects on stability and on the kinetics of folding. These results suggest that the domain association reaction is primarily controlled by hydrophobic groups located on both domains. The transition from the native form to the principal intermediate, which has a folded amino domain and an unfolded carboxyl domain, and the transition from the intermediates to the unfolded forms are both stabilized by a protonation even whose pK is 7.8. The relevant residue which is likely to be in the amino domain has a pK very similar to that for one of the four histidine residues in the protein.

This work was supported by PHS grants GM23303 and KO4 AG00153.

T-Pos23 THE EFFECTS OF CHARGE SUBSTITUTION IN THE FOLDING OF THE α SUBUNIT OF TRYPTOPHAN SYNTHASE. N. Tweedy and C. R. Matthews, Intr. by W. D. Taylor, Department of Chemistry, The Pennsylvania State University, University Park, PA 16802.

The urea-induced unfolding of the Gly 211 → Arg 211 single amino acid substitution variant of E. coli tryptophan synthase (E.C.4.2.1.20) has been studied by equilibrium and kinetic techniques to determine the role of this residue in folding and to elucidate the folding pathway. Equilibrium studies show that the Gly 211 → Arg 211 substitution decreases the stability of the native state and partially unfolded intermediates relative to completely unfolded forms. The rate of the first step in unfolding, N → I_3, where I_3 is an intermediate species, maintains the characteristic urea dependence of wild type (Gly 211), but is >10-fold faster for Arg 211. A previous study on the Gly 211 → Glu 211 mutant protein (Matthews et al. (1983) Biochemistry 22, 1445) has shown the opposite effects, stabilization of the Glu 211 protein and a 10-fold decrease in the N → I_3 unfolding rate. These opposing effects from sidechains of opposite charge demonstrates the importance of an electrostatic interaction near position 211 in the folding of the mutants. Analysis of the Gly 211 → Arg 211 protein folding kinetics demonstrates the utility of the mutants in probing the kinetic models of folding.

T-Pos24 PROGRESS TOWARD A 3.0 ANGSTROM CRYSTAL STRUCTURE OF THE TRYPTOPHANYL-tRNA SYNTHETASE FROM BACILLUS STEAROTHERMOPHILUS. D. E. Coleman and C. W. Carter, Jr., Department of Biochemistry, University of North Carolina at Chapel Hill, Chapel Hill, NC 27514

We have previously reported the crystallization of a product complex of the tryptophanyl-tRNA synthetase from B. stearothermophilus (Coleman and Carter, 1984, Biochemistry 23, 361-385). The crystals (type IV) contain stoichiometric amounts of an enzymatically formed acyl-transfer product, tryptophanyl-2'(3')ATP, bound to the enzyme. This ligand is presumed to be bound to the binding site for the 3' terminus of the tRNA substrate.

The space group is $P4_12_12$ or its enantiomer with unit cell dimensions A=B=60.9Å, C=234.4Å. We have used the UCSD Digital Bioimage Group multireflection diffractometer to measure intensities to 3.0Å resolution for the parent and to various resolutions for several potential heavy-atom derivatives. Progress toward solving this structure will be reported. Supported by NIH grants GM 26203 and RR 01964.

T-Pos25 ELECTRON MICROSCOPY OF FROZEN HYDRATED CRYSTALS OF THE T4 DNA HELIX DESTABILIZING PROTEIN GP32*I R. A. Grant, M. F. Schmid, J. F. Deatherage, W. Chiu and J. Hosoda+, Dept. of Biochemistry, Univ. of Arizona, Tucson, Az. 85721, and Lawrence Berkeley Laboratory+, Univ. of California, Berkeley, Ca. 94721

Gp32*I is a DNA helix destabilizing protein (M.W. 29,000) derived from gp32, the product of gene 32 of the bacteriophage T4, by proteolytic removal of 50 amino acids from the carboxy terminus. Both gp32 and gp32*I bind cooperatively to single stranded DNA. Under low salt conditions gp32*I crystallizes as thin platelets suitable for electron diffraction analysis. A low resolution (20 Å) 3 dimensional reconstruction of this crystal in negative stain has been determined. In order to obtain higher resolution data we have collected low dose images of ice-embedded gp32*I crystals. Low dose images are typically very noisy due to the poor statistics of image formation. We have developed computer techniques for aligning and adding low dose images of frozen, hydrated gp32*I crystals in order to improve the signal to noise ratio of the data and recover high resolution structural phase information that is buried in noise. Eleven image areas corresponding to about 50,000 unit cells were aligned in reciprocal space by applying the phase shifts that minimized the RMS phase deviation between their Fourier coefficients. Composite structure factors were obtained by vector addition of the aligned Fourier coefficients. The average figure of merit for the phases of all the composite structure factors out to 7 Å resolution was 0.74. The protein dimer is well resolved in the projection map calculated from the composite structure factors.

T-Pos26 NEUTRON SCATTERING FROM DENSE PROTEIN SOLUTIONS. R. Nossal, S-H. Chen and C. Glinka. Physical Sciences Lab., DCRT, NIH, Bethesda, MD 20205, Department of Nuclear Engr., MIT, Cambridge, MA 02139, and Reactor Div., NBS, Gaithersburg, MD 20899.

Small angle neutron scattering (SANS) has been used to examine concentrated BSA solutions of up to 20% protein wt/vol. Spectra were obtained for several solvent conditions, including low ionic strength near the isoelectric pH and a wide range of ionic strength in NaCl solutions near neutral pH. At higher protein concentrations, scattering spectra show distinct features which can be ascribed to strong intermolecular interactions. Scattering data are fit to theoretical curves derived from models of intermolecular interaction consisting of hard-core plus exponentially decaying repulsive potentials. For all experimental conditions we are able to account for intermolecular structure using DLVO repulsive potentials. We demonstrate that it is possible to extract size parameters and molecular weight using concentrated solutions, rather than employing a series of dilute samples approaching the zero-concentration limit. By relating an experimentally determined strength parameter to the DLVO potential, we obtain the effective charge on the protein. Also, interpretation of the data in terms of a detailed model yields the number of exchangeable protons in the molecule and the degree of hydration.

T-Pos27 USE OF NONLINEAR REGRESSION ANALYSIS OF SMALL-ANGLE X-RAY SCATTERING DATA TO DETECT NON-HOMOGENEOUS ELECTRON DENSITIES IN TWO PROTEINS. Helmut Pessen, Thomas F. Kumosinski, and Eleanor M. Brown, Eastern Regional Research Center, USDA, Philadelphia, PA 19118.

Regions of different electron densities within a macromolecule have characteristic effects on Guinier plots, and it is known that analysis of such plots can give information about these regions. To overcome the limited sensitivity of graphical methods we have employed nonlinear regression analysis to study the holo and apo forms of bovine lactoferrin (Lf) and of the dogfish-muscle (M_4) and beef-heart (H_4) isozymes of lactate dehydrogenase (LDH). Sedimentation analysis found Lf to be a dimer at pH 7.0, where two moles of ferric iron are bound per mole of protein, but a monomer at pH 2.5, where the iron is dissociated. In both cases nonlinear regression analysis of the excess scattering curves showed double Gaussians without residual function and indicated two regions of different electron densities with a common electronic centroid. The holo form appeared as a 160,100-dalton particle with electron densities corresponding to radii of gyration (R_G) of 47.7 and 20.0 Å; the apo form, of 77,200 dalton, had R_G values of 36.7 and 15.3 Å, higher total hydration, and a higher fraction of total molecular weight attributable to the lower density region. For H_4 LDH, a known tetramer, we found a molecular weight of 141,000, R_G of 37.1 Å, hydration of 0.34 g H_2O/g dry protein, and a scattering-equivalent oblate spheroid of axial ratio 0.4; corresponding values for M_4 isozyme showed small but significant differences. A further difference was that H_4 had a larger amount of the higher-density region than M_4, and this region was as anisotropic as the total molecule, whereas in M_4 it was less so. The results demonstrate the value of this kind of analysis and its possible use in detecting similar effects in so-far unsuspected systems.

T-Pos28 EFFECTS ON THE NH_2-TERMINAL REGIONS OF LOSING THE LOOSE ENDS IN A COENZYME DEPENDENT SYSTEM. Ana Iriarte, Kenneth Kraft and M. Martinez-Carrion. Departments of Biochemistry, University of Navarre, Pamplona, Spain and Virginia Commonwealth University, Richmond, Virginia 23298.

Proteolytic loss of the NH_2-terminal region of the isozymes of the pyridoxal phosphate (PLP) dependent aspartate transaminase induces a catalytic loss and conformational changes. The effect of various proteases varies and the loss in activity is produced after removal of a 19 amino acid NH_2-terminal peptide. Differential scanning calorimetry shows that new conformations of lower thermal stability are produced. These arise from the creation of at least 2 distinct core proteins missing the amino terminal region. Spectrometric (UV, CD,NMR, FTIR) investigations give indications that the contact amino acids at the active site retain affinity for PLP and the enzyme's substrates and their analogs. Partial catalytic events can be followed in this system. None of the amino acids in the sections removed by protease form past of the catalytic site, yet they overlap the hydrophobic region of each companion subunit in these dimeric proteins. Ridigity over several structural domains in the remaining core protein appears altered as consequence of losing the NH_2-terminal portion. The resulting core protein becomes available to endoprotease action to which native protein is resistant.

T-Pos29 PHOSPHORYLATION OF HYDROXYLYSINE RESIDUES IN COLLAGEN. Y. Urishizaki and S. Seifter. Department of Biochemistry, Albert Einstein College of Medicine, Bronx, N. Y., 10461.

O-Phosphohydroxylysine (PHyl) was synthesized and its position of elution determined using the single column system of a Beckman Model 119 BL amino acid analyzer and its movement established on thin layers of cellulose using electrophoresis and chromatography. ^{32}P-inorganic phosphate was incubated with confluent layers of calf aorta smooth muscle cells and of IMR-90 human fetal lung fibroblasts for periods of 4 hours in presence of ascorbate. Cells were scraped, washed with buffer, and hydrolyzed in 2N HCl for 4 hours at 95° C, conditions under which PHyl is stable. HCl was removed by evaporation, the material applied to Sephadex G-50 and eluted with water. Dried eluate was resolved on the analyzer and yielded two peaks containing ^{32}P. The second corresponded to synthetic PHyl emerging at 16.7 minutes. Additional incubations were performed with ^{32}P-inorganic phosphate and [^3H] 4,5-lysine. Although lysine goes into most proteins, only in collagenous proteins does it become hydroxylated. In this experiment, then, the hydroxylysine should be labeled in both sidechain and phosphate group. Indeed such a result was obtained; a compound emerged at peak 2 corresponding to PHyl, and this was doubly labeled. Examined by electrophoresis at pH's of 3.5 and 1.9 and by chromatography, the material was clearly distinguished from other phosphoamino acids and phosphoethanolamine, and contained the ^{32}P and ^3H labels in almost theoretical stoichiometry. Preliminary experiments in which homogenates of cells were incubated with γ-^{32}P-ATP showed a small but significant amount of PHyl, suggesting that a protein kinase phosphorylates hydroxylysine residues in cell-associated collagens. Supported by NIH grants AG00374, AM17702 and AM20541.

T-Pos30 METARHODOPSIN INTERMEDIATES OF SYNTHETIC ANALOG PIGMENTS. Geoffrey Renk, Jesmael Zingoni, Yat Sun Or and Rosalie Crouch, Medical University of South Carolina, Charleston, S.C.29425

The chromophore binding site of rhodopsin has been studied extensively using synthetic analogs of retinal to probe the structural requirements of pigment formation and function. These have helped to explain the absorption spectrum of rhodopsin and the physical behavior of the chromophore during early photochemical events, such as cis-trans isomerization. We reported previously the syntheses of a retinal analog containing a spin label 1 and of an acyclic retinal analog 2, and the properties of the pigments the 9-cis isomers formed with bovine opsin. We report here the photochemical behavior of these isorhodopsins under conditions which favor the formation of a stable Metarhodopsin I or II state. The artificial pigments used in this study were stable to NH OH and excess 11-cis retinal in the dark. The pigments were illuminated with white light at 0°C at pH 8.5 or 5.1, conditions which produce a stable photoequilibrium favoring metarhodpsin I or II, respectively. The spin-labelled analog pigment and the acyclic analog pigment showed similar stable shifts in the λmax of the UV-VIS spectrum 8-12nm towards shorter wavelenghths in response to light indicating that formation of a meta state is not dependent on the presence of the retinal ring. The EPR spectrum of the spin-labelled pigment showed no significant change when motional effects were removed at low temperature, suggesting that protein conformational changes involve the polyene chain of the chromophore rather than the ring portion. The photchemistry of other relevant analogs will also be discussed.

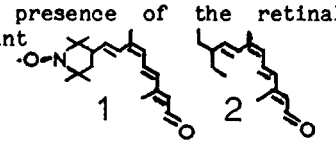

(Supported by NIH EY04939)

T-Pos31 FOURIER-TRANSFORM INFRARED STUDIES OF OCTOPUS RHODOPSIN, ITS METARHODOPSIN FORMS, AND OCTOPUS HYPSORHODOPSIN. Kimberly A. Bagley, Laura Eisenstein, Department of Physics, University of Illinois at Urbana-Champaign, 1110 West Green Street, Urbana, IL 61801; Thomas G. Ebrey, Department of Physiology and Biophysics, University of Illinois at Urbana-Champaign, Urbana, IL 61801; Motoyuki Tsuda, Department of Physics, Sapporo Medical College, Sapporo 060, JAPAN.

Infrared difference spectra are presented between octopus rhodopsin, its two metarhodopsin forms (acid and alkaline metarhodopsin), and its low temperature (20K) photoproduct, hypsorhodopsin. The analogous difference spectra are also presented for octopus rhodopsin which has been suspended in deuterium oxide, and hence, in which all exchangeable protons are replaced by deuterons. Comparison of the difference spectra for octopus rhodopsin in water and deuterium oxide has been used to identify the state of protonation of the Schiff base linkage in octopus rhodopsin, acid metarhodopsin, alkaline metarhodopsin, and hypsorhodopsin. The data presented are also discussed in terms of the isomeric state of the chromophore in these various intermediates and changes occurring in the opsin during the photosequence. This work was supported in part by grants HEW PHS GM32455 and HEW PHS EY01323.

T-Pos32 RHODOPSIN IN POLYMERIZED BILAYER MEMBRANES. P. N. Tyminski, L. H. Latimer, D. F. O'Brien Research Laboratories, Eastman Kodak Company, Rochester, NY 14650

Purified bovine rhodopsin was inserted into preformed partially polymerized lipid vesicles by the following procedure. Sonicated vesicles composed of equal parts of dioleoylphosphatidylcholine (PC) and dienoylPC were photolyzed with 254 nm light to polymerize the dienoylPC and form domains of dioleoylPC and poly(dienoyl)PC. Rhodopsin-octylglucoside(OG) micelles were slowly added to the vesicle suspension to give 15 mM OG (below the OG cmc). The suspension was incubated, then dialyzed and purified on a sucrose gradient. Ultracentrifugation revealed two populations of lipid membranes, a lipid (rhodopsin-free) band at the top of the gradient and a denser rhodopsin-lipid band. The narrow rhodopsin-containing band was harvested and found to contain 90 phosphorus groups per rhodopsin. The rhodopsin:poly(dienoyl)PC-dioleoylPC membranes were compared with control membranes of rhodopsin:dioleoylPC(1:90) (prepared by insertion) and rhodopsin:egg PC-egg PE(1:50-50) (prepared by detergent dialysis). Limited proteolysis by thermolysin of the rhodopsin in each of the two membranes prepared by insertion shows one population of rhodopsin. These rhodopsins are cleaved at the carboxyl terminus and correspond to rhodopsin in the normal orientation found in rod outer segment disc membranes. In contrast, thermolysin proteolysis of the membranes prepared by detergent dialysis revealed two populations of rhodopsin, one in the normal orientation (proteolyzed) and one in the retrograde orientation (unproteolyzed) found in symmetrical reconstituted membranes. The effect of the membrane environment on the photochemical functionality of the rhodopsin and its ability to activate the ROS peripheral enzymes, G protein and phosphodiesterase, will be described.

T-Pos33 INHIBITION AND ENHANCEMENT OF PHOTORECEPTOR POTENTIAL BY SOME DIVALENT CATIONS. T. Nakamura* and T. Yoshizawa (Intr. by Govindjee), Kanebo Institute for Cancer Research, Kobe 652, Japan and Dept. of Biophysics, Kyoto University, Kyoto 606, Japan

Calcium (Ca^{2+}) is one of the candidates for the intracellular transmitter in visual photoreceptors. Moreover, other divalent cations have been reported to modify the responses of some receptor cells (e.g., hormone receptors). We have tried to examine the effects of these cations (Ca^{2+}, Mg^{2+}, Mn^{2+}, Zn^{2+}, Ba^{2+}) on photoreceptors by electrophysiology. We recorded "Fast PIII" responses (receptor potentials) from a frog retina perfused with aspartate ringer and 0-5 mM of the divalent cations. At the 5 mM level, all these cations inhibited Fast PIII, but at the level of 1 mM, Mg^{2+} did not inhibit. Fast PIII was rapidly reduced by Ca^{2+} and recovered rapidly after removing Ca^{2+}. For the other cations, Fast PIII decreased rather slowly; it reversed at most 40% after Zn^{2+}-treatment, and it "overshot" to about 120% and then reversed 50 to 80% after Mn^{2+}-treatment. This "overshooting" after Mn^{2+} was dependent on the concentration of Mn^{2+} and the period of the incubation. Thus, Mn^{2+} can enhance Fast PIII. However, when the incubation was long (e.g., $\geq$ 20 min), the "overshoot" was small or not seen. When the retina was incubated with Mn^{2+} and Zn^{2+}, the "overshoot" was not seen, so it seems that the enhancement by Mn^{2+} competes with the reduction by Zn^{2+}. Mn^{2+} and Ca^{2+} might affect the same site of the receptor to reduce its response, and Mn^{2+} and Zn^{2+} might affect another site to enhance and reduce respectively its response. *Present address: University of Illinois, Dept. of Physiology and Biophysics, 524 Burrill Hall, 407 S. Goodwin Avenue, Urbana, IL 61801 U.S.A.

T-Pos34 VOLTAGE DEPENDENT CONDUCTANCES PRESENT IN SINGLE ISOLATED CONE PHOTORECEPTORS. A.V. Maricq and J.I. Korenbrot, Department of Physiology, University of California at San Francisco, San Francisco, CA 94143

The electrical properties of the vertebrate cone photoreceptor are not nearly as well understood as those of the rod photoreceptor. This is in part due to the unavailability of large numbers of isolated cone photoreceptors suitable for electrophysiological studies. We have succeeded in enzymatically dissociating large quantities of single cone photoreceptor cells (10,000 - 50,000 cells per retina), from the retina of the lizard, Sceloporus orcutti. Most of these cells lack an outer segment, however their axons and synaptic terminals remain intact.

These cells can be recorded from for several hours with patch electrodes. In whole cell patch clamp experiments, the resting potential of these cells is typically -45 - -50 mv. The input impedance is generally greater than 2 gigaohms, the cell capacitance is typically 8 - 15 picofarads, and the maximum currents generated under voltage clamp are usually less than 0.5 nanoamps. Under current clamp, voltage records exhibit a characteristic nose-shaped response to hyperpolarizing pulses. Under voltage clamp, and while holding the cell at -60 mv, depolarizing voltage pulses revealed a complex mixture of currents. Depolarizing pulses up to -20 mv exhibited a rapidly activating inward current which did not appreciably inactivate during the 150 ms pulse. Depolarizing pulses beyond -20 mv elicited, in addition to the rapidly activating inward current, a large slowly inactivating outward current. Hyperpolarizing pulses generated a slowly activating inward current. Single channels recorded in the cell attached configuration demonstrated a non-homogeneous distribution over the synaptic terminal, nuclear, and ellipsoid regions of the cell.

T-Pos35 **DIFFERENTIAL SPECTROPHOTOMETRY OF PHYCOMYCES PHOTOMUTANTS.** B. A. Horwitz, C. H. Trad and E. D. Lipson, Department of Physics, Syracuse University, Syracuse, NY 13210.

Blue light responses of Phycomyces include phototropism, photocarotenogenesis and photodifferentiation. The photoreceptors for blue light in Phycomyces and other organisms have so far eluded identification, though flavins are believed to serve as chromophores. Some photomutants have receptor lesions, as shown by action spectra (Galland and Lipson, Photochem. Photobiol. in press). To correlate pigment differences with photoreceptor mutations, we measured in vivo absorption spectra of carotene-deficient albino strains (carA, carB, carA carR and carB carR), which respond normally to light. For mycelial samples, the spectra and their second derivatives show cytochrome bands, as well as peaks near 455 and 485 nm. The 485 nm peak was similar in strains C2 (carA), C1 and C5 (carB), as well as C173 (carB carR). This peak is thus unlikely to be due to carotene, and might belong to flavoprotein(s). In L6 (carA madB), it is shifted to 478 nm. In several carA strains, the trough between the 485 nm peak and the 520-530 nm cytochrome bands was filled in by a new 495 nm component. This change was found in C148 (carA madC); L5 and B77 (carA madA); L10, L11 and L14 (carA madE), as well as B99, C169 and S40 (carA). The 495 nm peak clearly is not specific to the mad genotypes. Work with subcellular fractions should help show which spectral differences are associated with photoreception. In vivo differential spectrophotometry has revealed spectral components related to the photoreceptor in Trichoderma, another fungus that responds to blue light (Horwitz, Gressel, Malkin and Epel, submitted). (Supported by NSF grant PCM-8316458).

T-Pos36 **SYSTEM ANALYSIS OF PHYCOMYCES LIGHT-GROWTH RESPONSE WITH SUM-OF-SINUSOIDS TEST STIMULI.** P. Pratap, A. Palit and E. D. Lipson, Department of Physics, Syracuse University, Syracuse, NY 13210.

The fungus Phycomyces blakesleeanus responds to blue light over the intensity range from 10^{-9} W m^{-2} to 10 W m^{-2}. The elongation rate of the sporangiophore changes transiently in response to changes in the ambient light intensity; this light-growth response is related to phototropism. Together, these responses serve as a model for photosensory transduction in primary receptor cells. We have studied the input-output relationship of the light-growth response using the sum-of-sinusoids method (Victor and Shapley, Biophys. J. 29:459, 1980). This (nonlinear) relationship can be expressed mathematically by a set of weighting functions called kernels. All experiments were done on the Phycomyces tracking machine under control of a microcomputer. The linear kernel of the system was determined at 12 wavelengths (383-529 nm, at temperature T = 20°C), and at four temperatures (17-26°C at 477 nm). These linear kernels were interpreted in terms of two models: a kinetic model, which contains a first-order process and two identical second-order processes in cascade (Lipson, Biophys. J. 15:989, 1975), and a model consisting of a cascade of first-order chemical reactions. A fit of the experimentally determined kernel to these models gives estimates of the time constants of the individual processes, the latency, and an overall amplification factor. The latency is the only parameter that varies significantly with wavelength and temperature. Because the latency in the cascade model depends on the rates of the individual reactions, light may not only act at the input, but also affect intermediate reactions in the transduction chain. (Supported by NIH grant GM29707).

T-Pos37 INVESTIGATION OF ENZYME TURNOVER OF VOLTAGE INDUCED ATP SYNTHESIS IN SOLUBILIZED, RECONSTITUTED MITOCHONDRIAL ATPase. Barry E. Knox* and Tian Y. Tsong. Department of Biological Chemistry, The Johns Hopkins University School of Medicine, Baltimore, MD 21205

ATP synthesis activity of FoF1-ATPase has so far been demonstrated for the enzyme in its native membrane environment. For solubilized, reconstituted enzyme, only ATP/Pi exchange activity can be measured. The application of electric field has allowed us to directly demonstrate ATP synthesis in this isolated enzyme system [Knox & Tsong, J. Biol. Chem. 259, 4757 (1984)]. However, despite great efforts from several laboratories, no multiple turnovers have been induced with a single electric pulse. This contrasts the result with submitochondrial particles, with which 8-12 ATPs per ATPase were induced by a single electric pulse of 30 kV/cm, 100 μs. Here we compare ATP synthesis, ATP/Pi exange, proton translocation and ATP hydrolysis activities of purified enzyme using three reconstitution procedures: the detergent dialysis method [Kagawa & Racker, J. Biol. Chem. 246, 5477 (1971)], the detergent dilution method [Serrano et al., J. Biol. Chem. 251, 2453 (1976)], and the sucrose gradient method [Laird & Cunningham, To be published (1984)], using sodium cholate, CHAPS and octylglucoside. The first two methods produced reconstituted ATPase which catalyzed ATP/Pi exchange, proton pumping, ATP synthesis and hydrolysis, but again no multiple turnovers in synthesis with a single voltage pulse. The third method reconstituted only the ATP hydrolysis activity. Examination of effects of detergents on these enzyme activities suggests that detergent can render mitochondrial membrane or lipid bilayer leaky to ions under an electric field, and at detergent concentration of 0.05 mole %, ATP synthesis diminished because of lost of ion permeation barrier in these membranes. This work was supported by NIH Grant GM28795.

T-Pos38 BENZOYL BENZAMIDOFLUORESCEIN: A FLUORESCENT PHOTOAFFINITY LABEL FOR THE ADENINE NUCLEOTIDE BINDING SITES OF ENZYMES. J.E.Rosen and P.S.Coleman, Laboratory of Biochemistry, Dept. of Biology, New York University, NY, NY 10003.

Previously, we designed and used benzophenone derivatives of adenine nucleotides (BzATP & BzADP) as photochemically active covalent labelling substrates for the mitochondrial F_1-ATPase (JBC, 257:2834, 1982). We now present preliminary work with a new fluorescent benzophenone photoaffinity probe, 4-benzoyl-1-benzamidofluorescein (BzAF), and its effects on the ATP-requiring enzymes creatine kinase and submitochondrial particle (SMP) ATPase. Fluorescein, a fluorescent conjugated-ring moiety, has been employed in various derivative forms as a specific nucleotide binding site ligand for enzymes that possess an affinity for the adenine ring. Thus, FITC, diiodo- and tetraiodofluorescein, among other covalently reactive fluorescein analogs, were found to seek out and chemically crosslink to the NAD^+ domain of LDH, and to the ATP binding sites of yeast hexokinase, Na/K-ATPase, and the sarcoplasmic reticulum Ca^{2+}-ATPase. In our studies with creatine kinase and SMP ATPase, natural ATP and ADP effectively protected against enzyme inhibition due to photolysis in the presence of BzAF, indicating that this new fluorescein photolabel is site selective for adenine nucleotide domains on these enzymes. Pseudo-first order reaction conditions for photolytic enzyme inhibition by the BzAF yielded an apparent K_D of 65 uM and a rate constant for irreversible inactivation of 0.66 min^{-1} with the SMP ATPase.

T-Pos39 ANOMOLOUS ^{18}O EXCHANGE DURING ATP SYNTHESIS BY MITOCHONDRIAL F1 ATPASE. Jacqueline J. Sines and David D. Hackney, Carnegie-Mellon University, Pittsburgh, PA 15213

Oxygen exchange between water and phosphate has proven to be an effective probe for the catalytic mechanisms of mitochondrial F1 ATPase. ^{18}O-ATP distributions produced during oxidative phosphorylation using highly enriched Pi have been shown to be significantly skewed in favor of singly and doubly labeled species (Hackney, Fed. Proc. 42, 1923 (1983)). We present two types of mechanisms which can explain such label patterns. The first involves nonequivalence of Pi oxygens during their scrambling between reaction reversals. Such models invoke partial restriction of the movement of bound Pi, consistent with the predicted nature of the binding site. The second category is based on various possible elaborations of the alternate site cooperativity model, which can explain the substrate dependence of the product release rate. (Hackney and Boyer, J. Biol. Chem. 253, 3164 (1978)) Lags in product release during a single turnover which are predicted by such cascade mechanisms can also produce the observed elevations in intermediately labeled species. The mathematical techniques used to analyze these mechanisms promise to be of use, not only in oxygen exchange analysis, but in enzyme kinetics in general.

Supported by grant AM 25980 from the USPHS and by an established Investigatorship from the American Heart Association to DDH. JJS is supported by an NIH National Research Service Award (GM-08067) awarded to the Department of Biological Sciences.

T-Pos40 OUTER-MEMBRANE LYSIS INCREASES SUSCEPTIBILITY OF MITOCHONDRIA TO INHIBITION BY CATIONIC ANTICANCER DRUGS. C.A. Mannella, N. Capolongo and R.C. Berkowitz, Wadsworth Center for Laboratories and Research, New York State Dept. of Health, Albany, NY 12201 and Dept. of Biological Sciences, State Univ. of New York, Albany, NY 12222.

The anticancer drugs adriamycin and methylglyoxal-bis(guanylhydrazone) (MGBG) inhibit mitochondrial respiration. We find that the inhibitory affects of these drugs on isolated rat-liver mitochondria are markedly increased after the outer membranes of the organelles have been lysed, either by osmotic shock or by digitonin. For example, inhibition by MGBG of succinate oxidation in untreated mitochondria is generally incomplete; 50% inhibition (when achieved) occurs at MGBG concentrations of 30-80 mM. For mitochondria with lysed outer membranes, inhibition by MGBG is complete, 50% inhibition occurring at drug levels of 6-10 mM. (Quantitatively similar results are obtained with the naturally occurring polyamines spermine and spermidine.) Likewise, adriamycin incompletely inhibits succinate oxidation of untreated mitochondria at levels above 1 mM but completely inhibits the same reaction when applied to mitochondria containing lysed outer membranes (50% inhibition at adriamycin concentrations of 0.1-0.2 mM). One explanation for these results is that, contrary to conventional wisdom, the outer mitochondrial membrane may represent a permeability barrier to some small (MW < 5000) organic molecules, in particular those bearing a net positive charge. It is known, for example, that the channels (called VDAC) which have been isolated from mitochondrial outer membranes are more permeable to anions than to cations (Colombini, 1979, Nature, 279:643). (Supported by NSF grant PCM 83-15666.)

T-Pos41 REYE'S SYNDROME: GENERATION OF ALLANTOIN FROM THE OXIDATION OF URATE BY CYTOCHROME $\underline{c}^{+3}$. M. E. Martens and C. P. Lee, Department of Biochemistry, Wayne State University School of Medicine, Detroit, Michigan 48201.

As indicated by the results of a previous study in this laboratory (Segalman and Lee, Arch. Biochem. Biophys., 214, 522, 1982), allantoin in the presence of calcium ions may be one possible agent responsible for the mitochondrial injuries in Reye's syndrome. It has been shown that uricemia is associated with this disease and that the severity of the neurological symptoms correlates with the plasma uric acid levels. Humans lack the enzyme, uricase, which catalyzes the oxidation of urate by molecular oxygen to allantoin. Therefore, an investigation of possible alternative sources of allantoin has been initiated. Urate is a strong reducing agent which can reduce cytochrome $\underline{c}^{+3}$ non-enzymatically. When carried out at pH 8.0, in addition to the reduction of cytochrome $\underline{c}^{+3}$, CO_2 and H^+ were also produced, with a stoichiometry of cytochrome $\underline{c}^{+2}$:H^+ equal to 2:1. In each case, the reaction rate was proportional to the concentrations of urate and cytochrome $\underline{c}^{+3}$. The participation of molecular oxygen in this reaction could not be demonstrated. Based on these results, the following balanced reaction can be written: urate$^-$ + 2 cyt. $\underline{c}^{+3}$ + 2 H_2O $\longrightarrow$ allantoin + 2 cyt. $\underline{c}^{+2}$ + H^+ + CO_2. We propose that allantoin can be generated from the oxidation of urate by cytochrome $\underline{c}^{+3}$, and that this is a potential source of allantoin in human tissues. This could be of particular importance in patients with Reye's syndrome, in whom the elevated plasma uric acid may push the tissue levels of allantoin over the threshold required for mitochondrial membrane damage to occur. (Supported by grant from the National Institutes of Health)

T-Pos42 EVIDENCE FOR A RELATIONSHIP BETWEEN HEXOKINASE-BINDING AND THE MITOCHONDRIAL VDAC PROTEIN IN AS-30D HEPATOMA CELLS: DCCD LABELS THE PORE PROTEIN AND INHIBITS HEXOKINASE BINDING. Richard A. Nakashima, Patrick S. Mangan*, and Peter L. Pedersen, The Johns Hopkins University School of Medicine, Department of Biological Chemistry, Baltimore, Maryland 21205 and *The University of Maryland, Department of Zoology, College Park, Maryland 20742

We have purified a pore-forming protein from AS-30D rat hepatoma mitochondria which shows the voltage-dependent, anion-selective channel-forming (VDAC) activity characteristic of the outer membrane pore protein of normal rat liver mitochondria. The purified fraction, when analyzed by SDS-PAGE and Coomassie blue staining, consists of only one identifiable species of approximately 35,000 daltons. It exhibits an amino acid composition similar to that reported for rat liver mitochondrial pore protein. When assayed for channel-forming activity in lipid bilayer membranes the purified protein exhibits a specific activity of 64 channels/min/μg protein. It has recently been reported that the outer membrane pore protein and the hexokinase receptor protein of rat liver mitochondria are identical and that DCCD binds to the rat liver mitochondrial porin. We have examined the effects of DCCD pretreatment of mitochondria on their ability to bind tumor hexokinase. Both AS-30D and rat liver mitochondria show a dose-dependent inhibition of hexokinase-binding following DCCD pretreatment, with 50% inhibition occurring at less than 2 nmol DCCD/mg protein. When AS-30D mitochondria were labeled with [^{14}C]DCCD at 2 nmol/mg one of the few proteins labeled was the 35 kD protein. Purification of the VDAC protein from [^{14}C]DCCD labeled mitochondria confirmed that the labeled 35 kD band was the VDAC protein. Experiments are currently in progress to determine the effects of DCCD-treatment on VDAC activity. (Supported by NIH Grant CA 32742)

T-Pos43 Inhibition Characteristics by Epoxycreatine on the Mitochondrial Creatine Kinase (CKm) Isozyme. Stephen M. Krause and William E. Jacobus. Dept. of Medicine, Div. of Cardiology, The Johns Hopkins School of Medicine, Baltimore, MD.

Since the identification of CKm as a dimer on the inner membrane of the mitochondrion it has been assumed that the activation characteristics for each monomer were identical because of the behavior of the released isozyme. Using the specific inhibitor epoxycreatine we studied the inhibitory characteristics of CKm and discovered that the isozyme exhibits two distinct inhibitory sites. These sites are characterized by two different t1/2 activation times with increasing inhibitor concentrations.

[epoxycreatine]	t1/2 site "A"	t1/2 site "B"
membrane bound CKm		
25 mM	73 min	122 min
40 mM	35 min	80 min
50 mM	29 min	75 min
69 mM	21 min	60 min
released CKm		
8 mM		253 min
20 mM		113 min

The bound form of CKm demonstrates a facilitation for substrate binding at site "A" which is lost when the enzyme is released from the membrane. This greater than two fold decrease in the inactivation of site "A" indicates a distinct preference of one of the sites for epoxycreatine when the enzyme is in the bound state. The released CKm dimer demonstrates only a single inactivation site which is similar to to the "B" site of the bound enzyme indicating no distinction or preference between sites. The results of this study indicate that the CKm exhibits two distinct binding sites for epoxycreatine when the isozyme is bound to the inner mitochondrial membrane. The implications of these findings are that the increased affinity at site "A" may indicate a preferred associaton of substrate for the CKm which may facilitate the entry of mitochondrial derived substrates to the active site of the CKm and contribute to the substrate functional coupling between the adenine nucleotide translocase and the CKm.

T-Pos44 PRACTICAL APPLICATIONS OF A GENERAL PURPOSE TCA CYCLE MODEL. Joanne K. Kelleher, Robert T. Mallet and Blackshear M. Bryan III, Dept. of Physiology, George Washington U. Medical Center, Washington, D. C. 20037

A model for steady state carbon isotope distribution in the tricarboxylic acid cycle (TCA) and related pathways has been developed. The model yielded 16 steady state equations containing five unknown flux ratios. To solve for the values of these unknowns an investigator need only measure labeled CO_2 production and specific activity (SA) ratios of citrate carbons. This theoretical work resulted in novel approaches to three important problems in energy metabolism. The first problem concerns the metabolism of glutamine, a major energy source for certain cell including intestinal epithelium and mammalian cells in culture. To determine net flux of carbon from glutamine into the TCA cycle we compare the rate of $^{14}CO_2$ production from (1,4-14C) succinate and (2,3-14C)succinate. To determine if glutamine is completely oxidized to CO_2 we determine the ratio, SA citrate C4+5 : SA citrate C2+3 during steady state metabolism of (2,3-14C)succinate. A second problem concerns a critical branch point in metabolism, flux of pyruvate to acetyl CoA versus flux to oxaloacetate.Our model yields an equation which detects pyruvate carboxylation by comparing the ratios of $^{14}CO_2$ production from radioisotopes of succinate and pyruvate. The third problem focuses on estimates of gluconeogenesis from labeled three carbon precursors. These estimates require a correction factor to compensate for isotope dilution as gluconeogenic flux interacts with the TCA cycle oxaloacetate pool. Our model yields a correction factor which is considerably more complex than that in current use. Specific tests are presented which allow an investigator to determine if use of this more complex correction factor is warranted in an experimental situation.

T-Pos45 ANTIMYCIN-SENSITIVE CYTOCHROME b REDUCTION: RECOGNITION OF AN ANTI-ELECTROGENIC ELECTRON TRANSFER IN THE bc_1 COMPLEX OF *Rhodopseudomonas sphaeroides* Ga, D.E. Robertson, C.C. Moser, K.M. Giangiacomo, S. de Vries, P.L. Dutton,Intro By R.LoBrutto,U. of Penna. Phila. PA 19104

Cytochrome b is reduced in flash activated chromatophores of *Rps. Sphaeroides* Ga via two independent routes, each distinguished by a characteristic sensitivity to either antimycin or myxothiazol. The well characterized myxothiazol-sensitive route proceeds via oxidant-induced reduction and involves the Qz site. The antimycin-sensitive route, involving the Qc site, may be revealed in chromatophores by raising the redox potential difference between Q pool and cyt b_{560} by one of two strategies: 1) Raising the pH to exploit the different Em/pH relationships of Q pool and cyt b_{560}; 2) Extracting quinone, thereby lowering the effective post-flash Eh of the Q pool It is not possible to explain the large extent of cyt b reduction solely on the basis of the redox properties of Q pool. Simulation of various possibilities has led us to propose that antimycin-sensitive cyt b_{560} reduction proceeds by two distinct modes: one dominant at high [Q] and directly Q pool mediated, the other circumventing Q pool and using Qb as the ultimate reductant. On the basis of extractions and redox titrations, the Qb to cyt b_{560} mode is expressed in inverse proportion to [Q pool], requires an unoccupied Qc site and implies collision and complex formation between the reaction center and the bc_1 complex. A change in the carotenoid band shift matching antimycin-sensitive cyt b reduction is opposite in direction to,and a significant percentage of the physiological phase III change and contains information on the relative locations of bc_1 complex redox components. Directed collisional complex formation for antimycin-sensitive as opposed to myxothiazol sensitive b reduction is also suggested by the differences in viscosity sensitivity of these reactions in purified protein hybrid systems.

T-Pos46 CHARACTERIZATION OF ELECTRON TRANSFER AND PROTON TRANSLOCATION ACTIVITIES IN TRYPSIN-TREATED BOVINE HEART MITOCHONDRIAL CYTOCHROME c OXIDASE. V.A. DiBiase and L.J. Prochaska, Biological Chemistry, Wright State University, Dayton, OH 45435.

Cytochrome c oxidase isolated from bovine heart mitochondria has been treated with trypsin in order to investigate the role of components a, b, and c (nomenclature of Capaldi) in cytochrome c binding, and electron transfer and proton pumping activities. Cytochrome c oxidase was dispersed in solution (Ludwig et al Biochemistry18, 1401 (1979)) with Triton X-100 (3 mg/mg enzyme) and treated with trypsin (1 mg/50 mg cyt. ox.) at pH 8.0 for ½ hour at 20°C. This treatment inhibited electron transfer activity by 9% when compared to a similarly treated control in a polarographic assay (493 sec^{-1}) and had no effect on the high (K_m = 6.1 x 10^{-8} M) or low (K_m = 2.2 x 10^{-6} M) affinity sites of cytochrome c interaction with cytochrome c oxidase. Direct thermodynamic binding experiments with cytochrome c showed that neither the high (1.04 ± 0.06 moles cyt. c/mole cyt. ox.) nor low (2.21 ± 0.15 moles cyt. c/mole cyt. ox.) affinity binding sites of cytochrome c on the enzyme was perturbed by the trypsin treatment. Control and trypsin-treated enzyme incorporated into phospholipid vesicles by cholate dialysis exhibited respiratory control ratios of 3.4 and 3.5, respectively. SDS-PAGE showed that components a and b were completely removed by the trypsin treatment. [^{14}C]-iodoacetamide labeling experiments showed that the content of component c in the enzyme was depleted by 85% upon trypsin treatment. These results suggest that components a, b, and c are not required for electron transfer activity in the isolated enzyme. (Supported by NIH HL 29051 and Miami Valley Chapter of the American Heart Association).

T-Pos47 EFFECTS OF LONG ALKYL-CHAIN COMPOUNDS ON ELECTRON TRANSFER AND ENERGY TRANSFER REACTIONS OF BEEF HEART SUBMITOCHONDRIAL MEMBRANES: ROLE OF THE ALKYL-CHAIN LENGTH AND FUNCTIONAL GROUP. N. Batayneh*, S. J. Kopacz* and C. P. Lee, Department of Biochemistry, Wayne State University School of Medicine, Detroit, Michigan 48201.

Free fatty acids, C_7 - C_{18}, at 0.5 mM exhibit an inhibitory effect on the NADH oxidase activity of beef heart submitochondrial membranes (SMP); the extent of inhibition being a function of the alkyl-chain length and the energy state of SMP. SMP in the oligomycin-recoupled state are less susceptible than in the uncoupled state. With succinate oxidase, a stimulation of the rate in the oligomycin-recoupled state and a slight inhibition of the rate in the uncoupled state were seen. The alkyl-chain length plays a significant role in both cases, with C_{13}, C_{14} fatty acids being the most potent. Replacement of the -COOH with the other functional groups altered only the magnitude of the effects. The degree of effectiveness of the C_{12} compounds on NADH and succinate oxidase activities follows the order: $-NH_2$ > -COOH > $-COCH_3$ > -OH. Bovine serum albumin completely removed the effects of free fatty acids on both NADH and succinate oxidases, but only a partial recovery (50 - 60%) in the case of amine-, alcohol-, or methylester-treated SMP. Similar results were also seen with F_1-deficient SMP. Analyses of the steady state kinetics of the reduction of cytochromes by succinate revealed that the site of the irreversible damage caused by alkyl amines is located between cytochromes b and c_1. These data indicate that: (1) there are specific lipophilic interactions between the membrane and long alkyl-chain compounds; (2) the sites of interactions are situated in the regions of complexes I and III of the respiratory chain; and (3) the alkyl-chain length and the nature of the functional group play a vital role in determining the effectiveness of theses compounds as inhibitors and/or uncouplers. Supported by grants from NSF and USPHS.

T-Pos48 COMPUTER MODELING OF EPR LINESHAPES IN CYTOCHROME bc COMPLEXES J.M. McGill and J. C. Salerno, Dept. of Biology, Rensselaer Polytechnic Institute, Troy, NY 12181

The low spin b type cytochromes of the cytochrome bc_1 complex of mitochondria and the cytochrome b_6f complex exhibit asymmetric EPR lineshapes at g max. Cytochromes b_{566} and b_{562} (bc_1 complex) have well resolved features near g=3.8 and g=3.4 which we have previously simulated by distributing the rhombic crystal field parameters (V) of each species about a characteristic value of $\bar{V}$. 'Cytochrome b_{563}' of the cytochrome b_6f complex does not exhibit two such well resolved peaks in our preparations; however, the asymmetric spectra are still either visibly double peaked or can be shown by computer simulation to be due to two components with g values of $\backsim$3.7 and $\backsim$3.4. The crystal field parameters necessary to simulate these features are Δ_1=3.3λ, $\bar{V}_1$=.4λ, $\delta_1 V$=.25 (g=3.7) and Δ_2=3.3 $\bar{V}_2$=.8λ, $\delta_2 V$=.18λ (g=3.4). The major difference between b_6f preparations is in the g=3.4 component.

In comparison, the values for b_{566} and b_{562} are Δ_1=3.3λ, $\bar{V}_1$=0 and $\delta_1 V$=.3λ and Δ_2=3.3, $\bar{V}_2$=.71λ, $\delta_2 V$=.15λ, respectively. During reduction of cytochrome b_{562} the peak position of b_{562} shifts from g$\backsim$3.4 to $\backsim$3.44. This can be simulated with the assumption that the peak shifts correspond to a decrease in V in response to reduction of a component with a midpoint potential of +80 mV and n greater than one. The lineshapes are not well modeled with the assumption that two components of b_{562} with different midpoints and different $\bar{V}$ are responsible. Response of the cytochrome spectra to inhibitors such as antimycin correspond to shifts in $\bar{V}$ and δ V.

T-Pos49 TOPOGRAPHICAL LOCATION OF REDOX ACTIVE CENTERS IN THE ENERGY COUPLING SITE II. T.Ohnishi and *G.Von Jagow, Dept. of Biochem. & Biophys, Univ. of Penn. Phila., PA 19104; *Inst. fur Physikal. & Biochem., Univ. of Munchen, Munchen, FRG.

We have examined the topographical distribution of redox active centers in the Site II segment of the respiratory chain utilizing a paramagnetic probe technique we have developed (1). We have examined the EPR signals of cytochromes b_{566} (g=3.78) and b_{562} (g=3.45) in a Complex III proteoliposome system (2). These peaks gave $P_{1/2}$ [half saturation parameter (3)] values of 7.0 and 0.2 mW at 6.2 K, which increase linearly with added dysprosium concentration. The $\Delta P_{1/2}$ values were 1.3 and 0.2 mW/mM Dysprosium, which correspond to effective distances of 15 and 22 Å, respectively, assuming r^{-6} dependence of $P_{1/2}$ and using a model system of C.vinosum HiPIP-type iron-sulfur protein (1). The effective distance of the Rieske iron-sulfur cluster was found to be similar to that of cyt. b_{566}. These data indicate that both cyt. b_{566} heme and Rieske iron-sulfur cluster are located closer to the cytosolic surface of the mitochondrial inner membrane with cyt. b_{562} heme located deeper, perhaps close to the middle of the membrane. These results are consistent with indirect estimates of the topographical distribution (electrogenic span) of cytochrome b_{566} and b_{562} hemes in mitochondria (4) and in photosynthetic bacteria (5). Presently the effective distances of redox centers from the matrix side of the membrane are being estimated. References: 1) Blum et al. (1983) BBA 748, 418. 2) W.D. Engel et al. (1980) BBA 592, 211. 3) H.Blum & T.Ohnishi (1980) BBA 621, 9. 4) A.Gopher & M.Gutman (1982) in Function of quinones in energy conserving systems (Trumpower, ed.) Academic Press, pp 511. 5) E.Glaser & A.Croft, (1984) BBA 766, 322. (Supported by NIH GM-25052 and NSF 81-17284 and the Deutsche Forschungsgemeinschaft.)

T-Pos50 CYCLIC VOLTAMMETRY OF ELECTRON-CONDUCTING BILAYER LIPID MEMBRANES **H. Ti Tien**, Membrane Biophysics Lab, Department of Physiology, Michigan State University, East Lansing, Michigan 48824 (USA)

Planar bilayer lipid membranes (BLM) have been extensively employed as models of biomembranes. A modified BLM, for example, containing photosynthetic pigments has been used as a model for the thylakoid membrane of chloroplasts, in which light-induced electron transport leading to eventual redox reactions have been demonstrated. Experimental evidence to show redox reactions in the dark in BLM has been less unequivocal owing mainly to the lack of (i) a suitable experimental technique, and (ii) a modified BLM for electronic processes. It is now possible to form BLM containing TCNQ (7,7',8,8'-tetracyano-p-quinodimethane), whose electronic properties are well described. This TCNQ-containing BLM is then investigated by cyclic voltammetry (CV), a widely used technique in electrochemistry, but only recently applied to the BLM system **(J. Phys. Chem., 88, 3172, 1984)**. This communication reports for the first time a voltammogram of cytochrome c using the TCNQ/containing BLM as the working electrode. Thus, it is shown that a suitably modified BLM can function as an electronic conductor in aqueous media partaking in redox reactions at the membrane/solution interfaces. This new type of BLM may be useful in the study of membrane bioenergetics. The experiments with TCNQ-containing and other modified bilayer lipid membranes are still at an early stage of development and wide open for the application and fusion of ideas from electrochemistry, membrane biophysics and biology.

(Supported by NIH GM-14971)

T-Pos51 RATE OF ELECTRON TRANSFER ACROSS THE CHROMAFFIN-VESICLE MEMBRANE. Gordon J. Harnadek, Elizabeth A. Ries and David Njus. Dept. of Biological Sciences, Wayne State Univ., Detroit MI 48202.

Ascorbic acid contained in catecholamine storage organelles (chromaffin vesicles) serves as a one-electron donor for the intravesicular enzyme dopamine β-hydroxylase. We believe that this internal store of ascorbate is maintained in vivo by electron transfer from a cytosolic electron donor through membrane-bound cytochrome b-561 to intravesicular semidehydroascorbate. We have been able to demonstrate electron transfer in the reverse direction in vitro by oxidizing internal ascorbate using external electron acceptors. Rates of electron transfer were measured in resealed membrane vesicles (ghosts) containing 100 mM ascorbic acid by adding an external electron acceptor (cytochrome c or ferricyanide) and following the reduction of the acceptor spectrophotometrically. To be certain that the external acceptors were being reduced by ascorbate sequestered within the ghosts, ascorbate oxidase was added to destroy any external ascorbate. To follow cytochrome c reduction, it was also necessary to add cyanide to inhibit mitochondrial cytochrome oxidase contaminating the chromaffin-vesicle ghost preparation. The rate of cytochrome c reduction is proportional to the ghost concentration (at low concentrations) and is increased at higher external pH. At pH 7.0, ghosts reduce 60 μM cytochrome c at a rate of 0.035 ± 0.010 μequiv/min·mg protein and 200 μM ferricyanide at a rate of 2.3 ± 0.3 μequiv/min·mg. Presuming that cytochrome b-561 is the mediator of electron transfer, its turnover number is 15 min^{-1} with cytochrome c and 17.5 sec^{-1} with ferricyanide. The protonophore FCCP accelerates the rate of cytochrome c reduction, probably because it dissipates the membrane potential generated by electron transfer. These rates of electron transfer are sufficient to support dopamine β-hydroxylase in vivo and are consistent with mediation of electron transfer by cytochrome b-561. Supported by NIH grant GM-30500.

T-Pos52 INACTIVATION OF BACILLUS SUBTILIS PHAGES BY 254 NM RADIATION, Lyndon L. Larcom, Abbie G. Freeman and Karen Schweikart, Departments of Physics and Microbiology, Clemson University, Clemson, South Carolina, 29631.

Three phages of Bacillus subtilis have been compared. Bacteriophages SPO2 and SPP1 are morphologically similar. For both, the DNA has a molecular weight of 25 x 10^6 and an AT content of 57%. In transfection, the DNA of phage SPP1 must undergo recombination for virus production to occur, but recombination is not required for infection with SPO2 DNA. The DNA of phage ϕ29 has a molecular weight of 11 x 10^6 daltons and an AT content of 64%. Dose-response curves were obtained for the phages and their purified DNA's in uvr^+ and uvr^- B. subtilis hosts. The phage with the highest UV sensitivity was ϕ29, even though it has the smallest target size. For all three viruses, the sensitivity of the irradiated DNA assayed in competent cells was higher than that of the intact phage in log-phase cells. Multiplicity reactivation of the virus in the uvr^+ host was observed for phages SPO2 and SPP1, but not for phage ϕ29.

T-Pos53 MODE OF ACTION OF HYPERTHERMIA IN RELATION TO PROTEIN DEGRADATION IN recA and uvrA DERIVATIVES OF E. coli K-12, N.Grecz, R.Jaw and T.McGarry, Biological Research Dept., King Faisal Specialist Hosp. & Research Centre, Riyadh, Saudi Arabia.

While the role of protein synthesis has been extensively studied in relation to the high-temperature protein (HTP) response induced by hyperthermia, the role of protein degradation is not well understood. Quantitative evaluation of the gene products in response to chronic hyperthermia (43.5 °C/ 60 min) in recA and uvrA derivatives of E. coli K-12 shows a 4-fold greater protein degradation in the recA+ uvrA+ strain AB1157 than in recA- uvrA- strain AB2480. The initial rate of induction of thermotolerance in the strain with high proteolysis (AB1157, k=0.4% per min) was about 7 to 8-fold lower than in the strain with low proteolysis (AB2480 k= 3% per min), and the subsequent steps in the HTP response, i.e. development, maintenance and decay of thermotolerance were all delayed in the presence of high proteolytic activity. Although the role of protease in the biochemical pathway of the HTP response is not well understood, one possible source is the recA gene product which codes for a protease, and plays a central regulating role in the SOS circuit which, in some aspects, overlaps the HTP response(1). The late stages of the HTP response are strongly affected by the presence of recA (as well as uvrA) gene function (2). Another potential source of proteolytic activity is the pleiotropic lon gene which codes for a protein with proteolytic activity and was recently identified as part of the HTP regulon (3). Thus, it is possible to speculate that at least two genes, recA and lon, are the potential contributors to the observed proteolytic activity within the HTP response.

Refs: 1. Walker, Micobiol. Revs. 48,60, 1984; 2. Grecz, et al. Mut. Res., in press; 3. Phillips et al. J. Bact. 159, 283, 1984.

T-Pos54 TEMPERATURE DEPENDENCE OF ELECTRON-IRRADIATION-INDUCED MASS LOSS AND RADIATION DAMAGE IN ORGANIC MATERIALS MEASURED BY ELECTRON ENERGY LOSS SPECTROSCOPY. M.K. Lamvik, D.A. Kopf and S.D. Davilla, Department of Anatomy, Duke University Medical Center, Durham NC 27710.

The statistical accuracy of electron beam methods for mass determination, chemical analysis, and elemental quantitation in organic materials is severely limited by specimen mass loss during electron irradiation. Typically 50%-90% of an organic film is lost for exposures of a few hundred electrons per square nanometer. Structural studies of unstained specimens face a similar limitation. It has been proposed that lower specimen temperature would delay the appearance of radiation damage effects. We have begun to measure radiation-induced changes in organic materials at temperatures between 4K and 300K with the aid of an electron energy-loss spectrometer. A CAMAC rack passes the data from a Gatan spectrometer to a VAX computer for online analysis. This automated system allows the extensive data collection required to sort out interrelated effects, such as dose rate and temperature dependence. Mass loss at room temperature can usually be described by a simple exponential function, while mass loss at 100K is a more complex process. Sublimed films of glycine at 100K tolerate 100 times the dose required at 290K to produce the equivalent damage, while the structure is visibly altered through a "bubbling" phenomenon. Collodion films show a range of rates at 100K with sharp discontinuities corresponding to observable structural changes in the film. Prior to the onset of the discontinuities, which occur at electron exposures of 3000 e/nm^2, the mass loss rate at 100K is as much as 50 times less than the rate at 290K. These measurements are being extended to other materials and temperatures.

Supported by NSF PCM 8306638.

T-Pos55 HEAT PRODUCTION BY TWO STRAINS OF X-IRRADIATED L5178Y CELLS.
Harry D. Youmans, W. Howard Cyr, LeRoy Schroeder, and Janusz Z. Beer. Center for Devices and Radiological Health, FDA, Rockville, MD 20857.

The heat produced by living cells cultured in vitro is a product of metabolism and the measurement of it rate of evolution in terms of power-time-curves is a direct assay of the overall metabolic activity of the population. Such data provide information beyond that obtainable from other measures such as cell density and plating efficiency. As such, the technique is particularly suitable to the assay of the effects of physical, chemical, or biological cytotoxic agents. In these experiments, thermal power-time-curves were obtained with a Prosen-NBS microcalorimeter for x-irradiated and un-irradiated mouse lymphoma strains, L5178Y-R (LY-R) and L5178Y-S (LY-S), grown as 3 ml specimens in fused optical-quartz vessels with Teflon stoppers. To adjust for different growth rates the initial densities were 3×10^4 cells/ml for LY-R and 1.5×10^4 cells/ml for LY-S. The exposed specimens received x-ray absorbed doses of 4 Gy to LY-R and 2 Gy to LY-S. The different doses are nearly equitoxic. The unexposed strains exhibited specific powers of about 1 pW/cell during logarithmic-phase growth, as expected from the literature. In this phase the increase in power paralleled the increase in cell density. In all cases the evolved power reached a maximum at about 60 hours of incubation followed by a decrease until termination of measurement at 80 hours. The decreasing power corresponded to an increase in the fraction of dead cells. The irradiated cells demonstrated less evolved power and less growth with an extension of the lag phase. These results indicate the utility of heat production monitoring to determine cytotoxic effects, as they occur, with accuracy.

T-Pos56 A ROLE FOR THE EARTH'S MAGNETIC FIELD IN BIOLOGICAL EFFECTS CAUSED BY ELF ELECTROMAGNETIC SIGNALS.
C. F. Blackman, S. G. Benane, J. R. Rabinowitz and D. E. House. Health Effects Research Laboratory, U.S. Environmental Protection Agency, Research Triangle Park, NC 27711.

Two independent laboratories have demonstrated that specific frequencies of electromagnetic radiation can cause changes in the efflux of prelabeled calcium ions from brain tissue slices [Rad. Res. 92:510 (1982)]. Under the steady-state magnetic field intensity of 38 μT due to the earth's magnetic field, 15- and 45-Hz electromagnetic signals (40 Vpp/m in air) have been shown to induce a change in the efflux of calcium ions from the exposed slices, while 1- and 30-Hz signals do not. We now show that the effective 15-Hz signal can be rendered ineffective when the net steady-state magnetic field is reduced with a Helmholtz coil to 19 μT. In addition, the ineffective 30-Hz signal becomes effective when the steady-state magnetic field is changed to ±25.3 μT or to ±76 μT. These results demonstrate that the net intensity of the steady-state magnetic field is an important variable. The results appear to fit a resonance-like relationship in which the AC frequency that can induce a change in efflux is proportional to the net magnetic field intensity times an index, 2n+1, where n=0,1. These phenomenological findings may provide a basis for evaluating the apparent lack of reproducibility of effects reported to be caused by low-intensity ELF electromagnetic signals. If the underlying mechanism involves a general property of biological tissue, then research conducted in the ambient electromagnetic environment (50/60 Hz) may be subjected to unnoticed and undesirable influences.

T-Pos57 MODIFYING EFFECTS OF "COMPETING LESIONS" ON RADIATION ASSOCIATED OSSEOUS TUMOR DEATHS IN DOGS.
Richard P. Spencer. Dept. Nuclear Medicine, Univ. Connecticut Health Center, Farmington, CT 06032

Administration of any of a number of "bone seeking" long lived radionuclides is followed by eventual appearance of bone tumors in dogs. This has been documented for the radionuclides Sr-90 and Ra-226. The "threshold dose" and latency period have been discussed in the literature. If up to a certain quantity of Ra-226 is injected into beagles, nearly all the dogs die of bone tumors. Beyond that administered dose of Ra-226 in dogs, however, deaths due to bone tumors begin to fall (see for example, Table 2 in Raabe et al, Health Physics 40:863, 1981). The reason is that, at higher doses of the administered radionuclide, animals die from other ("competing") lesions before they succumb to the bone tumors. An approach to describing this is as follows. The percent of dogs who die of bone tumors was plotted as a function of the dose level of radionuclide (Ra-226 injected, in units of microcuries per kilogram body weight). The percent of deaths was small at low doses of Ra-226 (5.5% at 0.064 uCi/kg). It peaked at over 92% deaths at 3.36 uCi/kg, and then fell to 66% at 10 uCi/kg. These values could be approximated by a function in which the percent (P) of dogs dying of bone tumors approached the asymptotic 100% while competing events increased linearly with dose. Thus: $P=100\ (1 - \exp AD) - BD$, where D is the dose; A & B=constants. A constraint is that $P+BD \leq 100$. Data are too sparse to permit extension to such events as redistribution and saturable mechanisms. At higher radionuclide doses, lesions other than bone neoplasms develop. These are principally hematopoietic tumors which are more rapidly fatal than the osseous neoplasms. (Supported by USPHS CA 17802, NCI).

T-Pos58 MOTIONAL AND STRUCTURAL ANALYSIS OF ETHER- AND ESTER-LINKED PHOSPHATIDYLCHOLINES BY ^2H NMR AND X-RAY DIFFRACTION

M.J. Ruocco, A. Makriyannis, D.J. Siminovitch and R.G. Griffin. F. Bitter Nat'l Magnet Laboratory, Massachusetts Institute of Technology, Cambridge, MA 02139.

^2H-NMR and X-ray diffraction studies of headgroup labeled dihexadecylphospho(α-$^2H_2$)choline (α-$^2H_2$-DHPC) yield quadrupolar splittings, spin-lattice relaxation times and structural behavior similar to dipalmitoylphospho(α-$^2H_2$)choline in the L_α and ripple bilayer phases. These results indicate the ether linkage has no effect on the dynamics and orientational order at the α-CD_2 segment. Chain labeled 1,2-[1,1-$^2H_4$]DHPC in L_α bilayers exhibit four quadrupolar splittings in contrast to three splittings for 1,2-[2,2-$^2H_2$]DPPC L_α bilayers. Lineshape simulations suggest the DHPC splittings arise from two pairs of inequivalent deuterons on the alkyl chains as a result of different orientations of the alkyl chains at the membrane surface. DHPC gel bilayers are interdigitated, most likely due to a conformational change induced at the bilayer interface by the ether linkage, which allows axial diffusion to persist to much lower temperatures than in DPPC. As a result only α-$^2H_2$-DPPC and 1,2-[2,2-$^2H_4$]DPPC gel spectra exhibit substantial lineshape changes at $T \leq 0°C$.

X-ray diffraction studies of equimolar DHPC/cholesterol (CHOL) dispersions at 20°C and 51°C demonstrate a non-interdigitated bilayer phase similar to equimolar DPPC/CHOL bilayers. Significant changes of 1,2-[1,1]DHPC ^2H-NMR spectra (i.e. four quadrupolar splittings → three quadrupolar splittings) in the presence of cholesterol suggest the steroid ring induces a conformational and/or motional change at the α-methylene segment of the alkyl chains.

T-Pos59 THE ROLE OF CHOLESTEROL IN LIPID POLYMORPHISM. L.T. Boni, A.M. Kleinfeld and R.R. Rando, Departments of Pharmacology and Physiology and Biophysics, Harvard Medical School, Boston, MA 02115.

Fluorescence polarization and lifetime measurements of the probe 1,6-diphenyl-1,3,5-hexatriene (DPH) was employed to investigate the acyl chain order in mixtures of cholesterol, phosphatidylcholine (PC) and phosphatidylethanolamine (PE). These mixtures included those which exhibited polymorphic phase behavior with increasing cholesterol. Bilayer to inverted hexagonal phase or lipidic particle phase was revealed by freeze fracture electron microscopy and 31-P NMR. For mixtures of 1:1 dilinoleoylPE /dilinoleoylPC, 1:1 dilinoleoylPE /egg PC and 2:1 dilinoleoylPE /egg PC, DPH polarization values increased from .10 to .17, .12 to .23, and .16 to .28 respectively as the mole per cent of cholesterol was increased from 0 to 45%. Lifetimes measured by the phase-modulation method at three frequencies are consistent with a single exponential decay. DPH lifetimes showed a slight increase for all systems studied as cholesterol content was increased, ranging between 8 to 9 nsec. These results suggest an increase in acyl chain order in going from bilayer to non-bilayer phase as induced by cholesterol. On the other hand, a decrease in the order of the acyl chains is expected for a bilayer to non-bilayer transition. This suggests a unique means by which cholesterol induces lipid polymorphism. This work was supported by NSF grant PSM-79-27214 and was done during the tenure of an Established Investigatorship of the American Heart Association to A.M.K.

T-Pos60 REVERSE-PHASE VESICLES EXHIBIT MULTIPLE PREFERRED MORPHOLOGIES. Mark L. Carlson and John C. Owicki, Dept. of Biophysics & Medical Physics, Univ. of CA, and Division of Biology & Medicine, Lawrence Berkeley Laboratory, Univ. of CA, Berkeley, CA 94720.

When reverse-phase vesicles (F. Szoka and D. Papahadjopoulos (1978) Proc. Natl. Acad. Sci. U.S.A. 75:4194-4198) made of dimyristoyl- or dipalmitoyl-phosphatidylcholine are centrifuged on a ficoll density gradient, up to eight relatively distinct bands form over the density range 1.006 to 1.044 g/cc (densities for DPPC). Extrusion of the vesicle preparation through a 0.2 μm filter prior to centrifugation eliminated the denser bands. Lipid concentrations in the fractions were determined from the fluorescence of traces of a fluorescein-labeled lipid that had been added to the vesicles. The fraction of lipid on the external monolayers was determined by quenching this fluorescence with anti-fluorescein antibodies in the external medium (A. Petrossian and J. Owicki (1984) Biochim. Biophys. Acta 776:212-227). Trapped aqueous volumes were determined with the permeable spin probe TEMPONE and nonpermeable Mn-EDTA quencher (R. Melhorn, P. Candau, and L. Packer (1982) Meth. Enzymol. 88:751-762). Volume/lipid results consistent with published reports were obtained, with the ratio generally declining with vesicle density. The denser bands were, however, local maxima. A gradual stepwise decline from 50% to 20% of the total lipid on the surface implied that the density changes were due to internal lamellae. The number of bands and behavior of the volume/lipid and external surface fraction suggested, however, that this was unlikely to be due to the simple addition of tightly packed concentric lamellae. Support: NIH #R01-AI-19605-02.

T-Pos61 LOW CONCENTRATIONS OF BILE ACIDS INCREASE THE RATE OF SPONTANEOUS PHOSPHOLIPID TRANSFER BETWEEN VESICLES. J. Wylie Nichols, Department of Physiology, Emory University School of Medicine, Atlanta, Georgia 30322.

The rate of 1-palmitoyl-2-[12-{(7-nitro-2,1,3-benzoxadiazol-4-yl)amino}dodecanoyl] phosphatidylcholine (C_{12}-NBD-PC) transfer between dioleoyl phosphatidylcholine (DOPC) vesicles was measured by a technique based on resonance energy transfer between C_{12}-NBD-PC and N-(lissamine Rhodamine B sulfonyl)-dioleoyl phosphatidylethanolamine (N-Rh-PE) (Nichols and Pagano [1982], Biochemistry 21:1720). Bile acids below their critical micelle concentrations increase the spontaneous rate of C_{12}-NBD-PC transfer without disrupting vesicle integrity. For example, in the presence of 0.1 mM taurodeoxycholate, the rate of transfer is 6 times faster than the control rate.

The dependence of the initial rate of transfer on donor vesicle, acceptor vesicle, and bile acid concentration can be predicted by a kinetic model based on alterations of the phospholipid monomer-vesicle dissociation and association rate constants depending on the extent of bile acid binding to the vesicles. Using this model, the influence of bile acid binding on the dissociation rate constant can be determined. Temperature dependence studies indicate that bile acid binding to the vesicles increases the rate of phospholipid transfer by lowering the activation enthalpy for phospholipid dissociation.

T-Pos62 CORRESPONDING STATES BETWEEN LIPID BILAYERS AND MONOLAYERS. Robert C. MacDonald and Sidney A. Simon, Department of Biochemistry, Molecular Biology and Cell Biology, Northwestern University, Evanston, IL 60201 and Department of Physiology, Duke University, Durham, NC 17711.

To understand the lateral forces within lipid bilayers and to permit more effective employment of monolayers at the air/water interface, we determined the surface pressure (π) of a monolayer at which the molecular area and chemical potential correspond to those in a bilayer of the same lipid. We generated π-N (N is the number of lipid molecules) curves by slowly adding a hexane-ethanol solution of phosphatidylcholine (PC) to a fixed area of water surface while recording π. Above the phase transition temperature of the lipid (T_ϕ), π-N curves are broken, straight lines (the break is at 80-85 Å/molecule), extending from lift-off to a maximum of nearly 50 dynes/cm. The latter is identical to the monolayer equilibrium pressure of liposomes (π_e; π of a suspension of large liposomes of the same lipid); evidently, solvent addition creates a surface defect through which lipid escapes when the pressure for liposome formation is exceeded. Below T_m a condensation region appears in the π-N relationship, but the maximum remains at π_e. (Liposomes held below T_ϕ produce a high, stable π in a day or so. In contrast, the π of water in contact with unhydrated lipid remains small for years.) Because A_m (area/molecule) at π_e occurs at the intersection of straight lines, we can unambiguously determine the A_m of monolayer lipid that has the same chemical potential as bilayer lipid. A_m below T_ϕ corresponds to that measured in bilayers by X-ray diffraction and it is 25% greater above T_ϕ than below T_ϕ. The temperature at which the expansion occurs is within 1-2° of T_ϕ, which was accurately determined from the temperature dependence of the surface potential of lipid spread to excess. Since monolayers at π_e correspond to bilayers with respect to T_ϕ, A, and ΔA, the lateral pressure of bilayers is about 100 (2x50) dyne/cm.

T-Pos63 EFFECTS OF THERMODYNAMIC FIELDS ON THE PHASE TRANSITION PROPERTIES AND STABILITY OF PHOSPHOLIPID BILAYERS: LANDAU THEORY OF ONE-COMPONENT SYSTEMS. Istvan P. Sugar and Thomas E. Thompson (Introduced by W.R. Pearson) Semmelweis Medical University, Institute of Biophysics, Budapest and Department of Biochemistry, University of Virginia, Charlottesville, Virginia 22908.

A theoretical model is developed to describe the temperature-, electric field-, hydrostatic pressure- and lateral tension-induced phase transition of phospholipid bilayers. By means of the calculated phase diagrams the Clapeyron-slopes and the critical parameters of the lecithin membranes are determined, e.g. the critical temperature and critical tension of dipalmitoyl phosphatidylcholine (DPPC) membrane are 38.2°C and 0.006 N/m chain respectively. Analysing the limit of bilayer stability the electric breakdown voltage and the osmotic breakdown tension are obtained and as a consequence the calculated pore edge energy per unit length is $4 \cdot 10^{-12}$ J/m. The transmembrane voltage--temperature phase diagram shows that 1.2-1.9 V transmembrane voltage induces a liquid crystalline--fluid phase transition of DPPC bilayer at 47°C. On the basis of a simple free-volume calculation, it is pointed out that in the fluid phase small, water-filled pores can be formed and as a consequence the ion conductivity of the membrane can increase dramatically. From these fluctuating small pores larger metastable- or unstable pores can develop having importance in the phenomena of the reversible- or irreversible electroporation (electrical breakdown) respectively.

T-Pos64 DETERMINATION OF GANGLIOSIDE ORGANIZATION IN PHOSPHATIDYLCHOLINE BILAYERS. T.E. Thompson, M.L. Johnson, M. Allietta, R.E. Brown and T.W. Tillack, University of Virginia, Charlottesville, Virginia, 22908.

The distribution of the ganglioside GM_1 as a minor component in liquid crystalline phosphatidylcholine bilayers can be determined using freeze-etch electron microscopy with ferritin-conjugated cholera toxin or with cholera toxin alone as the ganglioside marker. Although the markers are at least 100 times larger in cross sectional area than is the molecule of GM_1, the average number of GM_1 molecules under the marker can be determined from measurements of the fraction of bilayer area covered by the marker as a function of GM_1 mole fraction. The functional relation between these two variables, which can be derived from the general binomial term, is given by: $F = 1 - (1 - C)^{M/G}$

Here F is the fractional area of the bilayer covered by the marker when the mole fraction of glycolipid in the bilayer is C. M and G are the cross sectional areas of marker and glycolipid, respectively. The ratio of the value of M/G calculated from the known dimensions of the marker and the glycolipid to that determined from the experimental data is the average number of glycolipid molecules under the marker. Application of this analysis to GM_1 in liquid crystalline phosphatidylcholine bilayers indicates that on the average 1 molecule of GM_1 is under each marker. Thus in these systems, GM_1 is molecularly dispersed. This is in contrast to asialo GM_1, a neutral glycosphingolipid derived from GM_1, which is organized in compositional domains in liquid crystalline phosphatidylcholine bilayers. (Supported by USPHS Grants GM-26234 and GM-23573).

T-Pos65 DEPENDENCE OF ^2H SPIN-LATTICE RELAXATION RATES OF LIPID BILAYERS ON ORIENTATIONAL ORDER. James M. Beach, Michael F. Brown, Steven W. Dodd, Amir Salmon, and Gerald D. Williams. Department of Chemistry and Biophysics Program, University of Virginia, Charlottesville, VA 22901.

^2H NMR studies of multilamellar dispersions of saturated diacyl-sn-glycero-3-phosphocholines, as a function of chain length and temperature, with perdeuterated acyl chains at the sn-1/sn-2 or the sn-2 positions have been performed (1). In this work, a method of analysis which involves deconvolution of the experimental, superimposed powder-pattern spectra to obtain well resolved oriented spectra ("de-Pake-ing") (2) has been used to obtain the spin-lattice relaxation rates (T_1^{-1}). We have routinely applied this highly computational technique to provide experimental evidence for an approximately square-law dependence of the ^2H T_1^{-1} values on the bond segmental order parameter S_{CD}, at all temperatures, consistent with a relaxation expression of the form $T_1^{-1} = T_{1fast}^{-1} + (B\omega_0^{-1/2})|S_{CD}|^2$ where ω_0 is the fixed resonance frequency and B is nearly constant (3). Close agreement with the available data for specifically deuterated phospholipids suggests that the dominant relaxation contribution arises from the second term due to slower, collective bilayer disturbances (4). Similar studies of other systems, including lyotropic phases, are in progress.

(1) G.D. Williams et al., Biophys. J. 45, 169a (1984). (2) M. Bloom et al., Chem. Phys. Lett. 80, 198 (1981). (3) M.F. Brown, J. Chem. Phys. 77, 1593 (1982). (4) M.F. Brown et al., PNAS 80, 4325 (1983).

Supported by NIH grant EY03754, the Monsanto Company, a postdoctoral fellowship from NIH (J.M.B.) and an NSF predoctoral fellowship (A.S.). M.F.B. is an Alfred P. Sloan Research Fellow.

T-Pos66 INFLUENCE OF ACYL CHAIN UNSATURATION ON MOLECULAR DYNAMICS OF LIPID BILAYERS FROM ^{13}C T_1 RELAXATION TIME MEASUREMENTS. Jeffrey F. Ellena, Gerald D. Williams, Janel Sennewald, Robert D. Pates, Amir Salmon, and Michael F. Brown. Department of Chemistry and Biophysics Program, University of Virginia, Charlottesville, VA 22901.

^{13}C spin-lattice (T_1) relaxation time studies of unsaturated 1,2-diacyl-sn-glycero-3-phosphocholine (PC) vesicles have been performed as a function of frequency/magnetic field strength (15.0, 50.3, 90.5 MHz). The acyl chain length and the number of double bonds have been varied systematically. Profiles of $(NT_1)^{-1}$, where N is the number of directly bonded ^1H nuclei, show that the values of the CH=CH segments are increased relative to those of the adjacent CH_2 chain segments. For the homologous series of di(Cn:1) PC's at the same absolute temperature, where n = 14, 16, 18 denotes the number of chain carbons, little systematic change in $(NT_1)^{-1}$ of the CH_2 segments is observed with increasing chain length. However, the $(NT_1)^{-1}$ values of the CH=CH resonances appear to increase as the chain length is increased. For the homologous series of di(18:n) PC's at the same absolute temperature, where n = 1, 2, 3 indicates the number of double bonds, again little change in the $(NT_1)^{-1}$ values of those CH_2 groups between the carbonyl group and the Δ^9 double bond is evident; those of the CH=CH resonances appear to decrease as the number of double bonds is increased. The relaxation rates of all the resonances decrease with increasing frequency/magnetic field strength as observed for saturated PC's (1,2).

(1) M.F. Brown et al., PNAS 80, 4325 (1983). (2) M.F. Brown, J. Chem. Phys. 80, 2808 (1984).

Supported by NIH grant EY03754, a postdoctoral fellowship from NIH (J.F.E.) an NSF predoctoral fellowship (A.S.), and by the Monsanto Company. M.F.B. is an Alfred P. Sloan Research Fellow.

T-Pos67 **STABILIZATION OF DRY LIPOSOMES BY TREHALOSE.** **Lois M. Crowe, John H. Crowe, Christopher Womersley, Alan Rudolph, and Paul Uster. Department of Zoology, University of California, Davis.**

Trehalose is a carbohydrate found at high concentration in many organisms that normally survive dehydration. We have previously shown that is preserves structure and function in dry biological membranes. In the present study we show that this molecule can stabilize dry large unilamellar phospholipid vesicles (90 POPC: 10 PS). With trehalose both inside and outside the bilayer, > 90% of trapped solute was retained in rehydrated vesicles previously freeze-dried with sufficient trehalose to result in ca. 2.0 g trehalose/g phospholipid in the dry mixture. With no trehalose present essentially all the trapped material is leaked to the surrounding medium as a result of freeze drying. Additional studies were conducted in order to provide evidence concerning the mechanism by which trehalose stabilizes the dry vesicles. Freeze fracture suggested that trehalose inhibits fusion between the dry vesicles. Fusion was quantified by resonance energy transfer between fluorescent probes (Uster and Deamer. 1981. Arch. Biochem. Biophys. 209,385). The results showed that fusion was almost completely inhibited when the dry mixtures contained > 0.9 g trehalose/g lipid. Thus, the concentration of trehalose required to inhibit leakage completely from the vesicles is much greater than that required to prevent fusion. Previous studies showed that trehalose depresses the transition temperature (T_c) of dry phospholipids, and that maximal depression of T_c occurs at about 1.6 g trehalose/g phospholipid. We conclude that stabilization of the dry liposomes probably requires depression of T_c and consequent maintenance of the constituent lipids in a liquid crystalline phase. **[Supported by National Science Foundation (grant PCM 82-17538) and National Sea Grant (grant RA/41) to JHC and LMC.]**

T-Pos68 INFLUENCE OF TORUS ON THE CAPACITANCE OF ASYMMETRICAL PHOSPHOLIPID BILAYERS: AN HYPOTHESIS. M. Brullemans, S. Robert and P. Tancrède, University of Quebec, Photobiophysics Research Center, Trois-Rivières (Québec), Canada G9A 5H7.

We have undertaken a study of the electrical properties of planar asymmetrical bilayers formed according to the technique of Montal and Mueller. Phosphotidylethanolamine/phosphatidylserine asymmetrical bilayers were formed across Teflon films whose thickness varied from 6 to 25 μm. It is observed that the specific capacitance increases by about 10% as the thickness of the film is increased. Furthermore, the capacitance of the membranes being recorded throughout their formation, it is observed that the capacitance values increase markedly immediately before the membranes are completely formed and then rapidly decrease to their normal values when they are formed (closing-off phenomenon). These facts have led us to propose that Montal-Mueller membranes are surrounded by a transition zone whose associated electrical properties can affect the capacitance values measured for the membranes. Indeed, we show that both the thickness dependence of the capacitance and the closing-off phenomenon can be explained if a small torus (less than 1% of the overall membrane area) having specific conductivity properties characteristic of a moderately polar medium surrounds the bilayer. We show that a small torus of this kind bears important effects on the overall capacitance values of the membranes, particularly yielding, among other things, to large fluctuations of the capacitance values reported for a given set of experimental conditions (our results and Vodyanoy and Hall, Biophys. J. 46, 187-194, (1984)).

T-Pos69 KINETICS AND MECHANISM OF THE LAMELLAR AND HEXAGONAL PHASE TRANSITION IN PHOSPHATIDYLETHANOLAMINE. Martin Caffrey, Section of Biochemistry, Molecular & Cell Biology, Cornell University, Ithaca, New York 14853

A study of the kinetics and mechanisms of the thermotropic lamellar gel/lamellar liquid crystalline and lamellar/inverted hexagonal phase transition in dihexadecylphosphatidylethanolamine (DHPE) at various hydration levels has been carried out. Measurements were made using a real-time x-ray diffraction method at the Cornell High Energy Synchrotron Source. The chain melting and the nonbilayer transition were examined under active heating and passive cooling conditions using a temperature-jump to effect phase transformation. Measurements were made at hydration levels ranging from 0 to 60% (w/w) water and in all cases the transitions were found to 1) be repeatable, 2) be reversible with minimal hysteresis, 3) have transit times of $\leq$ 3 s, and 4) be two-state to within the sensitivity limits of the method. The shortest transit time recorded for the chain melting and lamellar/hexagonal transition was approximately 1 s. At 8% (w/w) water, the transit times were still on the order of seconds even though the transition does not involve the intermediate L_α phase. On the basis of the real-time x-ray diffraction measurements a mechanism is proposed for the lamellar/hexagonal phase transition. The mechanism 1) does not involve large or energetically expensive molecular rearrangements; 2) leads directly to a hexagonal lattice; 3) incorporates facile reversibility, repeatability and cooperativity; 4) accounts for an observed, apparent memory in the hexagonal phase of the original lamellar phase orientation; and 5) is consistent with the experimental observation of a predominantly two-state transition.

T-Pos70 EFFECT OF CHOLESTEROL ON DIETHER PHOSPHATIDYLCHOLINE BILAYER DISPERSIONS: A RAMAN SPECTROSCOPIC STUDY

William C. Harris, Ellen Keihn and Ira W. Levin, Laboratory of Chemical Physics, NIADDK, National Institutes of Health, Bethesda, MD 20205

For assessing lipid-sterol packing characteristics in model membrane systems, the vibrational Raman spectra of 1,2-di-O-hexadecyl-sn-glycerol-3-phosphocholine (DHPC) multilamellar dispersions were examined with 18 mole % cholesterol (CHOL). The thermotropic behavior of the pure diether and CHOL containing bilayers were studied in both the C-H stretching (2800-3100 cm^{-1}) and C-C stretching (1000-1200 cm^{-1}) mode regions, spectral intervals reflecting intermolecular and intramolecular order/disorder characteristics. Pure DHPC bilayers exhibit the pretransition and gel to liquid crystalline phase transition temperatures at 31 and 43°C, respectively. In contrast to the temperature behavior of dipalmitoylphosphatidylcholine-CHOL bilayers in which the primary phase transition T_m is broadened, T_m is increased to ∿49.5°C in the DHPC (diether PC) liposomes containing 18 mole % CHOL. As in diacyl-CHOL bilayer systems, CHOL disorders the DHPC gel phase and eliminates the pretransition, while ordering the liquid crystalline phase. Both the pure diether and CHOL containing liposomes exhibit greater inter- and intramolecular liquid crystalline disorder in comparison to their diacyl counterparts. On multiple recycling of the pure DHPC bilayers through T_m, the order characteristics of the liquid crystalline phase are increased. The CHOL containing liposomes always retain, however, their maximum disorder in the high temperature phase. It is suggested that the increased disorder in the diether liposomes results from the higher placement toward the headgroup of CHOL in the bilayer.

T-Pos71 MAGNETIC RESONANCE STUDIES OF ABSCISIC ACID - PHOSPHOLIPID MEMBRANE INTERACTIONS.

Stephen R. Wassall* and William Stillwell†, Departments of Physics* and Biology†, IUPUI, Box 647, Indianapolis, IN 46223.

The membrane as a site of initial interaction is a possibility that is currently under consideration for the as yet unknown mechanism of plant hormone action. Numerous studies have shown that abscisic acid (ABA), an inhibitor of many growth associated plant processes, affects membrane transport properties. Due to the complexity of the biological systems predominantly studied, however, no clear picture emerges from the sometimes conflicting effects observed.

We have recently applied magnetic resonance techniques to investigate the influence of ABA on simpler, more well defined phospholipid bilayer model membranes. The results confirm that the hormone modifies bilayer properties and that the extent of the effects depend upon phospholipid composition. In particular, they are consistent with a selective interaction with phosphatidylethanolamine (PE). Using lanthanide induced shift-NMR methods, furthermore, our previous observations that ABA interacts with PE to enhance lipid bilayer permeability to non electrolytes are extended to cations.

T-Pos72 THE MEMBRANE DIPOLE POTENTIAL IN A SELF-CONSISTENT TOTAL MEMBRANE POTENTIAL MODEL.

R. F. Flewelling and W. L. Hubbell, Jules Stein Eye Institute, UCLA School of Medicine, CA 90024.

Hydrophobic ions such as tetraphenylboron (TPB^-) and tetraphenylphosphonium (TPP^+) are proving to be invaluable probes of membrane electrical phenomena, whether in the form of dyes, spin labels, radioactive tracers or electrodes; many uncouplers of oxidative phosphorylation are also members of this class. Such molecules interact with membranes roughly according to a model first proposed by Ketterer, Neumcke and Lauger (J. Membrane Biol. 5: 225, 1971) which combined Born-image and neutral energy contributions. Despite its general success, this model fails to account for the enormous differences in hydrophobic anion conductances compared to those for structurally similar cations.

Recent data on the interaction of hydrophobic cations with membranes (Biophys. J. 41: 349a, 1983) permits the evaluation of a more complete model that explicitly incorporates the membrane dipole potential in a self-consistent manner along with Born-image and neutral energy contributions. The dipole potential is modeled as a two dimensional lattice of point dipoles located at each interface. The resulting membrane potential profiles show that a single set of realistic model parameters can entirely account for the detailed properties of both binding and translocation for the structural analogs TPB^- and TPP^+. Individual enthalpic and entropic contributions have been measured and can also be accounted for in detail.

The complete potential model now permits detailed analysis of hydrophobic ion interactions with membranes. It can also be applied to chaotropic ions and may have important implications for the energetics of protein incorporation into bilayers.

T-Pos73 MECHANISM OF THE TRANSITIONS BETWEEN LAMELLAR AND INVERTED HEXAGONAL PHASES

D. P. Siegel, Procter & Gamble Co., P.O. Box 39175, Cincinnati, OH 45247

The transitions between lamellar and inverted hexagonal (H_{II}) phases are proposed to occur via formation of IMI (inverted micellar intermediates; (1)), which assemble into two different H_{II} precursors (2). There is morphological and NMR evidence for the existence of all these intermediate structures. The formation and consumption rates of these intermediates and the time necessary to complete the $L_\alpha \rightarrow H_{II}$ and $H_{II} \rightarrow L_\alpha$ transitions can be predicted. The results are compatible with morphological, NMR, and synchrotron X-ray measurements. The predicted range of $L_\alpha \rightarrow H_{II}$ transition times is 0.2-8 s for unsaturated acyl-chain phosphatidylethanolamines subjected to small temperature jumps. The transition times depend on the structural dimensions of the L_α and H_{II} phases, the strength of the short-range forces resisting close apposition, and the degree to which the free energy necessary to closely-appose the membranes is available for inverted micelle formation. $H_{II} \rightarrow L_\alpha$ transition rates depend on the stability of certain defects within the bulk H_{II} phase, and should often be slower than the $L_\alpha \rightarrow H_{II}$ transition. Hysteresis in these transitions is due predominantly to the difference in water content of the two phases and the sluggish water transport properties of both. The theory is only qualitatively useful for $L_\alpha \leftrightarrow H_{II}$ transitions driven by cation binding (e.g., Ca^{2+}-cardiolipin) due to the severe Ca^{2+}-binding hysteresis that can occur.

(1) Biophys. J. 45:399 (1984).
(2) Biophys. J. (submitted).

T-Pos74 MEMBRANE-MEMBRANE INTERACTIONS VIA INTERMEDIATES IN THE $L_\alpha \rightarrow H_{II}$ TRANSITION

D. P. Siegel, Procter & Gamble Co., P. O. Box 39175, Cincinnati, OH 45247

The model presented in the accompanying abstract (and (1)) is used to predict the type and rate of vesicle-vesicle interactions that can occur via intermediates in the $L_\alpha \rightarrow H_{II}$ phase transition near the $L_\alpha \rightarrow H_{II}$ phase transition temperature, T_H. These interactions include lipid exchange without leakage or fusion, leakage after aggregation, and fusion. The predictions below are for dispersions of phosphatidylethanolamine LUV (diam.=ca. 0.1 μm). Starting at temperatures ca. 10^o K below T_H, the lipids of the outer monolayers of aggregated vesicles should exchange with a half-life of 10^{-3}-10^{-2} s. Fusion will be slow (>10^2 s), if it is observed at all. At $T \geq T_H$, the vesicles will leak after aggregation because of H_{II} phase formation between vesicles. This process should be complete within 10^{-1}-10^1 s after aggregation of a given pair of vesicles, and should be more rapid for vesicles with hyper-osmotic interiors. Fusion should <u>not</u> occur via intermediates in this phase transition at $T \geq T_H$, except in small unilamellar vesicles, where it should be slow (>10^2 s). These predictions are compatible with the observations of Bentz, Ellens, Lai & Szoka (2). The model is not quantitatively valid for lipids with $L_\alpha \rightarrow H_{II}$ transitions driven by cation binding (e.g., Ca^{2+}-cardiolipin), because of the large differences in lipid chemical potential produced by $[Ca^{2+}]$ asymmetries. In such cases, fusion should be observed much more frequently than in thermotropic systems.

(1) D. P. Siegel, Biophys. J. (submitted).
(2) BBA (submitted).

T-Pos75 EFFECTS OF STABILIZING AGENTS ON MEMBRANE PHOSPHOLIPIDS by Alan S. Rudolph, John H. Crowe, and Lois M. Crowe, Dept. of Zoology, University of California at Davis, Davis, CA 95616.

The ability of certain organisms to survive dehydration or freezing depends on accumulation of compounds able to stabilize biological membranes during the removal of water. We have previously shown that sarcoplasmic reticulum membranes retain structural and functional viability following a freeze-thaw event in the presence of two such agents: the disaccharide trehalose and the imino acid proline. In addition, resonance energy transfer experiments indicate that fusion between phospholipid vesicles is inhibited by as much as 90% in the presence of these agents. In the current investigation, we explore the interaction of proline, trehalose, and betaine with membrane phospholipids, using phospholipid monolayers and differential scanning calorimetry. We have studied these interactions as a function of head group and alkyl chain characteristics, employing DMPC, DMPE, POPC, and POPE. The results of these experiments indicate that all three of these agents spread phospholipid monolayers to some extent, increasing the critical area/molecule of phospholipid by 30-50% (in .5M protectant). Betaine spreads these lipids the most, with proline and trehalose equal in their effect. These agents also alter the gel to liquid crystalline phase transition; 1M proline results in a 2-3°C drop in peak transition temperature in aqueous dispersions of DPPC small unilamellar vesicles, and spreads the transition, indicating a decrease in cooperativity perhaps as a result of increased distance between alkyl chains of phospholipid. These results suggest that trehalose, proline, and betaine stabilize phospholipids during hydration stress by spreading phospholipids and altering dehydration induced gel formation. Supported by NSF (PCM 82-17538), and National Sea Grant (RA/41) to JHC and LMC.

T-Pos76 ENVIRONMENTAL INFLUENCES ON THE IONIZATION BEHAVIOR OF CHOLIC ACID. Donna J. Cabral, Donald M. Small & James A. Hamilton, Biophysics Institute, Boston University School of Medicine, Boston Massachusetts 02118

The ionization behavior of cholic acid in a variety of molecular environments was studied using ^{13}C NMR spectroscopy. The apparent pKa of the carboxyl group was determined from plots of chemical shifts vs. pH. Aqueous micellar sodium cholate (NaC) can be titrated from high pH only to pH 6.5 before precipitation of cholic acid begins, resulting in loss of the NMR signal. Using NaC with 90% ^{13}C-enrichment of the carboxyl carbon (C24), a full titration curve was obtained for monomeric NaC at a concentration (0.2 mM) below the solubility of cholic acid. The pKa of monomeric NaC was 4.6. Incorporation of 10 wt% NaC into sodium taurocholate micelles also prevented precipitation of cholic acid, and a complete titration curve with pKa=5.3 was obtained. NaC in a model membrane (egg lecithin vesicles) and in a protein environment (bovine serum albumin, BSA) was studied using 90% [24-^{13}C] NaC. In vesicles with 3% NaC, two carboxyl peaks of differing intensities were observed. The major peak had a pKa of 6.8 and the minor peak, 7.4. The minor peak may represent NaC in the inner monolayer of the vesicle bilayer in slow exchange with NaC in the outer monolayer. In a complexed with BSA (2 moles NaC/mole BSA), NaC exhibited a single, broad carboxyl resonance at all pH values except at very low pH (~2.0) where the peak was narrow (<10 Hz). Thus a complete titration curve for NaC bound to BSA was obtained with pKa=4.5. Therefore, at pH 7.4 the ionization state of NaC will depend on the local environment: monomeric NaC or BSA-bound NaC will be fully ionized, whereas membrane-bound NaC will be only half ionized.

T-Pos77 THE THERMOTROPIC PHASE BEHAVIOR OF A PLATELET ACTIVATING FACTOR: AN INFRARED SPECTROSCOPIC STUDY.

Ernest Mushayakarara and Henry H. Mantsch
Division of Chemistry, National Research Council, Ottawa, K1A 0R6, Canada.

The thermotropic phase characteristics of 1-O-octadecyl-2-acetoyl-sn-glycero--3 phosphocholine were obtained by infrared spectroscopic techniques. Phase changes of the headgroup, the interface and the acyl chain regions were monitored by using wavenumber displacement and bandwidth spectral parameters as functions of temperature.A sharp cooperative thermotropic transition, preceded by a second event at a lower temperature was observed. Crystal field splitting of the methylene bending modes is present in the interdigitated lamellar crystalline phase at temperatures below the first transition. At the first transition the crystalline phase transforms to a lamellar gel phase, which in turn converts to a clear micellar solution at the second transition. The rate of the reversed transformation from the micellar to the lamellar crystalline phase is negatively temperature dependent,e.g., 6 min at -1°C and about 12 min at 3°C.